The Wanganui-Wilberg Rock Avalanche: deposit, dynamics and dating

---

A thesis

submitted in partial fulfilment

of the requirements of the Degree

of

Master of Science in Geology

at the

University of Canterbury

by

Guillaume G. Chevalier

Department of Geological Sciences

University of Canterbury

March 2008

Table of Contents

Table of Figures

Table of Graphs

Abstract

The Wanganui-Wilberg landslide lies between Hokitika and Franz Josef townships, at the entrance of Harihari, on the true left bank of the Wanganui River, by State Highway 6. This apparently co-seismic landslide belongs to the class of events called rock avalanches - powerful destructive agents (Keefer, 1984) in the landscape. Other rock avalanches are numerous (Whitehouse, 1983), and widespread over the Southern Alps of New Zealand, and many appear to be co-seismic.

De Mets *et al.* (1994) used the model NUVEL-1A to characterize the motion of the Alpine fault: 37 mm/year at an azimuth of 071° for the strike-slip and a dip-slip of 10 mm/year normal to the strike direction. Although linear when seen from the sky, the detailed morphology of the fault is more complex, called *en échelon* (Norris and Cooper, 1997). It exhibits metamorphosed schists (mylonite series) in its hanging wall (McCahon, 2007; Korup, 2004).

Earthquakes on the Alpine fault have a recurrence time of *c.* 200-300 years and a probability of occurrence within 100 years of 88% (Rhoades and Van Dissen, 2002).

Thought to have been triggered by the AD1220 event (determined by dendrochronology), the Wanganui-Wilberg rock avalanche deposit represents only 20% of its original volume, which was *c.* 33 million cubic metres.

The deposit probably dammed the Wanganui River and, as a result, created a small and short-lived lake upstream. The next earthquake capable of triggering such events is likely to occur fairly soon (Yetton, 1998). Knowledge of historic catastrophic events such as the Wanganui-Wilberg rock avalanche is of crucial importance in the development of future hazard and management plans.

Acknowledgments

I would like to acknowledge the Mason Trust Committee of the University of Canterbury, Christchurch, for the financial support of this thesis. Tim Davies and Jarg Pettinga are deeply thanked for their time, kindness, support and patience. I also wish to thank people who helped me carry out field work during the year, and especially Anja Dufresne for her countless hours of help. For the ground-penetrating radar interpretations and for the realisation of the geomorpholgical map, I wish to acknowledge David Nobes and John Southward for their invaluable support. I am also grateful to the Sullivan family for allowing me to have unlimited access to their property. I am also grateful to Anna and her partner for allowing me to trench on their property. Andrew Wells is greatly thanked for the help provided during the dendrochronology survey and Sandra Hammond for the mounting of the cores. A more personal thankyou is addressed to the King family. Finally I would like to acknowledge Tim Davies and Anja Dufresne for reviewing this thesis.

Introduction

The Southern Alps of the South Island, New Zealand are bounded on their western margin by one of the most active fault systems on Earth: the Alpine Fault. The recurrence interval of major earthquakes on this remarkable geological feature is ~ 200 – 300 years (Rhoades and Van Dissen, 2002) and some of the effects on the landscape are still visible hundreds or thousands of years later. Co-seismic landslides are one of these effects.

In the vicinity of the township of Harihari (which lies midway between Hokitika and Franz Josef), on the true left bank of the Wanganui River, an anomalously high surface (compared to the riverbed) and a corresponding depression in the northern slope of Mount Wilberg are visible (fig. 1).

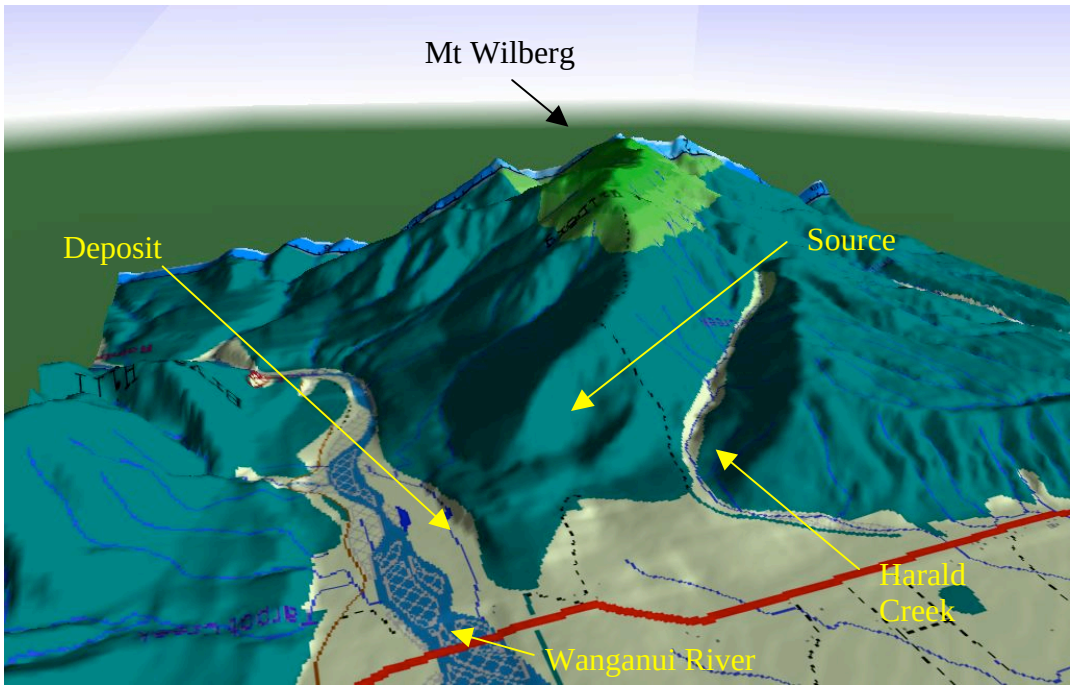

Figure 1: Modelled map of the Wanganui-Wilberg rock avalanche.

Mount Wilberg is on the western edge of the Southern Alps, in a zone, which exhibits a lithologic E-W gradient passing from greywackes to increasingly metamorphosed schists with

proximity to the Alpine Fault (Cooper and Norris, 1994). The Alpine Fault is a transform fault with an inception dated to the latest Oligocene - early Miocene (Balance 1970, Kamp 1986). Its strike-slip motion is 37 mm/yr at an azimuth of 071° and a dip-slip of 10 mm/yr normal to the strike direction (De Mets *et al.*, 1994).

As expected, Mount Wilberg confirms the presence of schists (seen in a nearby quarry) forming the major part of the bedrock and Harald Creek has evidence of the presence of cataclased mylonites and pseudotachylytes (metamorphised schists), and then of the Alpine Fault itself (McCahon *et al.*, 2007).

The purpose of this work is, first, to report the nature of the deposit in the context of other adjacent geomorphological surfaces. The dynamics of the landslide are then discussed in the light of what is remaining of the deposit. Finally an age determination is carried out to determine the likely triggering event for the Wanganui-Wilberg rock avalanche.

Chapter 1: Study Area

1.1 Introduction

The Southern Alps are a mountain range extending all along New Zealand's South Island. The geodynamic reason for this mountain range is the convergence of the Pacific plate with the Australasian plate. As these two plates collide, exhumation of material occurs. However, the Southern Alps are apparently in a dynamically steady state as erosion roughly balances uplift. On the western side of the range, moist winds coming from the Tasman Sea encounter the Southern Alps creating an orographic uplift, causing rainfalls up to 14,000 mm per year (Henderson & Thompson, 2000). Thus erosion is very intense and vegetation is very dense on this side of the Southern Alps. The eastern side is drier with less vegetation, and with lower uplift and slower erosion.

The higher peaks of the Southern Alps are concentrated in Central Westland, with about twenty of them over 3000m high including Mount Cook (3755m), the highest peak in Australasia.

1.2 Geology

The geology of the South Island presents three main domains. On the east coast, Quaternary deposits are dominant, showing sedimentary facies.

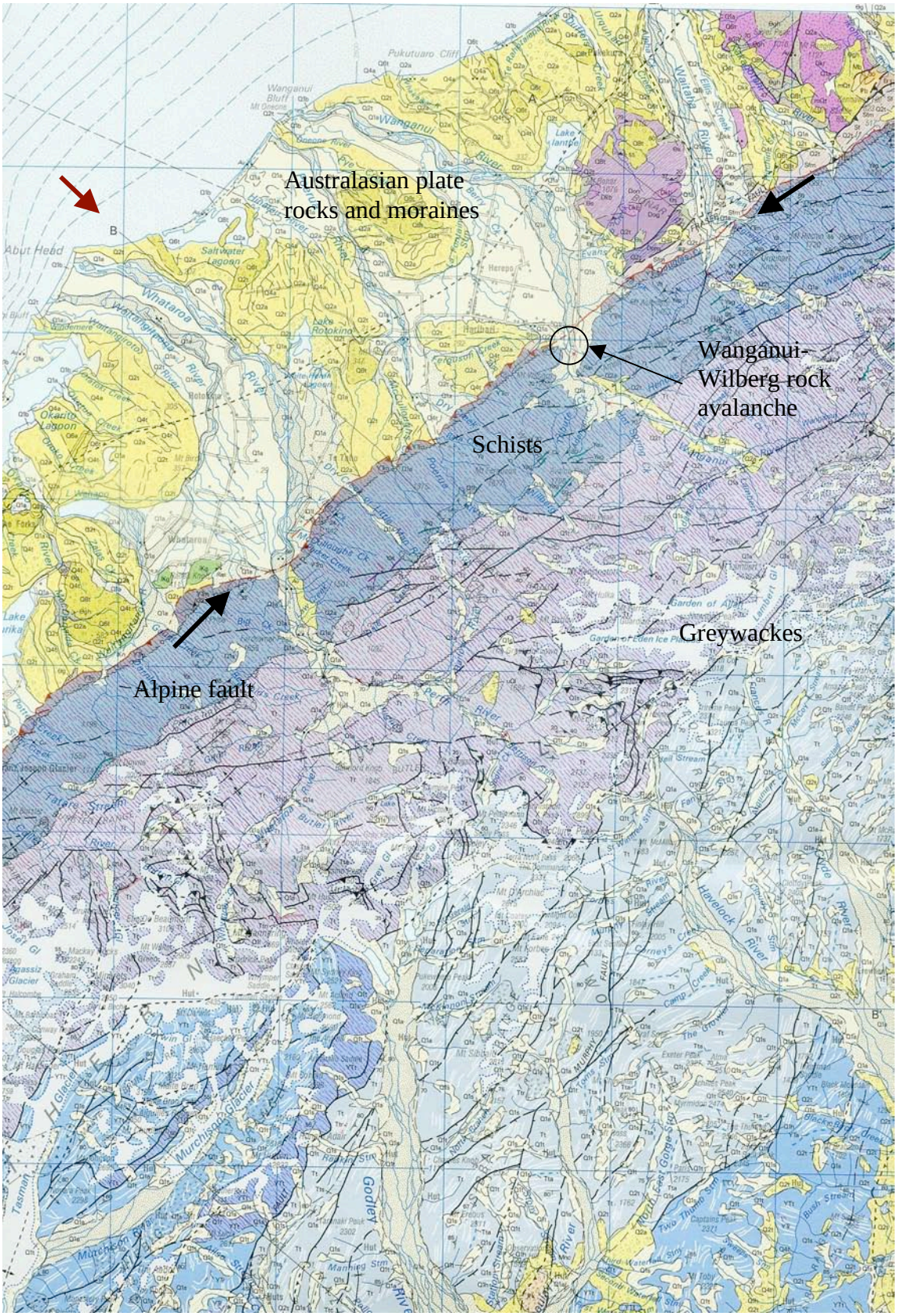

Figure 1: Geological map, showing the main divide of the Southern Alps and the West Coast of New Zealand. The circle marks the Wanganui-Wilberg site and the brown arrow points to the profile shown in fig.3 – from Cox and Barrel, 2007.

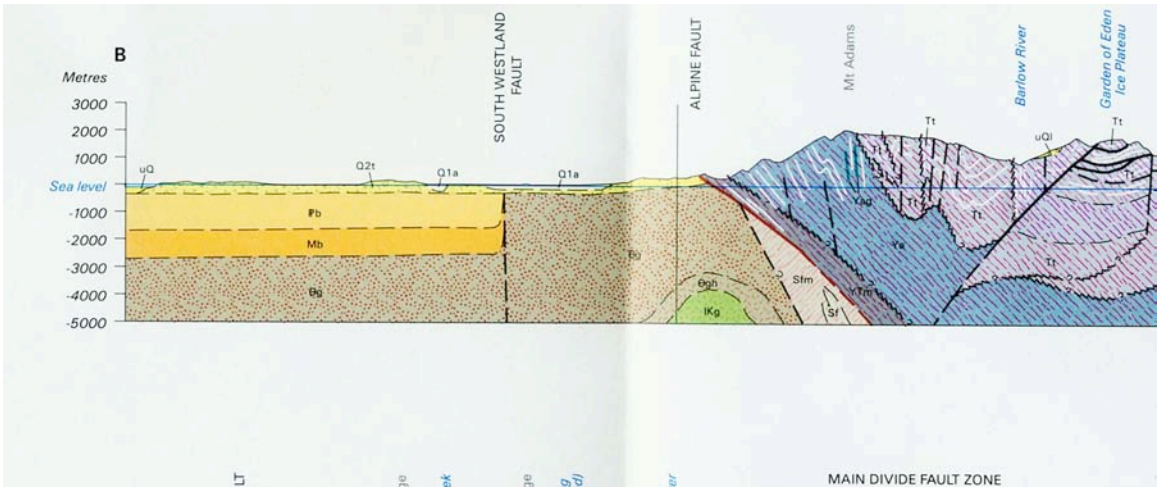

Figure 2: Cross-section shown on fig. 2 – from Cox and Barrel, 2007.

To the west of the main divide of the Southern Alps, the rocks change from greywacke to schist, the latter increasingly metamorphosed with proximity to the Alpine Fault zone. This zone forms the boundary between the Pacific and Australasian plates.

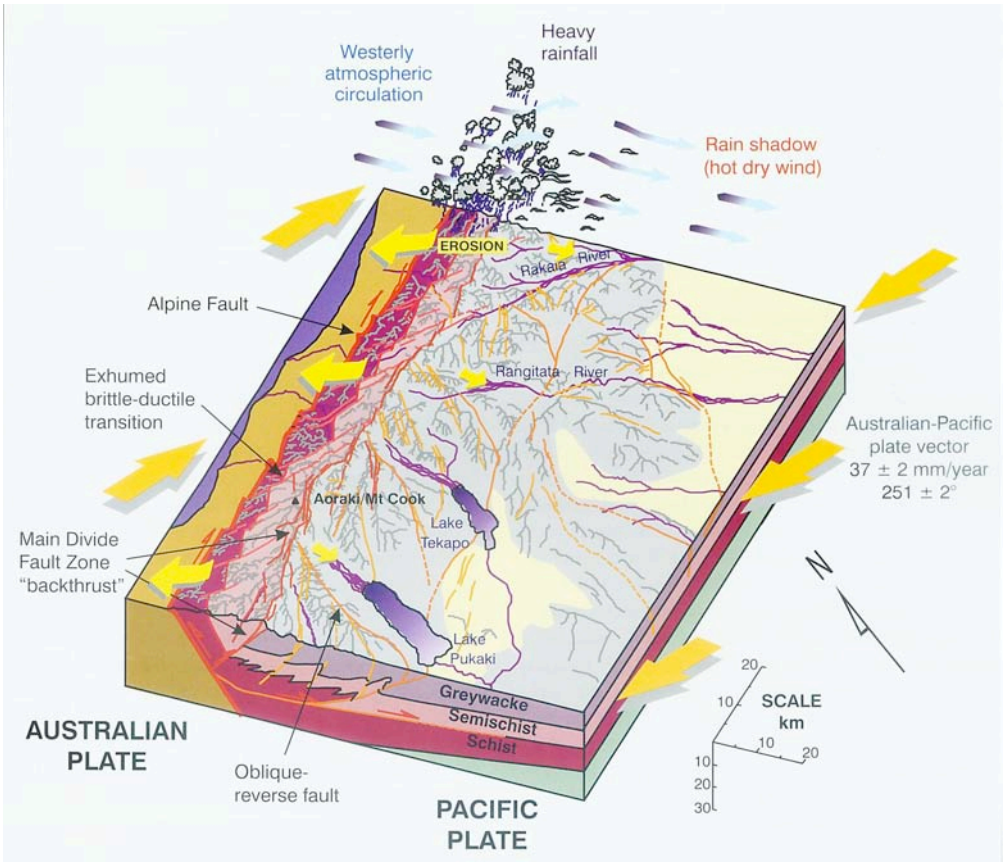

Figure 3: Block-diagram showing the geodynamic setting of the Southern Alps – from Cox and Barrel, 2007.

On the West Coast the subdued terrain of the Australian plate appears to be older but is mainly overlain by Quaternary moraine and sediment deposits. Central Westland, which is the regional name of the section of fault considered in this thesis, has an outstanding outcrop of the Alpine fault in the vicinity of Gaunt Creek, about 50 km south from Harihari. This 100 m high and 700 m long outcrop has already been studied and its geology described (Cooper and Norris, 1994). The general geological characteristics in the vicinity of the Alpine fault are reasonably consistent (fig. 2, 3 and 4), so we assume the geology in the vicinity of Harihari to show the same pattern as at Gaunt Creek, since the dense vegetation covering the Wanganui-Wilberg rock avalanche source area and deposit makes any geological survey there difficult.

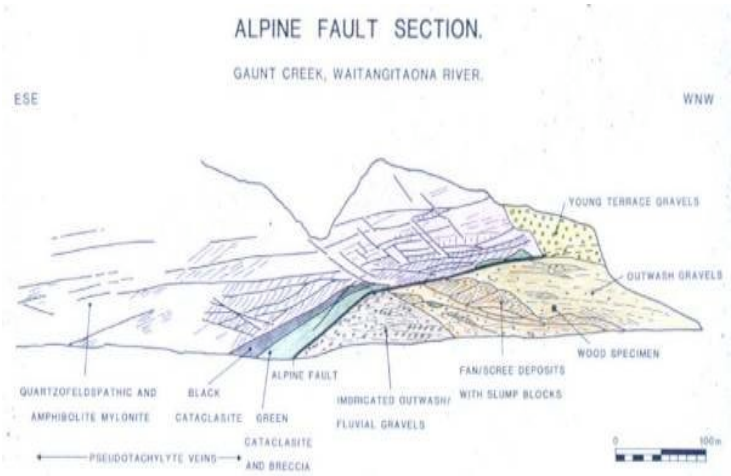

*Figure 4: Gaunt Creek (*http://www.otago.ac.nz/geology/features/aftrip/thrust.htm*, from Cooper and Norris, 1994).*

The sequential structural development of the Alpine fault zone from the last glaciation to the present day is reviewed by Cooper & Norris (1994). Initially, the mylonite and cataclasite layers were overlain by fluvio-glacial gravels. Due to convergence between the Pacific and Australasian plates, these two layers broke through the gravel and reached the surface. This may be the paleo-trace of the Alpine Fault. Convergence continued and a talus fan was generated west of the resulting mountain front. Then on top of this fan, fluvial gravel was deposited covering the trace of the fault at times of low convergence activity. This gravel is composed of the outwash of rocks from all areas west of the Main Divide. From time to time the fault managed to reach the surface again, pushing the fluvial outwash gravel away towards the WNW and carrying the mylonite and lenses of cataclasite with it. The present situation is well represented by the current outcrop visible in Gaunt Creek.

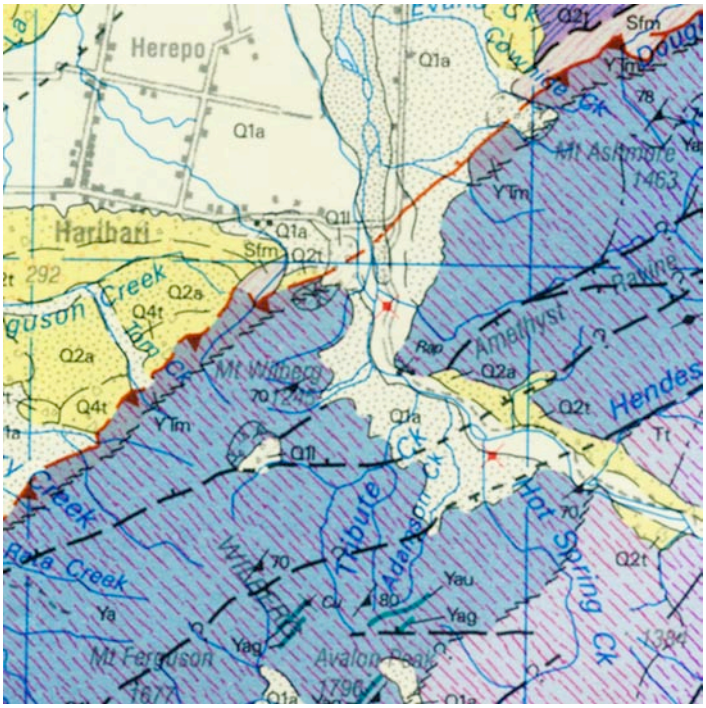

Figure 5: Geological map of the Wanganui-Wilberg site (from Cox and Barrel 2007).

Above the fault the cataclasite exhibits three different appearances. Closest to the fault is the basal cataclasite, which has a pale green matrix. The overlying cataclasite is called the black ultra-cataclasite, which is a dark green to black flinty fracturing cataclasite containing

mylonite. The end of the series is a coherent cataclasite derived from the Haast Schist, which is a major constituent of the Southern Alps formation.

The mylonite is thus found immediately adjacent to the Fault and is typical of the fault zone. It consists of fine-grained metamorphic rock, typically banded, resulting from the grinding or crushing of other rocks, being exhumed from over 20 km depth in this region. Norris and Cooper (2003) reviewed and explained the significance of the mylonite.

Bradshaw (1989) described the basement geology of New Zealand based on terrane classification. He shows that the study area consists of Haast Schist for the Eastern side of the fault and of Buller Terrane for the Western side, made of meta-sediments.

1.3 Tectonics

The Alpine Fault was first described by Morgan in 1908 and its presence confirmed by Wellman & Willett (1942). The Alpine Fault is a transform fault that separates the Australasian plate from the Pacific plate. It joins the east-dipping subduction zone to the south (Puysegur Trench and Macquarie Ridge) with the northern west-dipping zone (Hikurangi Trench and Kermadec ridge). It is considered as one of the greatest transform fault zones on Earth, often compared to the San Andreas system in California, USA.

The inception of the Alpine Fault is commonly dated to the latest Oligocene-early Miocene, which is concurrent with the age of the initiation of the volcanic arc on the North Island, having begun 20-24 Ma ago (Balance, 1970), following the initiation of the subduction by several millions years. Kamp (1986) also confirmed this, suggesting the plate boundary did not transect New Zealand until about 23 Ma ago. Originally thought to be of Cretaceous age, the Alpine Fault is in fact a young active structure.

It is now accepted that the Alpine Fault extends for 850 km, including about 200 km offshore south of Milford Sound. On satellite images the linearity of the Alpine Fault is striking along most of the South Island. Only in the region from Nelson to Marlborough does the fault split into segments: from north to south the Waimea, Wairau, Awatere and Hope Faults. The onshore Alpine Fault has been divided into 4 sections: the Wairau section from the northern coast of South Island to Lake Rotoroa, the North Westland section from Lake Rotoroa to Inchbonnie, the Central Westland section from Inchbonnie to Haast and the South Westland section from Haast to Milford Sound. This division, after Berryman *et al.* (1992), does not take into account the extension of the Alpine Fault into Cook Strait, nor that beyond the Fiordland section farther south.

Figure 6: Aerial image of the Alpine Fault, South Island, New Zealand (Simon Nathan. 'Geological exploration', Te Ara - the Encyclopedia of New Zealand, updated 21-Sep-2007, URL: http://www.TeAra.govt.nz/EarthSeaAndSky/Geology/GeologicalExploration/en

The rock avalanche studied in this paper occurred in the southern part of Central Westland.

Although the southern part of the South Island is almost purely dextral strike-slip, Central Westland experiences a slightly dipping component, which creates shortening. Based on the NUVEL 1A model, the strike-slip component is 37 mm/yr at an azimuth of 071° and the dip-slip component is 10 mm/yr normal to the strike-slip direction (shortening) (De Mets *et al.* 1994, Yetton 2000). Another survey based on GPS calculations gave a strike-slip component of 44 mm/yr at an azimuth of 077° and a dip-slip component of 15 mm/yr for the Pacific plate (Larson *et al.* 1997). The differences between the plate vector orientation and the slip direction of the fault are due to plate-motion accommodated elsewhere.

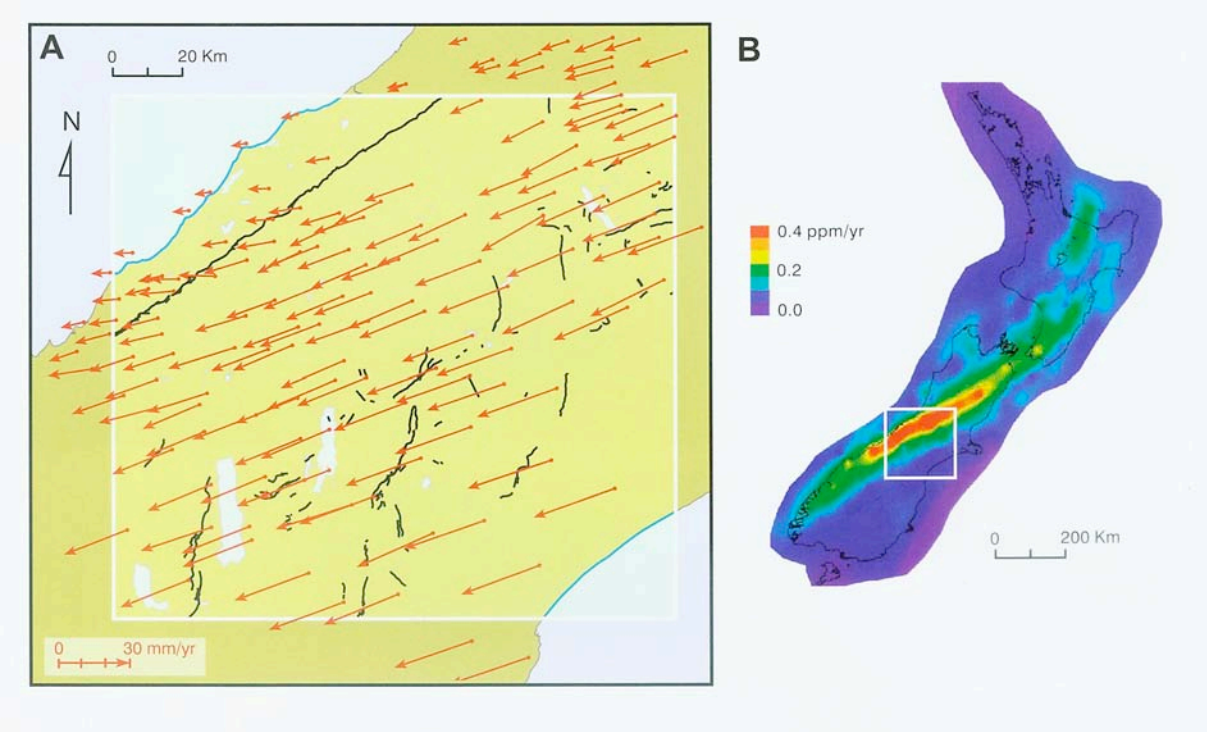

Figure 7: Plate movement map: A. motion vectors and B. strain rates – from Cox and Barrel, 2007.

This accommodation is partly owing to the development of the Alpine Fault between Nelson and Marlborough, and also to the structure of the fault itself. Although the fault trace appears perfectly linear on satellite images, field mapping at smaller scale shows another story. Near the surface, the Alpine Fault trace exhibits two main directions, almost N-S and E-W

(azimuth 015° and azimuth 080°, respectively). This shape of fault trace is commonly known as *en échelon*, also serial-partitioning, highlighted near Franz Josef.

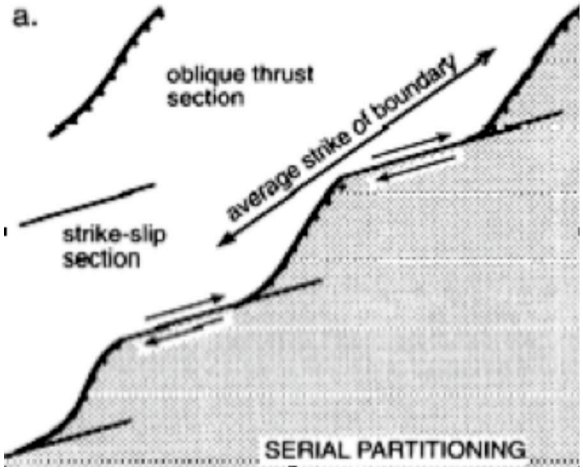

Figure 8: Plan view showing serial partitioning (from Norris and Cooper, 1997)

The Alpine Fault accounts for between 50 and 80% (60% is often mentioned) of the total accommodation of the plate vector (Yetton, 1999).

1.4 Seismicity

The M ~ 8 1717 AD event (Yetton, 1999) is the last major earthquake that the West Coast experienced, and five major events have been inferred in the last millennium or so, including the 930 AD event, main trigger for the Round-Top rock avalanche (Wright, 1998; Dufresne, in prep). This magnitude of earthquake is likely to produce an offset ranging between 6 m and 9 m. The 1717 AD event created a reported offset of around 8.5 m and uplift of about 3 m (Yetton, 1999), revealed by rivers and moraines straddling the fault trace giving information about displacement and uplift.

According to Yetton (2000), the recurrence time of an event producing an 8 m offset is ~ 300 years. A 240 years recurrence time will produce 6 m offset. These values were calculated

assuming a conservative horizontal plate motion component of 25 mm/yr. If the fault slip had been underestimated, then these recurrence intervals are likely to decrease.

There are many ways of determining the probability of an earthquake (e.g. the Poisson method; Savage (1994), Nishenko & Buland (1987)) that are not discussed here. Nevertheless, using the Savage theory, the probability of the next Alpine fault earthquake occurring within 50 years ranges between 16% and 51% and within 100 years between 49% and 85%. Perhaps more realistic is the Nishenko & Buland theory, which gives a 50 years probability of 67% (between 54 and 81) and a 100 years probability of 88% (between 80 and 95; Yetton, 1998)

The magnitude of an earthquake is commonly expressed by the media using the Richter scale (1930s), also known as the local magnitude (M_L). However, because measurements are based on a measurement of one aspect of the seismogram, they do not always capture the overall power of the surface: surface-wave magnitude saturates above $M_L = 8$. We also distinguish the surface magnitude (based on Richter scale), M_S, and the moment magnitude, **M** or M_W. The latter (Kanamori, 1977) is based on seismic moment deriving from the concept of moment in physics. Still calculated from seismograms, values of moments for observed earthquakes are not influenced by variables such as local circumstances. Accordingly the results obtained make it easy to objectively compare the sizes of different earthquakes. The moment magnitude is considered to be the most reliable way to describe earthquake shaking and is adopted in this paper, and many others.

Rock avalanches are generally triggered by earthquakes of **M** > 6.5 although this figure varies depending on the nature of the terrain (Shahrivar & Nadim, undated).

Although earthquakes are NOT predictable, the above probabilities indicate it is reasonable to assume that the next earthquake on the Alpine fault will occur in the coming century and the

offset produced will exceed 7 m; Yetton (1999) suggested it would be prudent to consider an **M**8 event.

The consequence of such an earthquake will be serious physical and economical isolation of the West Coast. Infrastructure will be extensively and intensively damaged. Although the West Coast will experience the most severe ground shaking, being closer to the epicentre, the effects on the east of the main divide will also be significant. It is not overestimating the forthcoming situation to say that New Zealand as a whole will pay a huge price for this inevitable event (McCahon *et al.* 2007).

Chapter 2: The Deposit

2.1 Introduction

Harihari is a small town on State Highway 6 halfway between Hokitika and Franz Josef. It lies at the foot of the Southern Alps between the Wanganui River on its east and the Poerua River on the west. The Tasman Sea is 20 kilometres north-west from the main settlement. Four mountains border this locality: Mts Bonar, Ashmore, Wilberg and Hercules. Lake Ianthe is a large kettle-hole lake trapped behind the last glacial maximum (LGM) moraines that make up most of the high ground west of the Alpine fault.

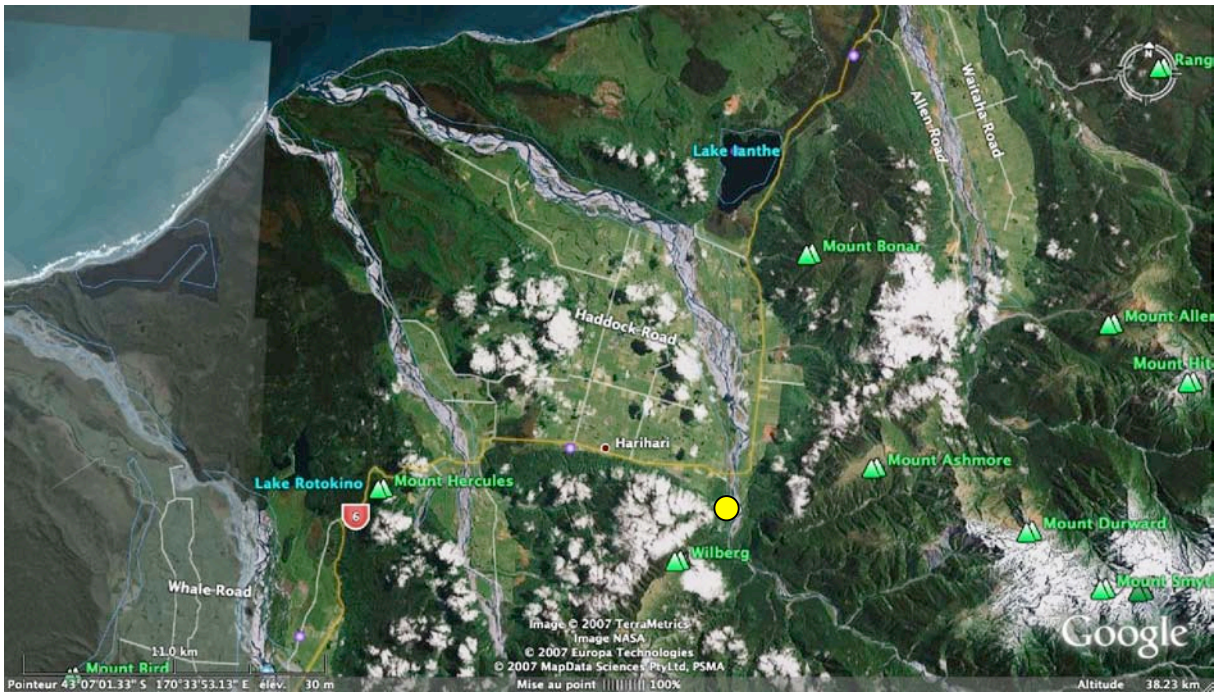

Figure 1: The Harihari area - picture from Google Earth. The yellow dot locates the Wanganui-Wilberg rock avalanche.

The Wanganui River, between Mount Wilberg and Mount Ashmore, has over time deposited a fluvial fan created from outwash from glaciers and subaerial erosion in the steep catchment. Sea level is known to not have changed during the last 6000 years (Dr Naish, www.gns.cri.nz/news/release/sedi.html). This thesis focuses on the Wanganui-Wilberg rock

avalanche. Also referred to as the Wanganui River rock avalanche, this event left a clear source scarp on Mount Wilberg. However, only a small part of the deposit of this landslide remains nowadays. River erosion is slowly removing its deposit.

Here we focus on the extent of the deposit. Aerial pictures and field inspection allowed a surface study, whereas a dug trench and ground-penetrating radar (GPR) allowed the subsurface deposit to be studied.

2.2 Aerial photographs

The vertical aerial photographs used during this thesis were obtained from New Zealand Aerial Mapping Limited (www.nzam.com). The first stereo pair of pictures was taken in 1948 in black and white at a scale of 1:16000. The second pair was taken in 1984 in colour at a scale of 1:17000. The closeness of the scales permits a direct comparison of the two.

Although the vegetation cover should be ignored, it can help to distinguish different parts of the landscape. On the true left side of the river we can distinguish (based on the vegetation) a large fluvial plain, a delta fan, the bedrock and the riverbed.

A stereoscopic pair emphasised apparent height surfaces differences. As a result we can distinguish the presence of ridges and incision of gullies. The surfaces separated by a terrace riser can either be of fluvial or glacial origin. At this stage it still is hard to be more precise, but in general the higher surfaces are glacial deposits and lower surfaces fluvial deposits.

The rectangular-shaped landslide deposit is clearly seen on both pictures.

Figure 2: Vertical aerial photo of the Wanganui-Wilberg rock avalanche, 1948, NZAM.

The landslide deposit lies adjacent to bedrock, a delta fan, and a fluvial plain, likely to have evolved into a flood plain considering the ripple marks visible on the ground, as well as the riverbed and some terraces of either fluvial or glacial origin.

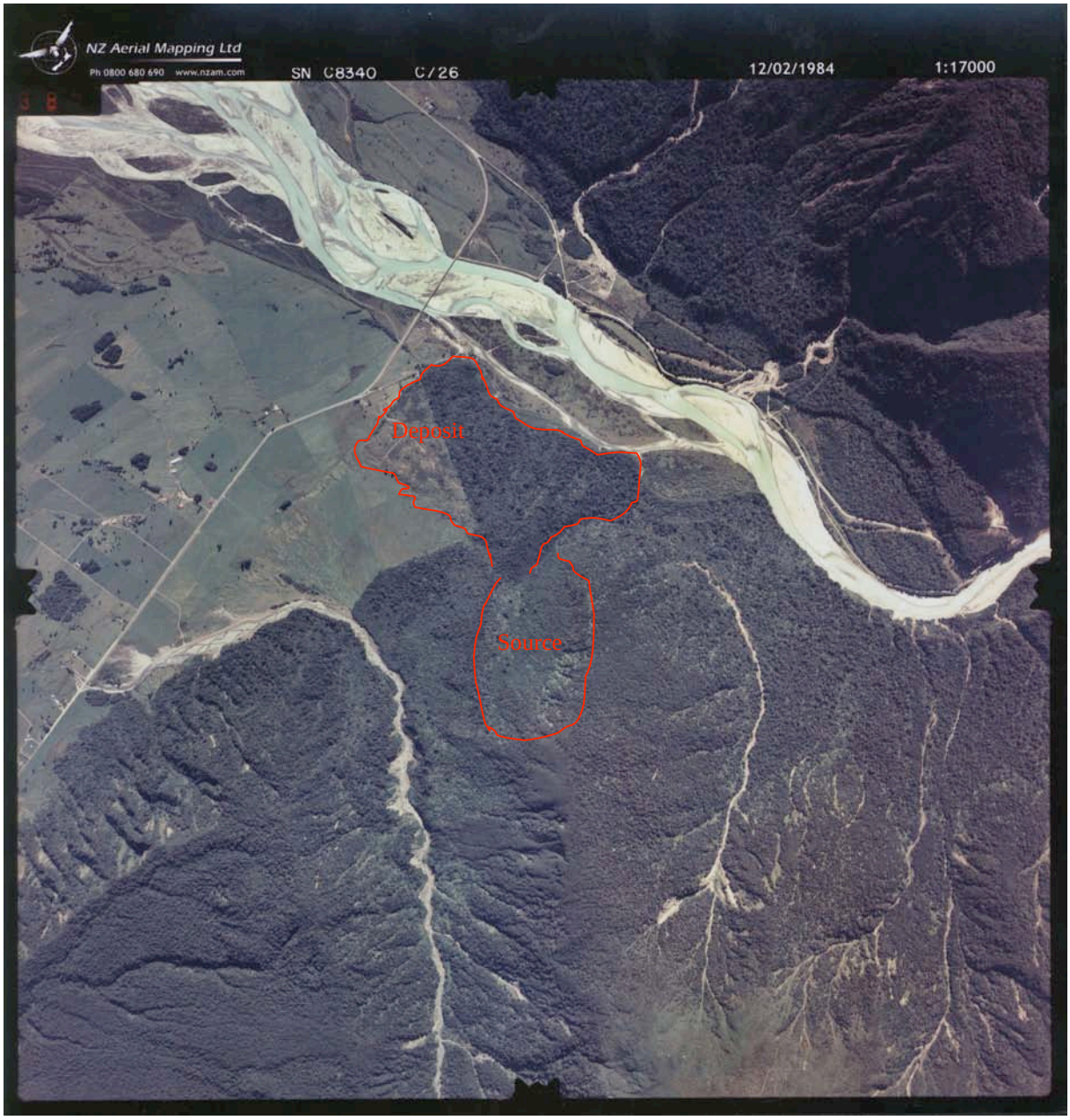

Figure 3: Vertical aerial photo of the Wanganui-Wilberg rock avalanche, 1984, NZAM.

The study of those two pictures also gives information about the development and behaviour of the river over a period of forty-six years. In 1948, the riverbed opposite the remaining landslide deposit was wider than it was in 1984. The Wanganui River was and still is incising into its bed, creating new fluvial terraces on each bank. It shows the phenomenon of degradation.

2.3 Geomorphology

Here the different constituents of the landscape are described. Field works and aerial photos reveal the presence of seven geomorphic units. Each of them gives information about the history of the Wanganui-Wilberg rock avalanche.

2.3.1 Unit 1: Bedrock

Although rarely visible in this area the bedrock can be inferred from the previous research carried out in the Southern Alps (Korup, 2004; Cooper & Norris, 1994) and from the presence of a quarry 4 km upstream of the Wanganui River on its true right bank. Gaunt Creek also gives information about the nature of the bedrock in the Alpine Fault vicinity (fig. 5).

Figure 4: bedrock outcrop, in the quarry, Wanganui River true right bank. Person for scale.

Dipping 70° toward the east, the bedrock consists of a metamorphic series of schists. Gaunt Creek is one of the most impressive outcrops showing the rock close to the Alpine Fault. Situated south of Whataroa this tributary of the Waitangitaona River gives an extraordinary vision of the complex series of events that has, and continues to, give birth to the Southern Alps western foot.

2.3.2 Unit 2: Glacial deposits

Between the riverbed and the bedrock often lie glacial deposits, also called moraines. In this area moraines of the last glaciation (LGM ~ 20,000 BP) are significantly higher than the present river level and are present on both banks.

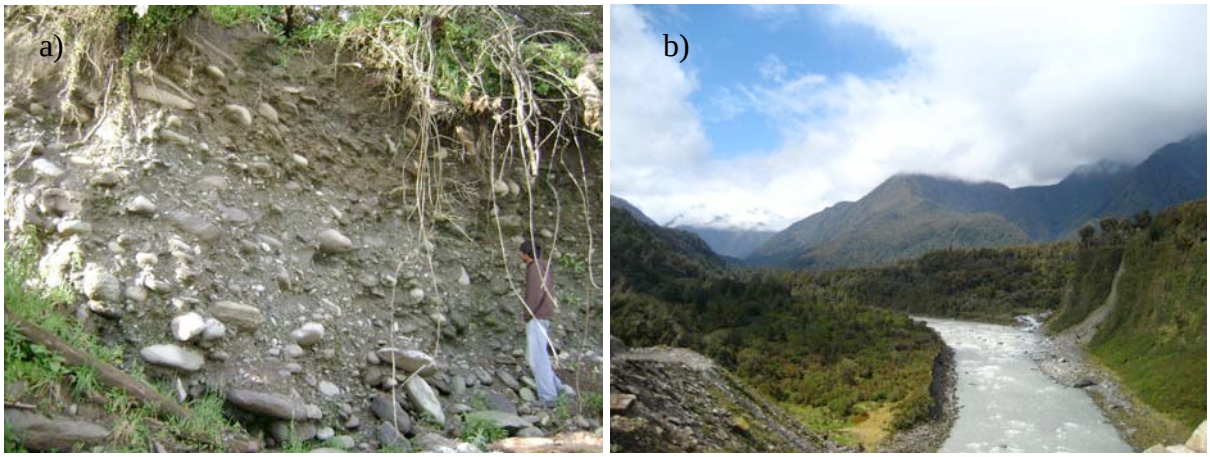

Figure 5: a) Glacial deposit outcrop by the riverbed, b) View from the quarry toward Wanganui River upstream.

A moraine consists of rounded rocks of all sizes. These rocks are carried by glaciers during their advance and deposited when they retreat. In this area moraines usually show distinct fluvial bedding, indicating the prominent role of water in their deposition.

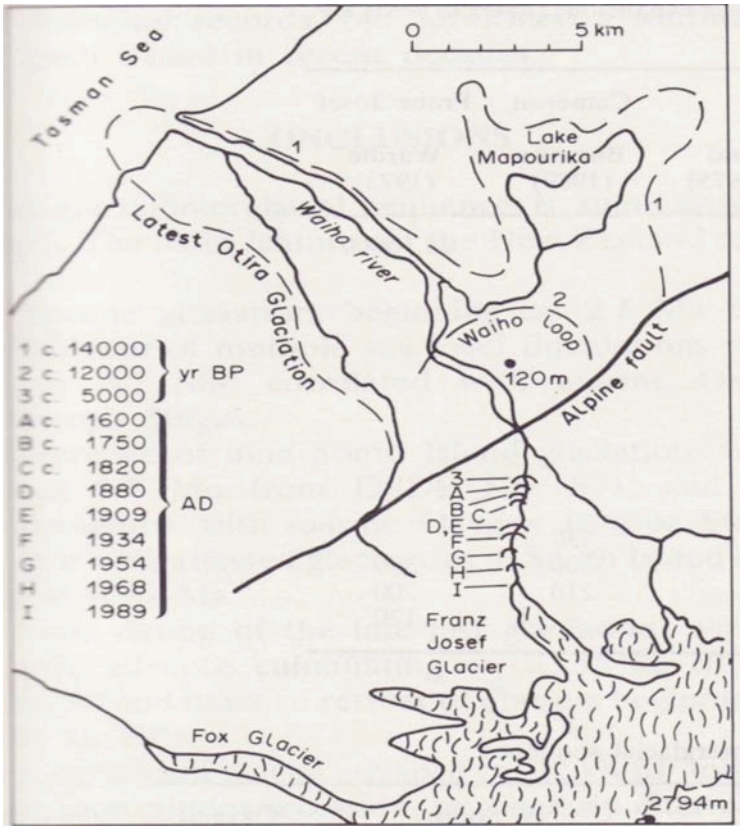

Figure 6: Latest Otiran and Aranuian advances of the Franz Josef Glacier after Warren (1967), Wardle (1973) and Sara (1979), from Suggate (1990).

Assuming that these moraines are related to the late Otira glaciation (the last) and not one of the post-Otiran fluctuations (Aranuian advances) described by Suggate (1990), and correlating the known dates available for Franz Josef Glacier (Warren 1967, Wardle 1973 and Sara 1979) with its relative closeness to the Wanganui River, the age of these moraines could be *c.* 14000 or *c.* 12000 BP (fig. 15).

2.3.3 Unit 3: Riverbed and fluvial terraces

These are usually the lowest points of the landscape in any section. Water only occupies a portion of its area. The rest of it is formed by fluvial terraces. Riverbed rocks compose the surface of this unit, and are sourced from erosion of the bedrock and the glacial deposits upstream of the Wanganui River or any other of its tributaries.

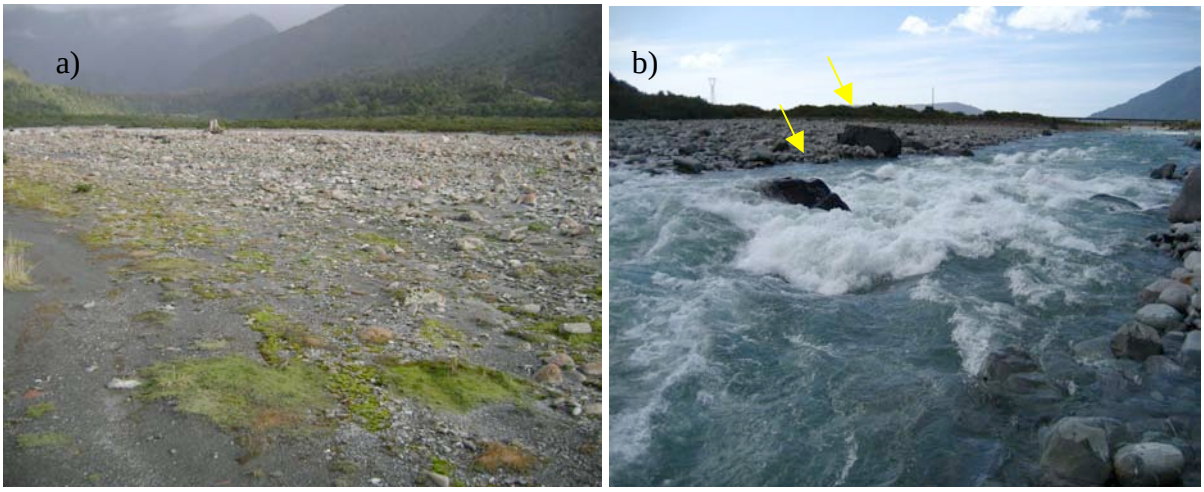

Figure 7: a) Temporarily inactive riverbed, b) Active riverbed (yellow arrows point to big ultracataclasite boulders)

Also to be mentioned is a lag of very large ultracataclasite boulders lying in the riverbed (cf. map) exhibiting a darker colour than other rocks. The fact that they are all aligned with the landslide source suggests that they may be part of the rock avalanche deposit. Moreover they could have originated from near the Alpine Fault as some similar boulders have also been recognized in Harald Creek.

2.3.4 Unit 4: Floodplain

Nowadays, the Wanganui River mainly flows on the true right side of its floodplain. On aerial photos the floodplain can be identified by traces of braided river channels and bars not obliterated by subsequent soil development; this indicates that the river has, in the past, flowed everywhere across the flat ground west of the mountains, at least as far west as Hari Hari.

Figure 8: View of the floodplain from the slopes of Mt Wilberg.

This low-lying surface is mostly used for farming activities. To prevent the area from flooding (like for instance in 1910 – last flooding event?) a stop-bank has been built on the true left bank. This is not the only stop-bank in the area. Two gullies, including Harald Creek, have had their flows re-directed by stop-banks. The one on the true right bank of Harald Creek was probably intended to protect State Highway 6 and is today almost concealed by vegetation.

2.3.5 Unit 5: Landslide deposit

The remaining landslide deposit is limited in extent by past erosion on the true left bank of the Wanganui River. Its vegetation is denser than on any other surface except the glacial terraces but does not completely conceal the typically large, protruding angular rocks. Rocks, mainly mylonite and other schists related to the proximity to the Alpine Fault, are angular and of a

wide range of different sizes up to several metres in diameter. Recent construction of a house on part of the deposit has required clearance of the surface rocks, which are now stockpiled (Fig. 18c).

Figure 9: a) Surface of the landslide deposit, b) outcrop of the landslide deposit dug by Mr Sullivan and c) surface rocks stockpiled.

The surface of the deposit is far from being flat. When a rock avalanche deposits, a hummocky landscape is often created ("Hummocky relief typical of rock avalanches “, Strom 2006) (see fig. 19 of the Round Top (New Zealand) rock avalanche deposit about 90 km north of the Wanganui-Wilberg rock avalanche).

Figure 10: Round Top rock avalanche deposit, showing a hummocky landscape (Photo by A. Dufresne).

The Wanganui-Wilberg rock avalanche, although thought to be younger than the Round Top event, has a smaller deposit extent due partly to the active river erosion and its emplacement with respect to the other geomorphological surfaces. Its hummocky character is mainly concealed by vegetation. The remaining deposit is close to the source and is thought to represent only a small portion of the original deposit.

Two details of this deposit are worth mentioning. The first one is two small lobes clearly coming from the deposit and overlapping the delta fan created by Harald Creek. They appear to be secondary sliding events (maybe simultaneously triggered), resulting from a destabilization of the deposit on its west edge. The other detail is the presence of a big boulder, “Trevor” (more comments in the chapter 4), which is in situ but not its original place at the base of the river-cut face of the deposit. The location of the boulder with respect to its former resting-place indicates the occurrence of severe earthquake shaking since the deposit was cut by the river to about its present extent.

2.3.6 Unit 6: Fluvially reworked landslide deposit

Only visible on the true left bank is a surface related to both the riverbed and the landslide deposit. As soon as the landslide reached the riverbed, water started to erode it. Enough time passed to severely reduce the extent of the deposit on the true right bank of the Wanganui River. On the true left bank erosion is still acting on the landslide deposit. Located between the riverbed and the landslide deposit, this surface shows rounded fluvial gravels and pebbles associated with bigger rocks from the landslide.

Figure 11: a) Typical association of large angular and small rounded rocks and b) surface of the fluvially reworked landslide deposit at the base of the present steep riverside face.

This surface, though strongly disturbed by water action, still exhibits the usual hummocks the deposit forms. Another feature that can be observed in this location is the flight of terraces, marking previous water levels; from where the fluvially reworked landslide deposit originated.

2.3.7 Unit 7: Debris flow fans

In the vicinity of the landslide deposit are three major debris flow fans including that of Harald Creek (see geomorphological map). They are the direct consequence of large inputs of

sediment brought by the erosion of bedrock from stream banks and beds. Debris flows can deposit huge quantities of sediments in short periods of time. Such events convey enough energy that trees and normally immovable rocks are transported.

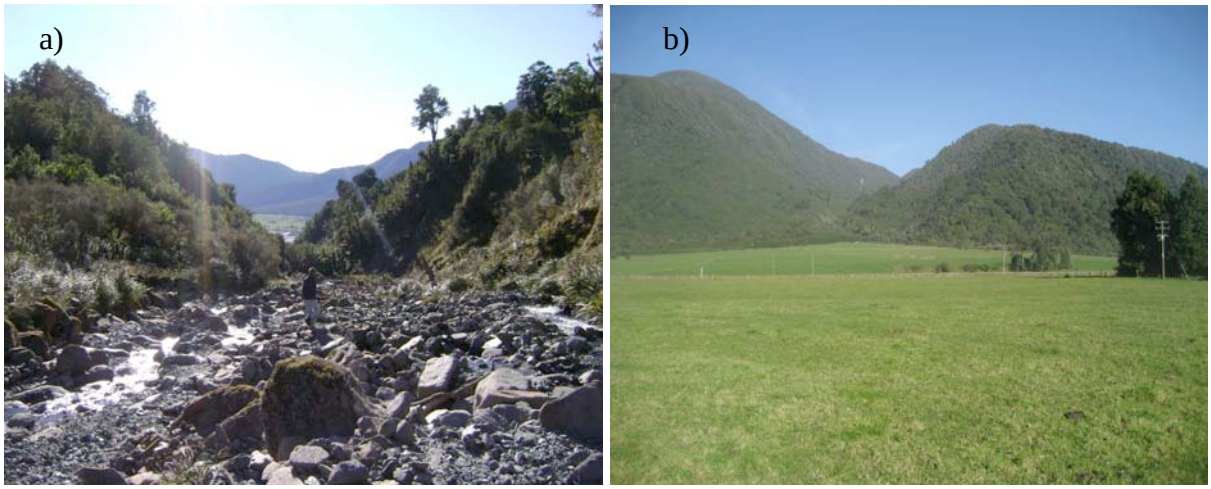

Figure 12: Debris flow channel; person for scale. a) Harald Creek (figure for scale) and b) the fan created at its exit.

2.4 Geomorphological map

The geomorphological map below, a result of combined field work and aerial photograph study, summarizes the surfaces discussed above.


a)
Geomorphological map
500 m
N

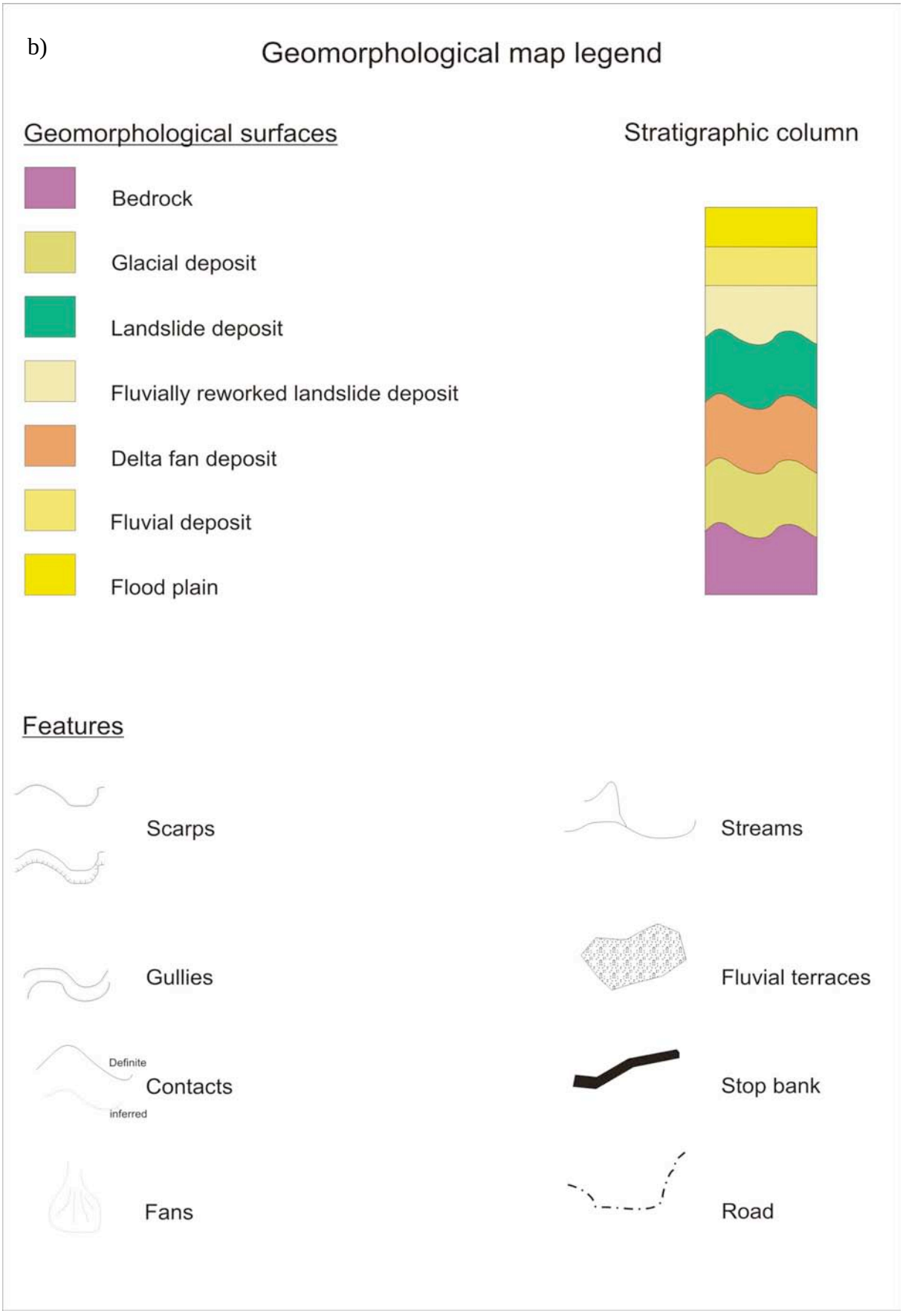

Figure 13: a) Geomorphological map and b) associated legend.

Interpretation: The riverbed, which is composed of a main active channel and of erosional terraces, is on its southern extent incised between glacial moraine surfaces that were once contiguous. These moraines lie on bedrock incised by gullies and streams of many sizes. Only the active 1984 water courses are shown on this map and one must keep in mind that their locations have been altered since 1984. More or less small soil slides are also shown (in Harald Creek and along the State Highway 6 on the western corner of the rock avalanche deposit). The source of the Wanganui-Wilberg rock avalanche makes up the centre of the map. Material derived from Harald Creek has created a large fan showing evidence of debris flow events. Nowadays Harald Creek's stream is controlled by a stop bank, as is the Wanganui River itself on its true left bank seen in the northern part of the map. Following a north-south trend is the contact of the Harald Creek fan with the landslide deposit. On the north side of State Highway 6 is the former active flood plain of the Wanganui River. It is bordered by the fan, the landslide deposit and obviously the riverbed. Focusing now on the landslide deposit, we saw that the immediate surfaces it lies against are the flood plain and the fan. The riverbed, the bedrock and the moraines are also bounded by it. In spite of thorough searching, no signs of landslide deposit have been found on the true right bank of the Wanganui River. On this same bank roughly between State Highway 6 and the riverbed is a complex network of small terraces likely to be the remnants of former riverbeds. A younger, similar terrace is visible on the 1984 picture (light green) with a noticeable "lens" shape (fig. 23, a)). This terrace was clearly part of the 1948 riverbed as seen in the aerial photograph. Another example (fig. 23, b) and c)) of this development is the active stream present in 1984 cutting the fluvially reworked landslide deposit, which is today colonized by vegetation.

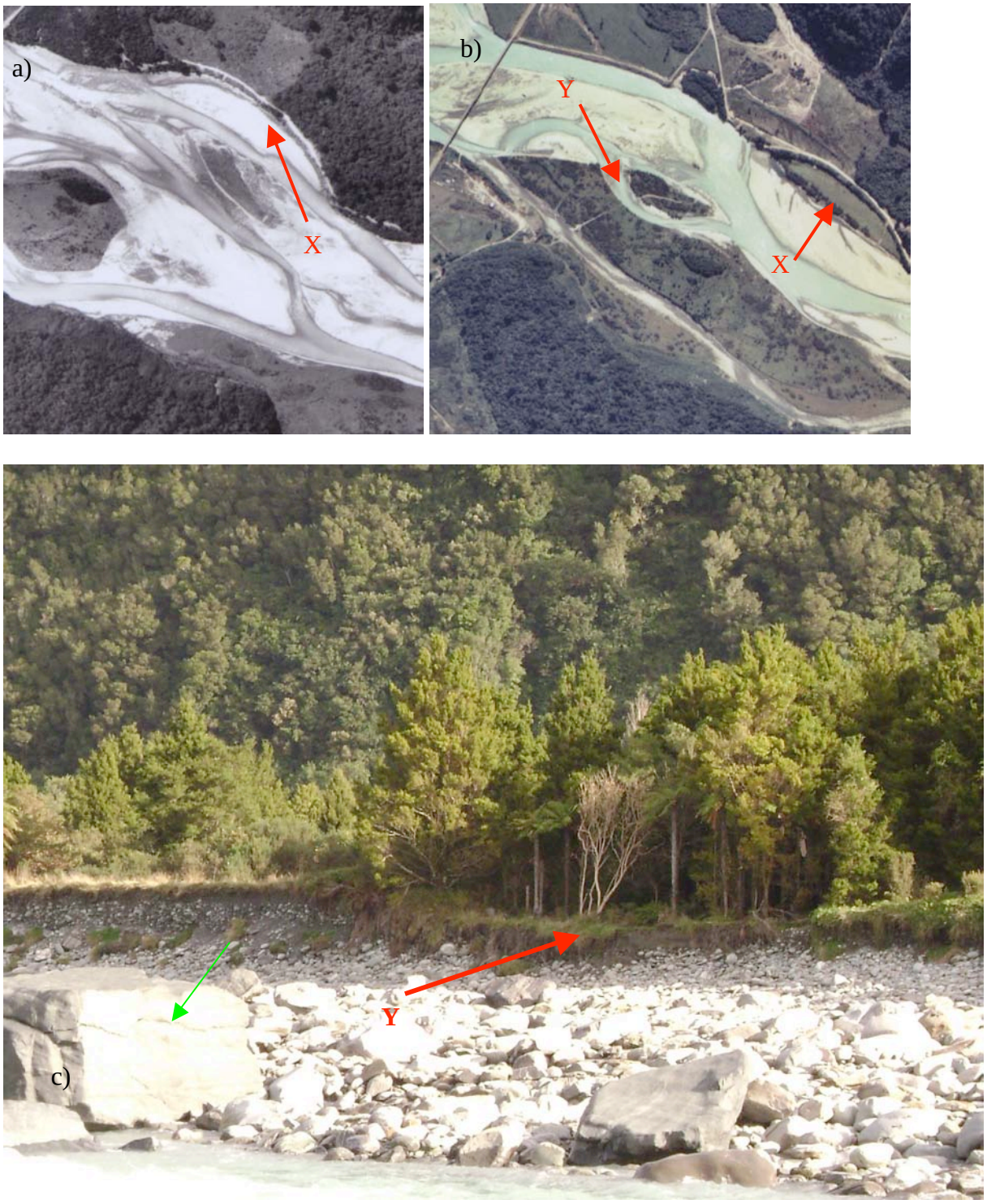

Figure 14: a) Detail from the 1948 and b) 1984 aerial picture just upstream from the bridge, with c) a recent picture taken on the field. "X" points to the "lens" terrace and "Y" a very recent terrace, the green arrow points to one of the big cataclasite boulders.

The current level of the Wanganui River is very low; the river has incised significantly into its bed since the 1984 aerial photos. This explains why a series of large boulders is only visible there, and not on either of the banks.

Figure 24: Some of the boulders making up the lag. Person for scale.

2.5 Trench

The study of the deposit cannot only be carried out by reporting what is visible at the ground surface. We also have to study the subsurface deposits. The first way to investigate the ground is to dig a trench.

The trenching place was carefully chosen to find the contact between the landslide deposit and the underlying surface(s). The surficial contact between the river-eroded landslide deposit and the flood plain was chosen, because the base of the landslide deposit was thought to be close to this surface.

Figure 25: Digging of the trench in progress.

The hole dug was more than 5 m deep, 3 m wide and about 5 m long. The local water table was encountered at about 5 m from the surface. Unfortunately the underlying presumed fluvial surface was not reached. Nevertheless, the hole provided an interesting profile perpendicular to the landslide travel direction.

Figure 26: Profile of the trench, view toward the west.

This picture montage shows the profile of the trench.

The upper third shows a recent landslide deposit (the big rock) next to fluvial deposit, which seems to have been pushed (accumulation of fluvial material behind the big rock).

As the depth increases the landslide deposit material becomes more dominant and the fluvial deposit tends to disappear. Angular rocks of various sizes are imbricated in a matrix of crushed small fragments.

The base of the hole still shows landslide material but rounded pebbles likely to be related to the moraine underlying the landslide deposit or to underlying fluvial strata are not uncommon. No paleosols have been found under the landslide deposit. The lowest third of the deposit shows a higher proportion of matrix.

Figure 27: Profile (fig. 26) in detail, the yellow arrows shows a sharp contact between the fluvial and landslide. The profile is c. 5 m high.

This hole shows that the surface of the rock avalanche has been eroded and fluvial material was deposited on the eroded surface. A subsequent small rockfall brought material from the landslide deposit over the fluvial deposit and pushed the fluvial material away from the landslide. This event could have been either triggered by an earthquake or by fluvial undercutting of the already eroded landslide.

The depth of the hole being 5 m one can assume that the base of the landslide deposit is more than 5 m from the current surface, resulting in an estimated deposit thickness of 10 m at this location.

2.6 Ground-penetrating radar

Ground-penetrating radar, or GPR, is a geophysical tool that enables the user to evaluate the subsurface geometry of depositional units (Jol and Smith, 1991; Leclerc and Hickin, 1997). The principle is similar to reflection seismic and sonar techniques (Davis and Annan, 1989): a beam in the form of an electrical impulse is transmitted, reflected and received. The basic principles are reviewed by Morey (1974), Annan and Davis (1976), Ulriksen, 1982), Benson *et al.* (1984), Davis *et al.* (1984) and Davis *et al.* (1985). In brief summary, a pulse of radio frequency energy is transmitted into the ground and the echoes returned and recorded as a function of the two-way travel time (TWT). Successive records or traces are plotted side-by-side to yield a profile, a cross-sectional view of the variation in the subsurface radar properties.

The GPR device consists of a transmitter, a receiver, a console, a 12 V battery pack, a computer and an electric remote trigger. All the components are connected to the console:

- the transmitter by a single fibre optic cable,
- the receiver by a dual fibre optic cable,

- the battery pack by a power cable,
- the computer by a serial RS232 cable, and
- the electric remote trigger.

Figure 28: pulseEKKO 100 GPR apparatus.

The applications of GPR are numerous (Davis and Annan, 1989): it can be used for mineral and groundwater exploration, geotechnical and archaeological investigations, as well as rock mechanics.

The arrival times of various reflections indicate the depths of reflecting layers showing different physical property contrasts (Nobes *et al.*, 2001). The propagation of the radar signal depends on the high frequency electrical properties of the ground (Davis and Annan, 1989). Topp *et al.* (1980) document the fact that "*electrical properties of geological materials are*

primarily controlled by water content". Nobes *et al.* (2001) mentioned three key subsurface variables able to influence the signal influenced: water quality, water quantity and clay content.

Davis and Annan (1989) and Nobes *et al.* (2001) both express concerns about possible electrical interferences caused by unwanted objects such as overhead cables, fences, buildings and/or cars.

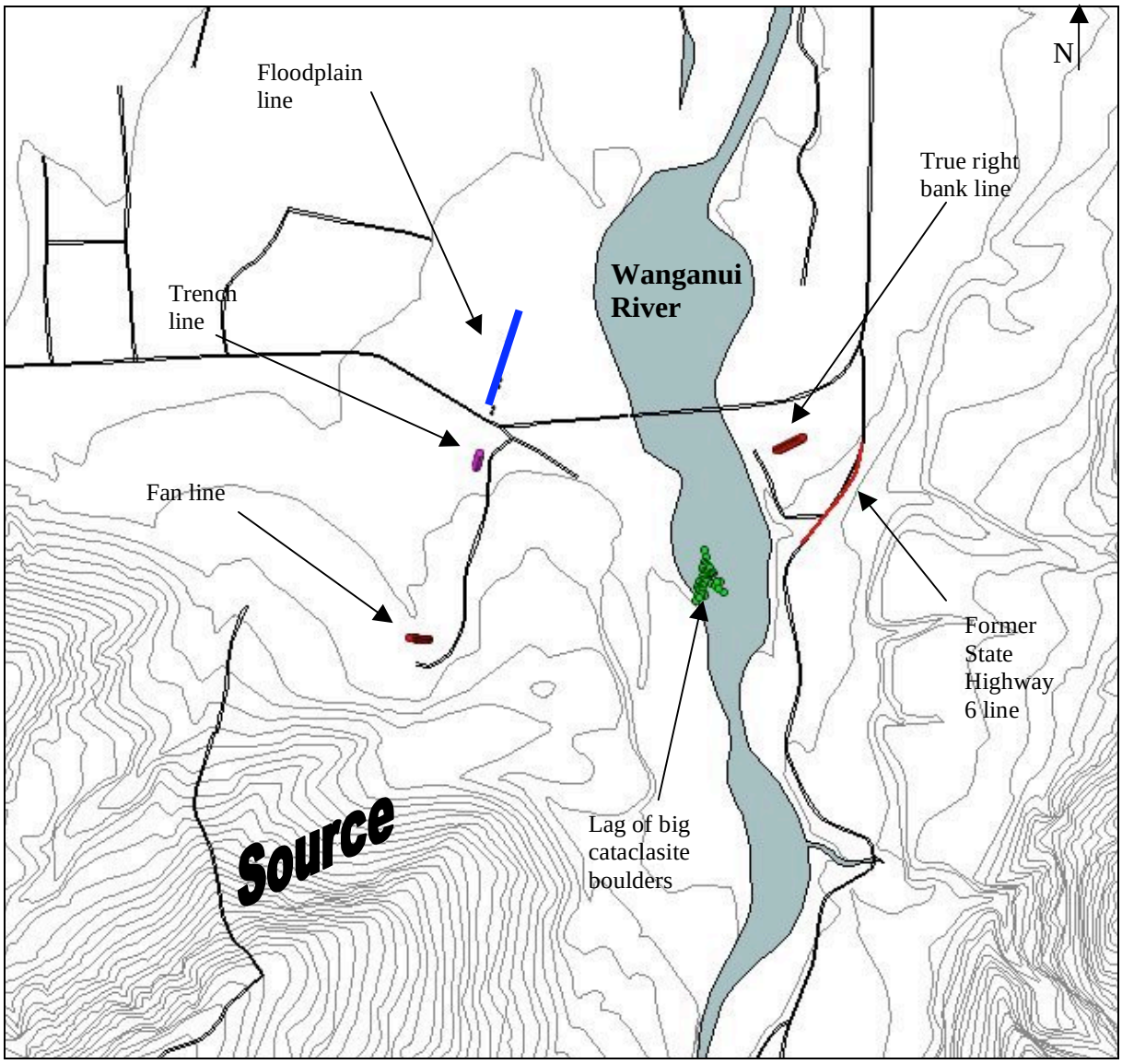

Figure 29: Map of the GPR lines done, also showing the lag of big cataclasite boulders.

The radar technique is most effective when the antennas are placed on or near the ground that is to be probed (Davis and Annan, 1989).

The equipment used (fig. 28.) allows surveying up to 20 metres underground, which in the case of the Wanganui-Wilberg rock avalanche was thought to be deep enough to reach the base of the deposit. Depths of up to 40 metres can be reached in environments with low electrical conductivities (Davis and Annan, 1989). However 10 metre and 5 metre depths were preferred in the present work for a better resolution of the signal. In parallel with the GPR survey a global positioning system (or GPS) survey was carried out. For the Wanganui-Wilberg rock avalanche study all the desired lines have been GPR and GPS surveyed. Five lines were chosen and plotted (fig. 29); the purpose of this survey is to find the likely extent of the landslide deposit.

- The first line was intended to explore the contact between the landslide deposit and the Harald Creek fan;
- The second line was designed to extrapolate what was seen in the trench;
- The third line was intended to probe the fluvial plain;
- The fourth line was obtained on a true right bank recent fluvial terrace on the extrapolated axis of the Wanganui-Wilberg rock avalanche;
- The fifth line was acquired on the former State Highway 6, nowadays the road leading to the Wanganui track, or the quarry, to assess the buried extent of a lag of big boulders visible into the riverbed.

The results are presented below.

The prominent “pyramid”-shaped features are diffractions (Nobes *et al.*, 2001).

"*The depth to the reflectors is determined from the signal propagation velocity in the ground which must be obtained from independent velocity soundings or, if the reflectors can be correlated with geological logs, from the associated depths and times*" (Davis and Annan, 1989). One independent velocity sounding is a common mid-point (CMP) survey, as discussed in Nobes *et al.* (2001). However as the speed of the signal could not be determined in the field, different speeds were tested and 0.1 m/ns seemed to work best at collapsing the diffractions in general. It is more than probable that different velocities worked best at the different sites and along different segments of each profile. The appendix shows each line with a different speed of penetration (p. 85). The time travel being a two-way time travel, 200 ns at a velocity of 0.1 m/ns gives a depth of 10 metres.

2.6.1 Line 1: "Fan"

This 65 m long profile extended over the contact of the Wanganui-Wilberg rock avalanche with the Harald Creek fan.

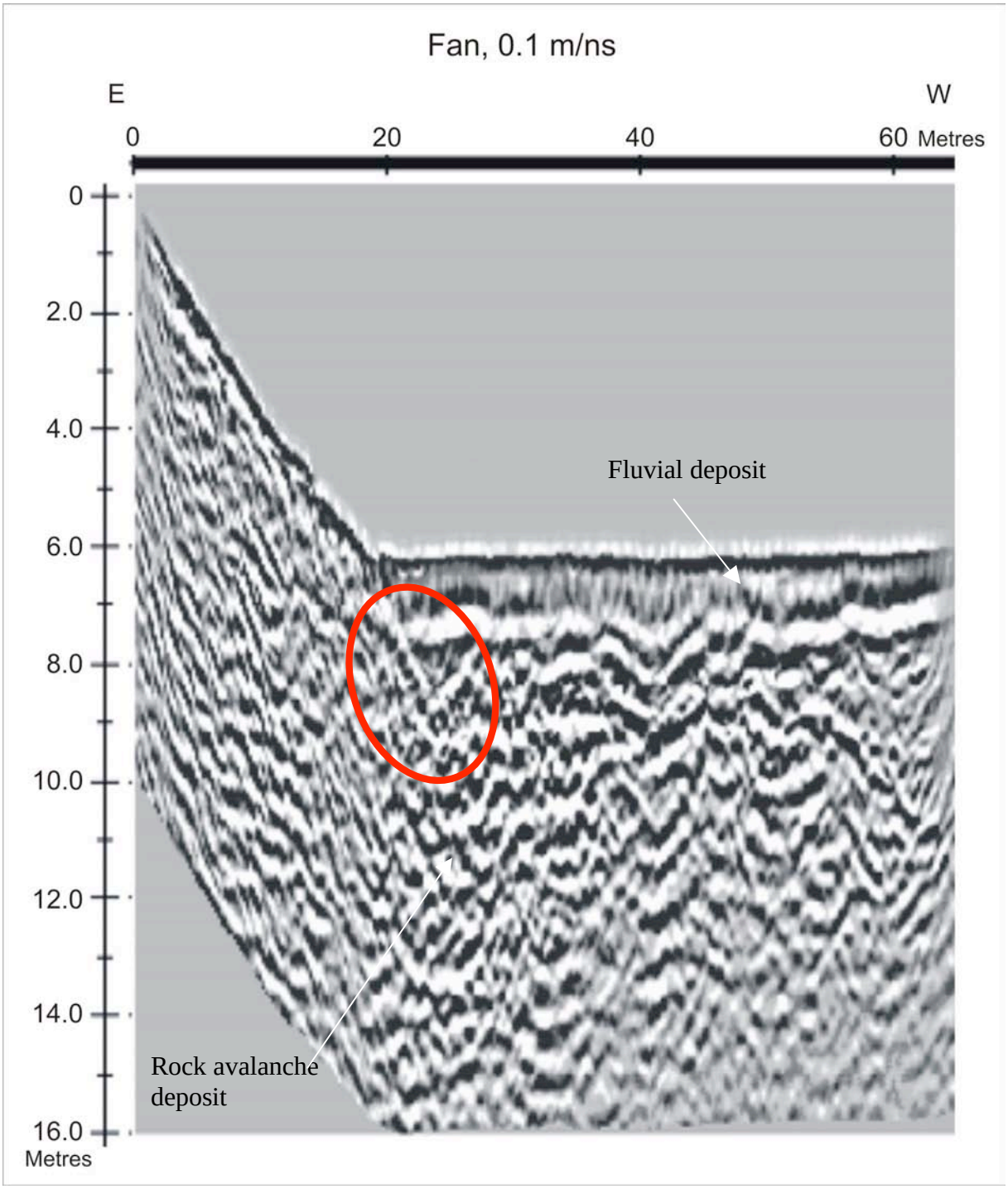

Figure 30: "Fan" profile, red oval showing onlap.

We know from the field the surficial first 20 m are rock avalanche deposit. From 20 to 65 m the continuous reflectors belong to the Harald Creek fan. At 20 m, and about 1.5 m from the surface, onlaps (red circle, fig. 30) are seen. The deposition layers of the fan are nicely continuous whereas the rock avalanche deposits exhibit rather chaotic reflector assemblages.

These reflectors are hardly able to be followed on the profile even if the signal is strong, and show a relatively high degree of scattering of the signal, probably due to the presence of rocks (coarse material) (cf. appendix). So this profile tells that the fan deposit formed over the rock avalanche and that the rock avalanche deposit extends underneath the Harald Creek fan deposit.

2.6.2 Line 2: “Hole”

This 50 m long GPR profile aimed at looking at the contact between the Wanganui-Wilberg rock avalanche deposit and the flood plain. It followed the dug trench (the profile starts a few metres away from it) to allow correlation between the trench and the GPR profile. The trench was a little more than 5 m deep and the signal was chosen to reach this depth. Moreover it permitted a greater resolution of the profile and hence a better trench/profile correlation.

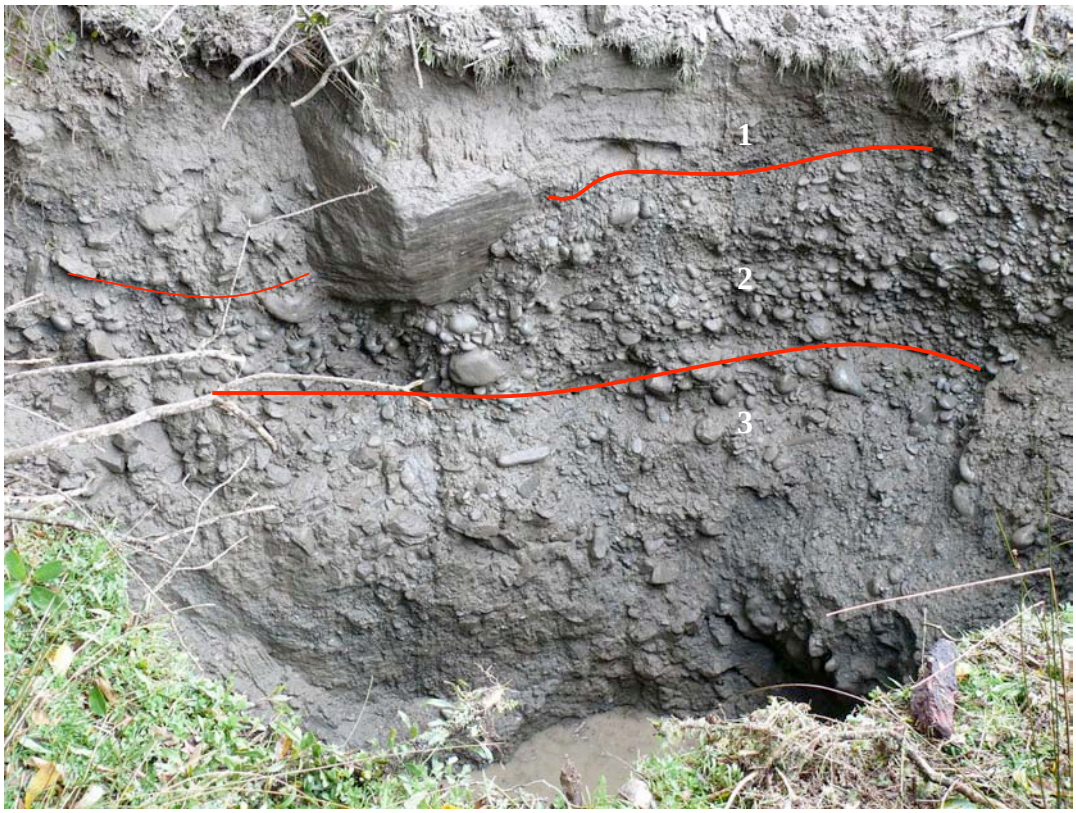

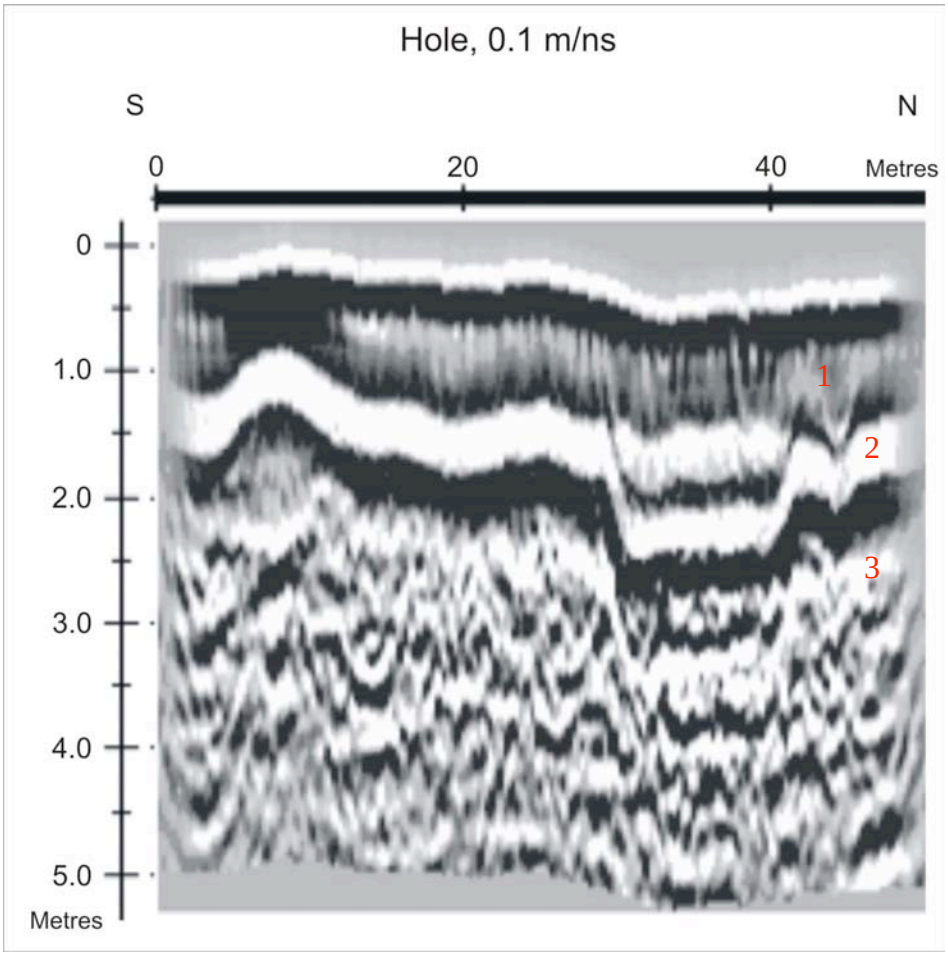

Figure 31: Picture of the trench and its GPR profile. Both have the same orientation.

The trench exhibits three clear layers noted “1”, “2” and “3”, which are also marked on the GPR profile. Layer “1” is made of fine material with few medium-sized rocks. The profile shows a weak signal for this layer that corresponds to the fine material probably accumulated during overbank river flows. Layer “2” shows a greater concentration of medium-sized rounded rocks. The GPR profile shows for this layer between *c.* 30 and 40 m from the trench an old river channel, which has been infilled. Layer “3” corresponds to angular rocks, part of the rock avalanche deposit. The GPR profile exhibits a similar chaotic reflector relationship as previously seen for “Fan”, typical of coarse material. Both the photograph and the GPR profile suggest that a rock avalanche deposit extends under the edge of the floodplain.

2.6.3 Line 3: “Floodplain”

This 300 m long profile runs entirely on the floodplain, on the same line as the trench and its corresponding GPR profile (“Hole”).

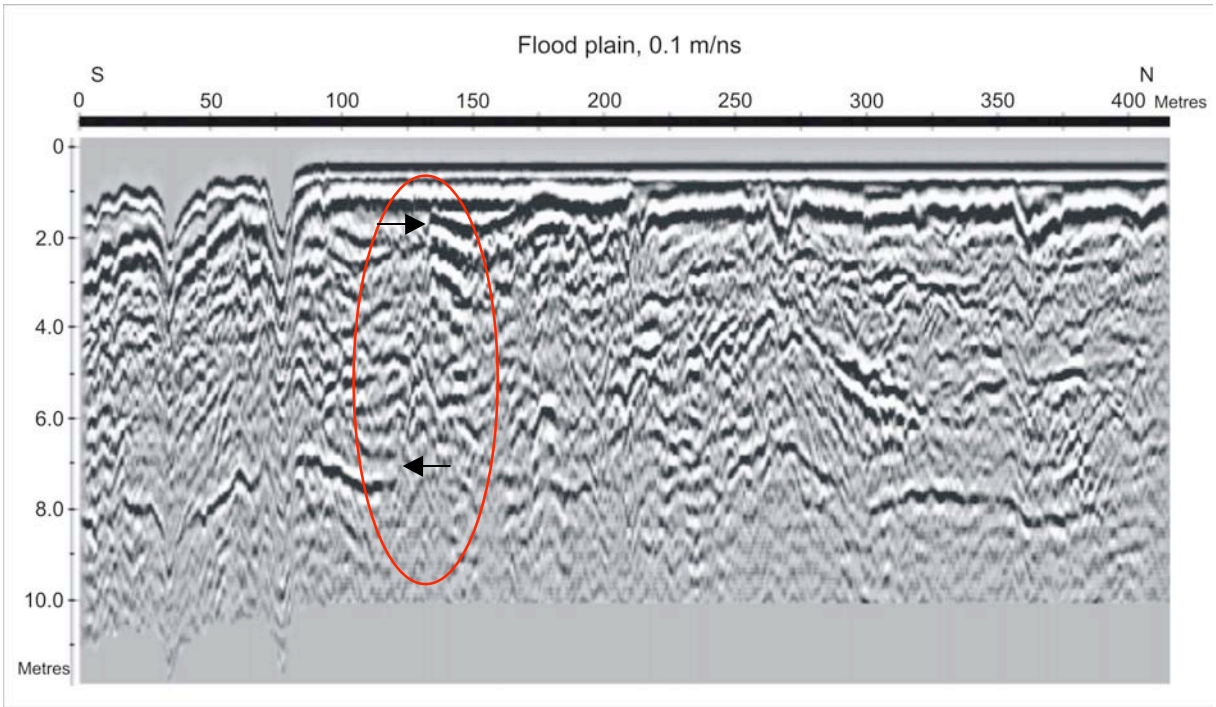

Figure 32: GPR profile of the floodplain.

This profile first surprises with the presence of a break in the continuity of the subsurface reflectors, as highlighted by the red oval (fig. 32). It seems that the reflectors may have been displaced by 6 m (arrows on fig. 32). The confirmation and final interpretation of this feature may require digging a trench in this area. An explanation could be the presence of a fault, but this seems very unlikely in alluvial materials, even so close to a major known fault. Interpreting this feature as a river cut suggests that the reflectors are NOT the same.

Finding strong reflectors up to 8 m deep has not been seen on the different profiles. So far the rock avalanche deposit has exhibited reflectors with a rather similar intensity all through the deposit.

The GPR profile of the first metre or so below the surface shows a very incised surface underlying a flat depositional one. The different incisions have been filled while a progradation occurred, seeming to propagate toward the south.

This profile shows less difference with increasing depth. The fine material is not only recognizable at the surface, as well as coarse material at depth.

Also noted is the increase of either water content or fine-grained material deeper than 8 m.

2.6.4 Line 4: “True right bank”

This 100 m long profile was obtained on a fluvial terrace on the true right bank of the Wanganui River.

As for lines 1 and 2, the surficial fluvial deposit is clearly noticeable. The ENE end looks disturbed. It is possible that a fence less than 5 m from this end point created electrical interference with the signal.

Because of the possibility that boulders may be present two profiles are presented: the first at low speed and the second at higher speed.

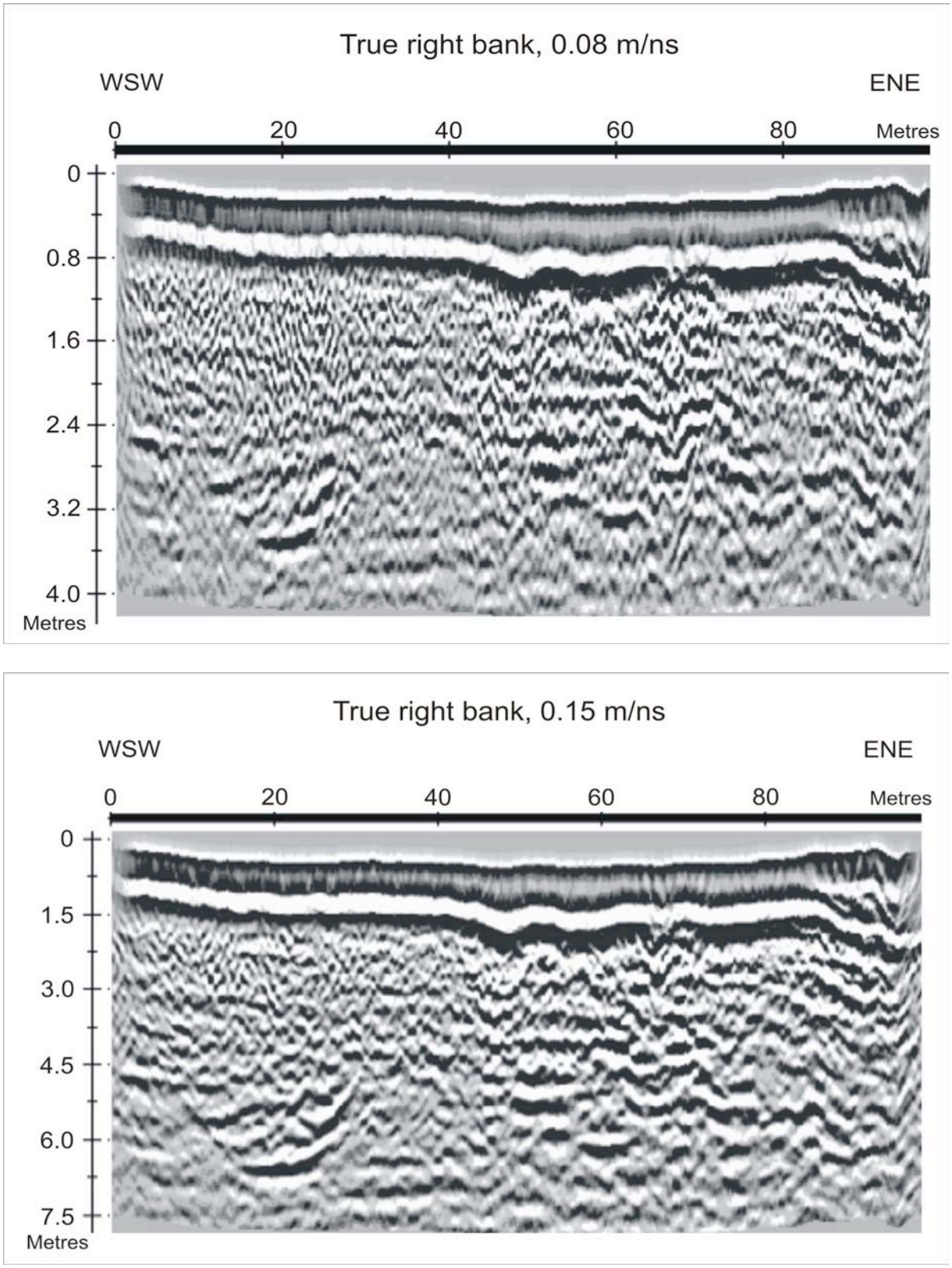

Figure 33: GPR profiles of line 4, at 0.08 m/ns and 0.15 m/ns.

At low speed such big boulders as the ones seen in the riverbed induce scattering of the signal, which tends to diminish at higher speed.

At low speed (0.08 m/ns), between 0 and *c.* 40 m on the abscissa axis and, between 0.8 and 2.4 m in depth, the signal shows a high degree of scattering. Looking at the higher speed migration profile it appears that this area's scattering is less pronounced. It is very likely indeed that this scattering is due to the presence of big boulders, which could be the continuation of the lag of big cataclasite boulders visible in the riverbed (fig. 37).

2.6.5 Line 5: "Road"

This GPR profile is 400 m long and exactly follows the former State Highway 6.

This line is actually the merging of three smaller lines and it appears that problems arose during the data processing from this combination, which do not allow any relevant interpretation. The different profiles are nonetheless presented in the appendix.

Although the Wanganui-Wilberg rock avalanche deposit is now confined to the true left bank of the Wanganui River, the possibility of finding it underneath the surface of the true right bank as well as farther away on the true left bank seems to be high. Most of the profiles acquired on this site present a clear near-surface fluvial stratification with, underneath, lots of reflectors more or less continuous but all exhibiting a certain consistent degree of disorder. This disorder could be caused by the buried part of the Wanganui-Wilberg rock avalanche deposit.

It is concluded that the Wanganui-Wilberg rock avalanche is very likely to have originally extended very much farther to the east (across the river) and a bit to the north (across part of the floodplain) than it does today. Both (present-day) northern and eastern edges show clear evidence of river incision.

Chapter 3: Dynamics

3.1 The Source

The source of the Wanganui-Wilberg rock avalanche has a SW-NE orientation, which appears to be parallel to the reported Alpine Fault trace (McCahon, *et al*. 2007). The head of its scarp is about 650 m.a.s.l and its base round 100 m.a.s.l. When compared to Keefer's (1984) database, the 550 m length of the scarp seems quite normal for a rock avalanche. By "best-guessing" the former contour lines and comparing them to the current situation, it is possible to estimate the volume of rocks that Mount Wilberg lost. Although the errors due to the use of this technique may possibly be high, this estimate gives a volume of 33 million cubic metres (previous estimates: 9-17 million cubic metres; Wright, 1998).

Figure 34: Reconstruction of previous assumed contours lines used for the volume estimates, the ridge is represent by the dashed line.

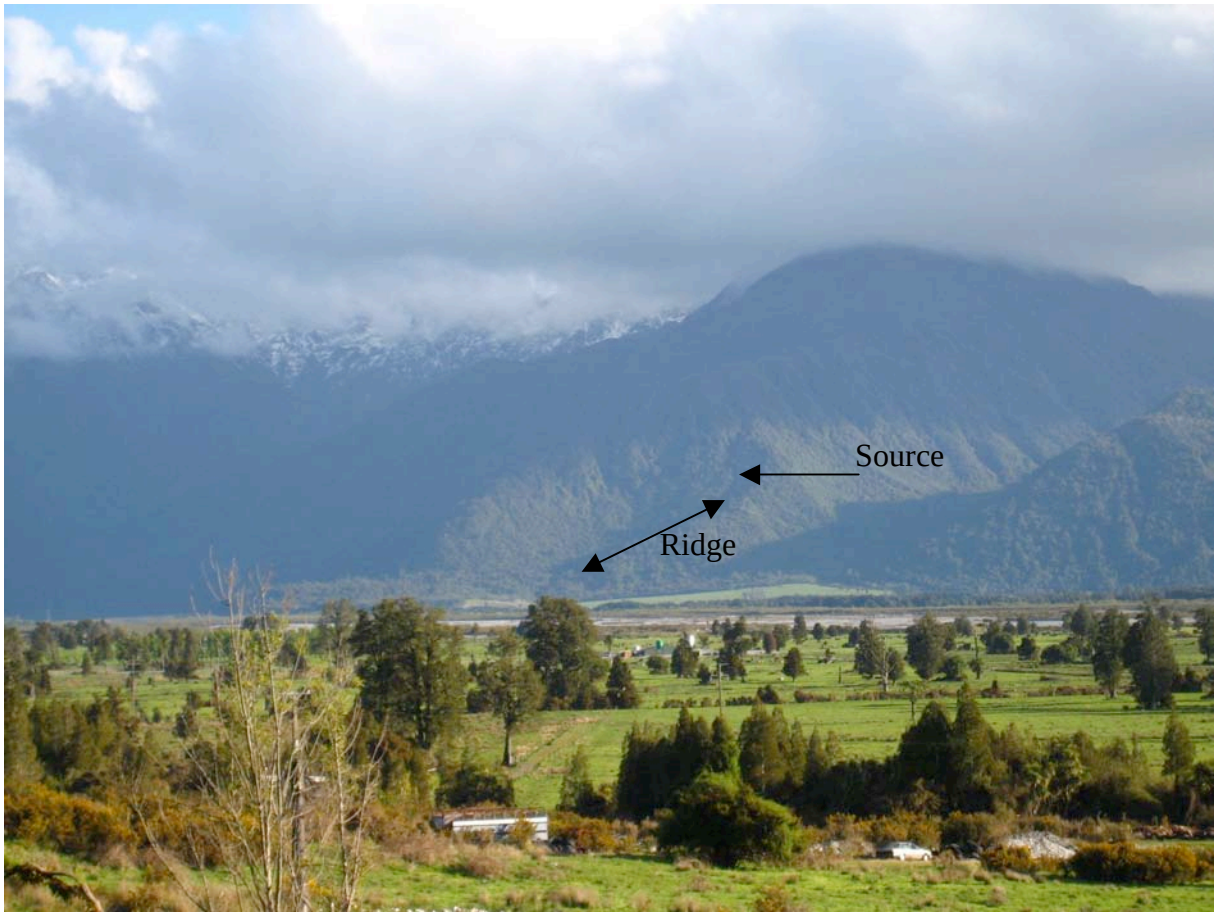

Figure 35: Source area, view from the north.

Havenith *et al.* (2003) reported that "*significant downward motion implies the development of a sliding surface*" when referring to rock avalanche initial motion. The shaking event triggering the Wanganui-Wilberg rock avalanche must have created a sliding surface that was exposed by the motion of the landslide out of its source; this surface today is probably covered by subsequent small-scale slope erosion deposits, and is certainly covered by dense vegetation.

The most striking feature of this source is probably its orientation. One would expect the Wanganui-Wilberg rock avalanche source to follow the greatest dipping slope, like Round Top.

Figure 36: Round Top source; this rock avalanche fell directly towards the camera, perpendicular to the original contour lines.

On the contrary, the direction of initial motion of the Wanganui-Wilberg rock avalanche is parallel to the ridgeline, although the source comprises only the slope to the north of the ridgeline. The reasons for such a peculiar initial sideways motion are probably related to proximity of the Alpine Fault, and more specifically to the rock structures related to it. This suggestion is supported by the presence, at the northern foot of the source area, of a substantial ridge that appears to have directed the initial motion of the slide (figs. 34, 35). This ridge seems likely to be made of resistant material; if it were rock avalanche debris it would not have been present at the initiation of the slide, which must then have moved initially perpendicular to the contours. The ridge is however covered by dense vegetation and its geology could not be ascertained.

When hiking near the top of the source, an expected “step” has been seen (*c.* 2.5 hours walk).

Figure 37: The step obove the source.

This step, at least 30 m long, is joining two steep portions of Mount Wilberg slope. It is likely that this flat surface could be helpful in future reconstruction of the historic slope and could maybe give information on the failure surface position in regard to the slope.

3.2 The Deposit

Direction of motion

Having a source scarp and knowing the initial direction of the runout, the question is how it moved. The answer to this question is subject to doubt. However a “best guess” would be the fall of an initially intact block of rock from Mount Wilberg. We then consider that all the parts of the deposit, a short time after the shaking event causing the Wanganui-Wilberg rock avalanche to detach from the rest of the mountain, moved in the same direction with the same velocity.

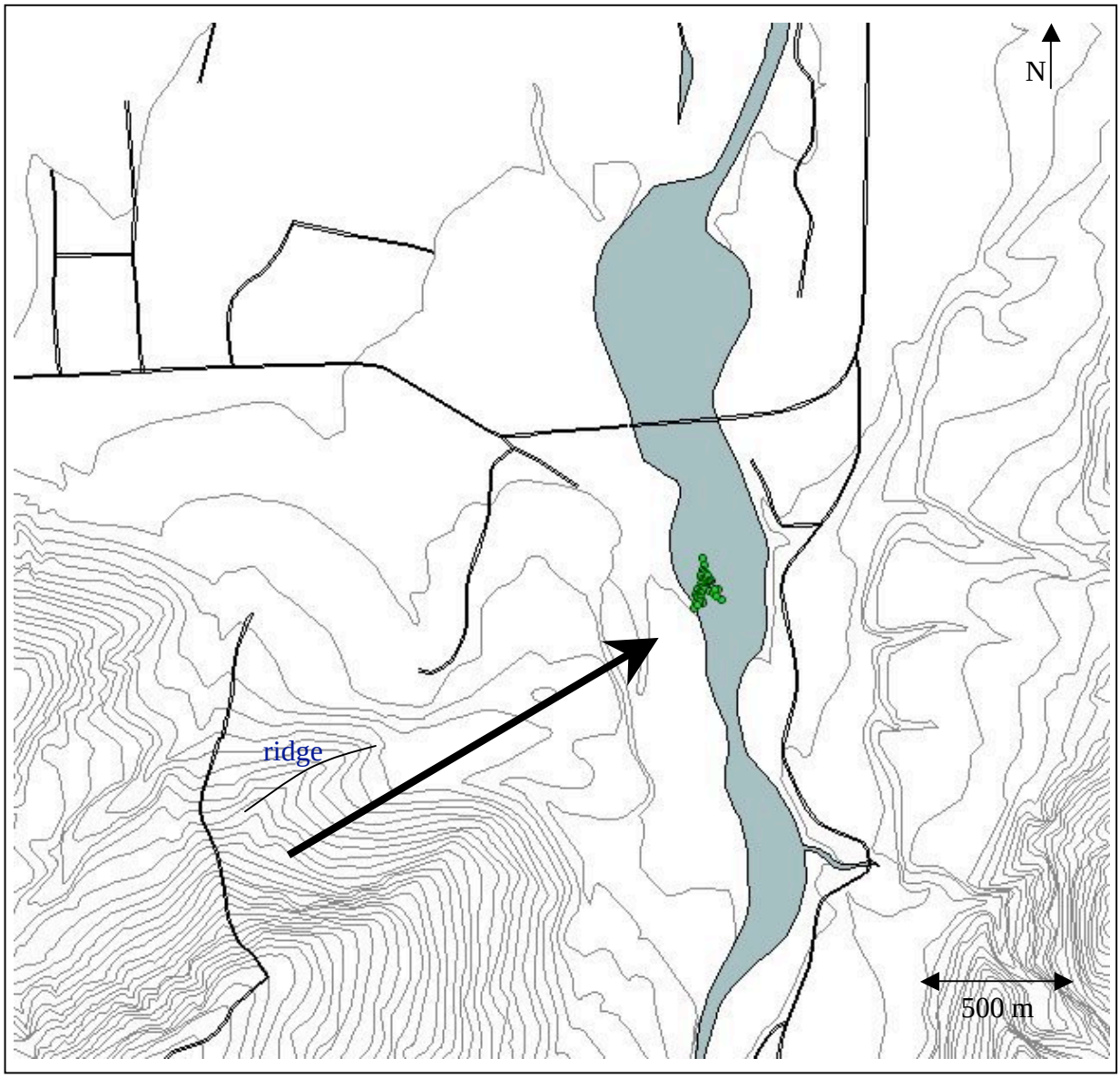

Figure 38: Boulders lag in relation to the source, showing the direction of the motion vector.

The site provides a feature that could verify this assumption of a single dominant motion vector: a lag of large cataclasite boulders in the current riverbed. These boulders are thought to have been part of the hanging wall of the Alpine Fault, since ultracataclasite forms very close to the main rupture surface of a major fault (Toy, 2007).

The fact that these boulders have remained intact must be due their greater strength; and/or a shorter runout distance (Weidinger 2002, Legros 2002), though the lack of segregation by size in rock avalanche debris makes the latter suggestion unlikely. Tracing a line between the foot of the scar at the fault hanging wall and these boulders shows a likely path of travel before it

was disturbed by the surrounding topography. Even if runout can curve and go uphill (Jibson *et al.* 2005), we assume that between the source and the resting place of the boulders, the motion was linear. Since the runout was on a glacial terrace, probably of flat surface profile, there is no reason to infer a curved path. The GPR profiles of the old State Highway 6 and the true right bank of the Wanganui River also confirm the presence of boulders near the surface.

Velocity

The range of speed for a landslide is very wide, and assessing it in the field is difficult when the deposit is severely eroded and there is no evidence of interaction with obstacles. Models and calculations however allow an estimate of the order of motion speed. Davies *et al.* (2006) have determined a maximum speed of *c.* 40 m/s for Waikaremoana Landslide (New Zealand), whereas Jibson *et al.* (2005) report landslide speeds reaching up to 100m/s (Plafker *et al.*, 1971) and Keefer (1984) highlighted "*their ability to transport material thousands of metres at velocities of tens or hundreds of kilometres per hour*". Possibly the best comparisons are the 55 x 10^6 m^3 Falling Mountain rock avalanche, which Davies & McSaveney (2002) have modelled achieving a peak velocity of the order of 100 ms^{-1}; and the 10^7 m^3 Acheron landslide, modelled to achieve a maximum speed of ~ 45 ms^{-1} by Smith *et al.* (2006). Determining the speed of the Wanganui-Wilberg rock avalanche is impossible; the model used for the Falling Mountain and Acheron events is not suitable for the Wanganui-Wilberg rock avalanche because the plan form of the whole deposit is not known. What can be said is that it almost certainly took a few seconds to perhaps a minute for the material to be deposited (Pollet, 2004).

The Wanganui-Wilberg rock avalanche deposit represents today about 20% of the initial volume that fell from Mount Wilberg. The 6.8 million cubic metres of the remaining deposit were estimated by multiplying the planform area by an assumed average thickness of 10 m, a

depth suggested by the exposures in the river-cut face. However, as for the volume determination of the source, the error could be important. Nevertheless a big proportion of the deposit remains invisible (about 80%), either washed away by erosion or lying beneath the surface (covered by subsequent sedimentation), as the GPR profiles show.

The runout distance of a landslide depends on the volume of material (Legros, 2002) and is linked to the degree of fragmentation of rocks (Weidinger *et al.*, 2002). The Wanganui-Wilberg rock avalanche deposit runout has not been determined in the field. However, comparing the Wanganui-Wilberg rock avalanche with the Round Top rock avalanche (Wright 1998, Dufresne, PhD *in prep*), which has a volume of 45 million cubic metres and a known runout of 4.9 km, one could estimate the runout of the Wanganui-Wilberg rock avalanche, which in that case would be $4.9*(33/45)^{0.33} =$ 4.4 km because the runout distance scales with the cube root of the volume (Davies, 1982). The following graph shows the relationship between volume and runout distance and how Wanganui-Wilberg rock avalanche and Round Top rock avalanche are to be placed compared to 56 other rock avalanches.

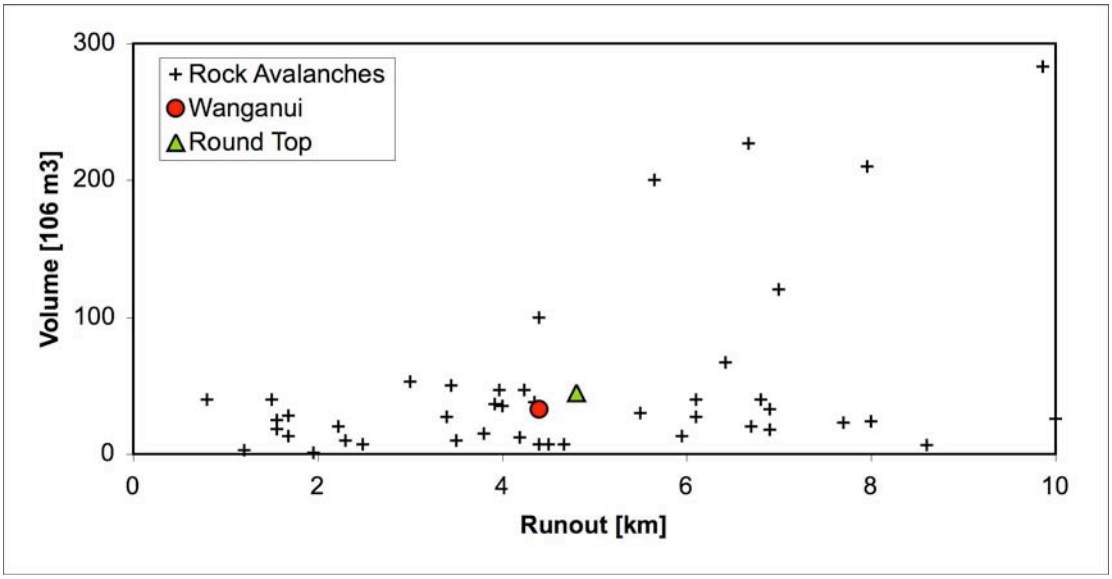

Graph 1: Volume (in million cubic metres) versus runout distance (kilometres) plot, provided by A. Dufresne.

Some other data have been plotted using the assumptions cited above, based on Legros (2002).

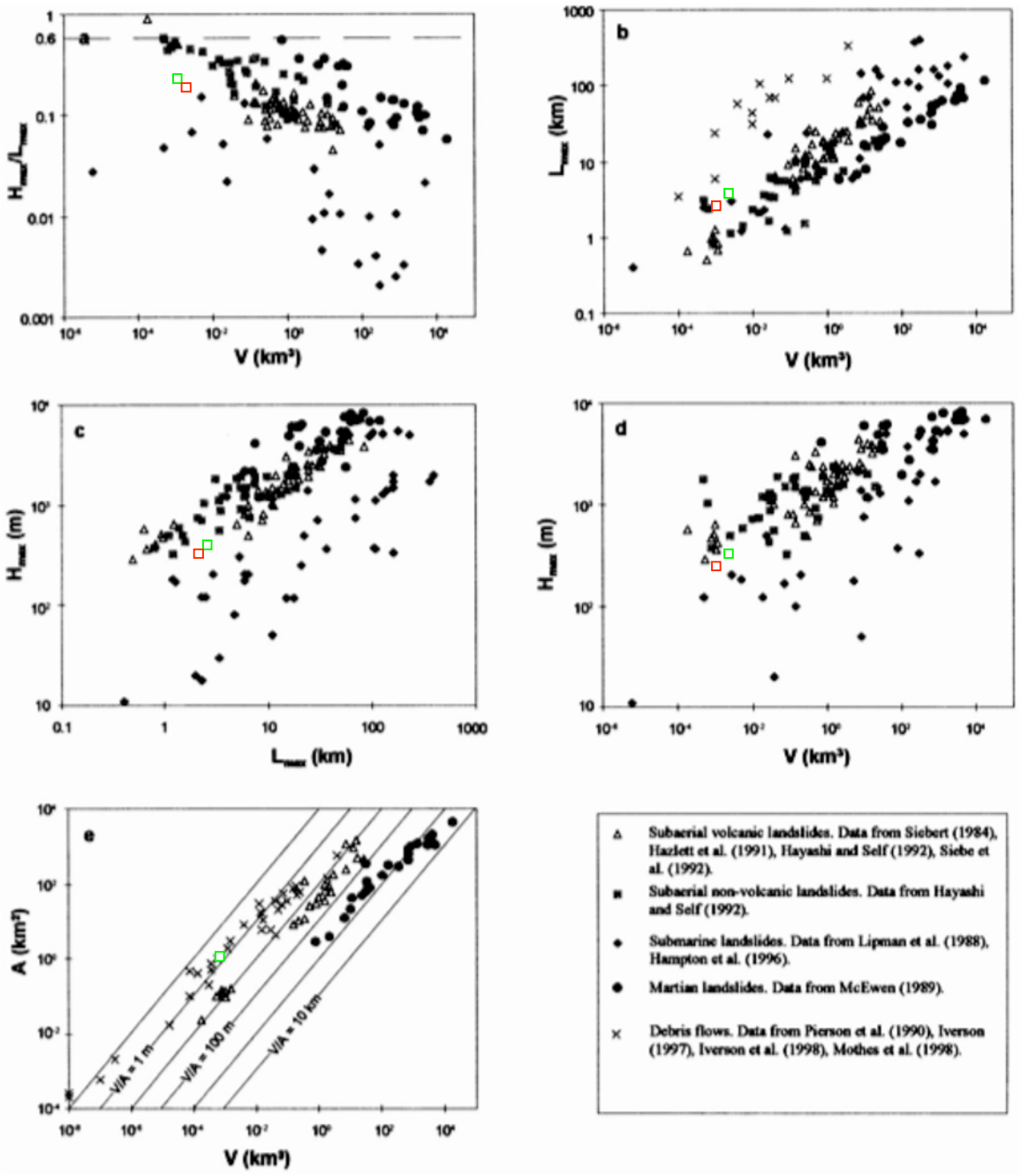

Graph 2: Graph from Legros (2002) showing the Wanganui-Wilberg (red square) and the Round Top rock avalanches (green square); a) Height max/Length max vs Volume; b) Length max vs Volume; c) Height max vs Length max; d) Height max vs Volume; e) Area vs Volume. Note Wanganui-Wilberg rock avalanche is not shown on e) because of its unknown area.

One of the parameters taken into account in these graphs is H/L, also known (wrongly) as the friction coefficient. H/L is often used to compare landslides (Wright, 1998). For the

Wanganui-Wilberg rock avalanche, H/L is equal to (550/4400) = 0.12. This figure represents a low apparent friction coefficient when considering the volume of the deposit (graph 2). Dynamically it means that the friction forces between the substratum and the sliding mass are low in comparison with the sum of gravity and internal forces driving the motion, and favour a longer distance of propagation (Davies et al. 2006). Legros (2002) also mentioned water as being partly "responsible for the long runout of landslides". However, there are many other possibilities for explaining long-runout rock avalanches (e.g. Davies *et al.*, 1999); the Wanganui-Wilberg rock avalanche site does not provide good evidences for low friction mechanism and further research is needed to emphasize this point.

The lag of large boulders is about 1.5 km away from the source, less than half of the expected runout distance (4.4 km). Moreover the moraine facing the Wanganui-Wilberg rock avalanche on the true right bank of the Wanganui River is less than 3 km away from the source. In that case it seems likely that this glacial deposit may have been hit by the slide. However when a slide is hitting a subvertical surface, it leaves a mark on the facing slope, like Acheron rock avalanche displays (fig. 39) (Smith *et al.* 2005). Any such evidence at Wanganui-Wilberg is either concealed by vegetation or has been eroded by the river.

Figure 39: Acheron rock avalanche, showing remaining evidence of the impact against the slope (arrow).

The farther the boulders are transported, the smaller the boulders (Weidinger *et al.*, 2002). Being between 1 and 2 km away from the source, the large boulders have undergone less travel than most of the little boulders, which could perhaps support the runout length calculated above.

In the light of the information provided in this paragraph:

- The slide originated from the rupture of a sliding surface and followed an initial path determined by the rock structure immediately adjacent to the Alpine Fault, as an intact block.

- The deposit is the result of the subsequent fragmentation of this block during the rest of its travel. The initial deposit extended much farther to the north and east than the present-day remnant.
- It probably dammed the Wanganui River by reaching the glacial deposits present on the opposite (right) bank.
- The river soon overtopped the created dam and started the erosion process, leaving today about 20% by volume of the original deposit.

Chapter 4: Dating

4.1 Introduction

The most common way to date an event such as a landslide is to use radiocarbon dating on organic matter on or in the deposit. Based on the chemical abundance of ^{13}C over ^{14}C, this method has the advantage of giving an absolute age. Another method is based on abundance of other chemical compounds (i.e. ^{11}Be), and it also gives absolute ages. These methods are often expensive and demand an access to radiochronology laboratory. There are also difficulties with calibration in many cases, particularly with ^{14}C in young deposits.

However, alternative methods exist. Dating living vegetation, although less precise, gives good results. Trees and lichens (Bull, 1996) can be used. Here again the age found is meant to be absolute even though errors are more likely important. Again, relating the vegetation age to the deposit age involves estimating the time for vegetation to become established as well as the place of the particular type of vegetation in the establishment sequence on the initially bare landslide deposit.

Beside absolute ages one can also use relative ages; by comparing the deposit surface to the surrounding surfaces, it is possible to determine an order of deposition. This is based on stratigraphic and structural relationships encountered in the field.

This paper first tries to answer the question of the Wanganui-Wilberg rock avalanche deposit age by using dendrochronology and relative age studies.

4.2 Why was the Wanganui-Wilberg rock avalanche not triggered by the last event of degradation?

Degradation is understood as any events that can cause a destabilization of the substrate. It can correspond to large rainfall, change in the water table level, earthquake and anthropogenic actions (Crozier *et al.* 1995)

The answer to this question lies on the west margin of the deposit, over the contact between the deposit and Harald Creek. Two slumps apparently coming from the deposit, overtop the contact. It has been assumed from GPR data that Harald Creek fan has developed over the deposit since it was emplaced. One can assume, from the study of the western margin, that the Wanganui-Wilberg rock avalanche fell, the fan developed and only then the slumps occurred. If this last event triggered the slumps, it could not have triggered the Wanganui-Wilberg rock avalanche. It must be older.

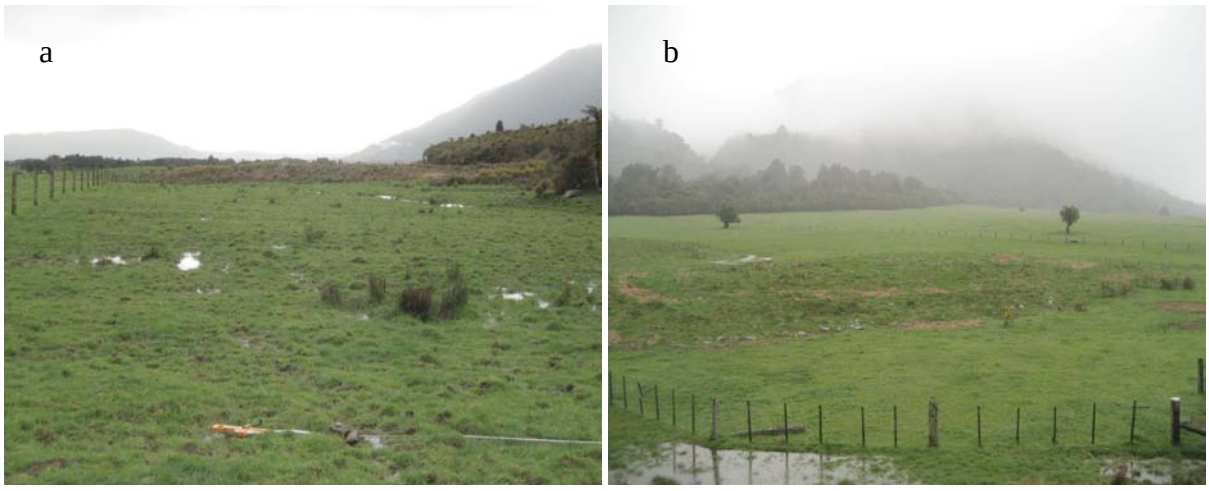

Figure 40: Slumps, view toward a) the North and b) the South-West.

4.3 Why did the last major earthquake not trigger the Wanganui-Wilberg rock avalanche?

The Alpine Fault is very active. Many earthquakes have shaken New Zealand since its emergence. In the last millennium four major events have been deduced and accepted (Larsen *et al*, 2005). AD 1717 is the date of the last major event and also the last one capable of triggering the Wanganui-Wilberg rock avalanche. Such an event is capable of creating a GPA (ground peak acceleration) of >10 ms^{-2} (Murphy *et al*., 2002)

Figure 41: Big boulder, known as "Trevor", northern edge, by the former State Highway 6, hidden by vegetation.

Present on the northern edge of the deposit, just next to the former State Highway 6, a large ultracataclasite boulder known as "Trevor" displays an interesting feature. It seems that it lies on a fluvial terrace. However, looking behind the boulder is found a little ridge about a metre high and, behind it, there is a "gap" in the deposit. The boulder is large: 5 m long, 3 to 4 m wide and about 7 m high. Between 5 and 10 m away from the current location of the boulder

the “gap” seems exactly the right size and shape to have, at one point, contained the boulder. Dynamically, it means that the boulder moved. However such a big boulder cannot “jump” over the remaining little ridge unless it received enough energy from the surroundings to do so. A GPA of 10 ms^{-2} (or 1.0 g) would be sufficient to create this effect because the force of gravity holding the boulder onto the ground could be completely overcome, while any lateral acceleration could then displace it. It is possible that the AD 1717 event caused the boulder move. Assuming that this boulder is part of the Wanganui-Wilberg rock avalanche deposit and that it moved in AD 1717, then the Wanganui-Wilberg rock avalanche deposit must have been first deposited, then eroded by the river to expose the boulder by 1717; so the deposit could not have been created by the latest earthquake. It is older – in fact in general it tells us that the event triggering the Wanganui-Wilberg rock avalanche was not that of 1717, but it could have been any of the previous ones.

4.4 So which earthquake triggered the Wanganui-Wilberg rock avalanche?

A rock avalanche such as the Wanganui-Wilberg rock avalanche is very likely to have been triggered by a major earthquake. Three well-substantiated earthquakes remain as possible triggers: AD 1220, AD 1425 and AD 1620 (Larsen *et al*., 2005). To answer this question a dendrochronology survey was carried out on the bigger trees present on the deposit and on an adjacent moraine. This involved sampling trees selected on the basis of their large size as being the oldest present, by coring them and counting the number of rings between the centre and the edge.

Figure 42: Trees reconnaissance before dendrochronology (the arrows are pointing to the biggest trees)

The drilled trees were either Rimu or Miro. Rimu (*Dacrydium Cupressinum*) is a coniferous tree that grows slowly throughout New Zealand. Most surviving large trees are 20 to 35 m tall, and can reach 50 m for the tallest. Miro (*Podocarpus Ferrugineus*) is a softwood forest tree, which can be up to 90 ft tall. It colonizes the lowland forests all around New Zealand.

Both these trees are considered to be scattered forest trees and emergent above the general canopy of the broadleaf trees.

Figure 43: Dendrochronology in progress and some of the resulting cores.

Once the cores were obtained using a Swedish Increment borer, they were mounted onto wooden sticks to make the counting process easier. The result is shown below.

Figure 44: Mounted cores.

The growth rings were counted using an Olympus SZ-STU2 microscope. Three cores were unable to be used in the counting process. Their rings remained uncountable even after the mounting process. However ten tree cores were able to give information about the age of the surface where they grew. The ages so determined cannot be said to be absolute as none of the cores showed the chronological centre (centre of the tree). However three cores show growth ring arcs, which allow the calculation of the chronological centre position (Norton *et al.*, 1987; Duncan, 1987).

For these reasons the calculated age is considered to be a minimum age; i.e. less than the age of the deposit.

Tag	**Straw**	**Species**	**DBH (cm)**	**Notes**	**Minimum age counted**	**Chronological centre calculation**	**Minimum age determined**
674	40	rimu	148	On scarp edge	1570	N	**1570**
666	85	rimu	85		??	N	??
665	98	miro	90	Elevated establishment microsite	1530	Y; + 40,7 yrs	**1490**
671	5 & 192	miro	135	Huge tree, branching wide and high. Took two cores	1550 & 1480	N	**1550 & 1480**
667	107	rimu	105	Near creek	1650	Y; + 101,32 yrs	**1549**
661	64	rimu	109	Just off the landslide deposit, on the moraine edge. Broke corer.	1290	N	**1290**

670	162	rimu	106	Just off the landslide deposit, on the moraine edge	1430	N	**1430**
660	103	rimu	c.150	DBH estimated	1670	N	**1670**
663	95	rimu	132	On fan apex.	??	N	??
662	55	rimu	118	Rotten core at end.	??	N	??
669	54	miro	c.200	DBH estimated	1650	Y; + 98,7 yrs	**1551**
668	804	rimu	c. 190	Rotten centre. Broke corer. DBH estimated	1640	N	**1640**

Figure 45: Age table (Tag=tree identification; straw=core identification; DBH=tree diameter).

When an event such as an earthquake or a windstorm occurs, one of the effects on the forests is a renewal of the big trees. The bigger ones are likely to fall and create holes in the canopy. Light manages to reach the ground and new trees can develop.

The trees on the moraine (Tag 661 & 670) respectively give ages of AD 1290 and AD 1430. Those two are the oldest trees cored. They closely match the AD 1220 and AD 1425 Alpine fault events.

On the landslide deposit trees seem to be rather younger. None of them are older than the 1425 event. Five trees' establishment seems to have followed the AD 1425 event (Tag 674, 665, 671, 667 & 669) while two trees on this same surface record the AD 1620 event (Tag 660 & 668).

However a stock of a Matai tree was also found on this same deposit. A slice of a portion of the stock had been cut in the field. It was dried and polished with sandpaper, to determine an age assessment by dendrochronology.

Figure 46: Piece of Matai on site and after drying and treatment.

The counting process revealed at least 700 rings and the chronological centre was not reached. This result tends to infer the presence of the deposit before at least AD 1300. That would infer the AD 1220 event is the most recent that could have created the surface by triggering the Wanganui-Wilberg rock avalanche.

4.5 Conclusion

When based on dendrochronology the age determination of any event remains subject to imprecision when the chronological centre of the tree is not reached. However it can give us a minimum age for the tree and also for the surface on which it grows. The tree coring suggests that the Wanganui-Wilberg rock avalanche was triggered by the AD 1425 event. But the Matai piece tells it could be of an even older age. The only sure thing is that neither the AD 1717 nor the AD 1620 triggered this landslide.

Discussion

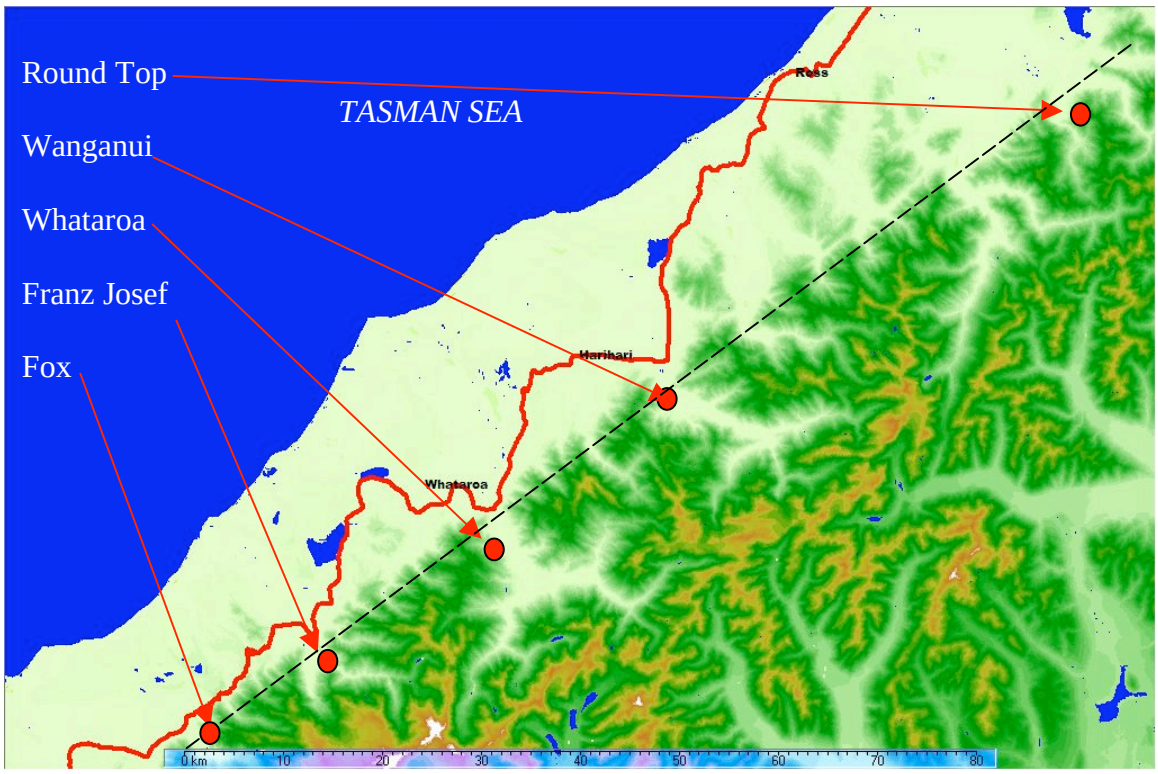

Figure 47: Location map of some landslides, either historic or expected. Dashed line = Alpine Fault, red line = State Highway 6.

Franz Josef

The extraordinary West Coast of New Zealand's South Island is a very active tectonic region. The Alpine Fault, which crosses all the South Island of New Zealand, has influenced numerous geomorphic features including landslides like the Wanganui-Wilberg rock avalanche or the Round Top rock avalanche. Some other places also show the required conditions to experience that kind of hazard soon. Franz Josef is one of them. The likelihood of seeing this slope (Fig. 47) collapsing is increased by its configuration that fulfils Keefer (1984) conditions: elevation of the slope, steepness, fluvial/glacial undercutting at its foot. Moreover, during recent field trips the step-profile of the slope and the presence of shallow rockfalls as well as cracks (L. Tatard, *PhD in prep*) have been pointed out. Not to be forgotten

is the presence of the Alpine Fault, extremely close to this potential failure site. Franz Josef Township is right on the runout path, which, if nothing is done before it is actually triggered, could be partially or entirely erased from the Earth.

Figure 48: Franz Josef Township, showing its closeness to the possible future source.

Round Top and Acheron rock avalanches

The Round Top rock avalanche provides an interesting source of comparison. Although both the Wanganui-Wilberg rock avalanche and the Round top rock avalanche deposits look very different (fig. 49), their common aspects are also numerous (table 2): their volumes are in the range of several tens of millions cubic metres, both are hummocky, their ages are close (AD 1220 and AD 930), both have the Alpine fault at the foot of the source, and neither was affected by strong topographical constraints during runout.

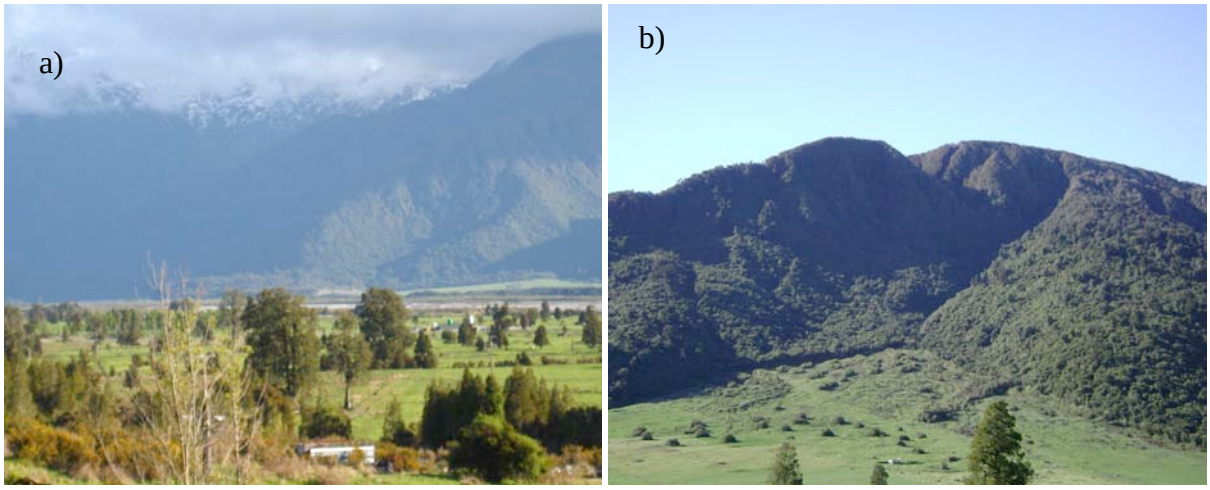

Figure 49: Source scarps of the a) Wanganui-Wilberg, and b) Round Top rock avalanches.

Another rock avalanche visited during this study was Acheron (Smith *et al.*, 2005) and its site provides views of a rock avalanche that has been directed by a pre-existing valley.

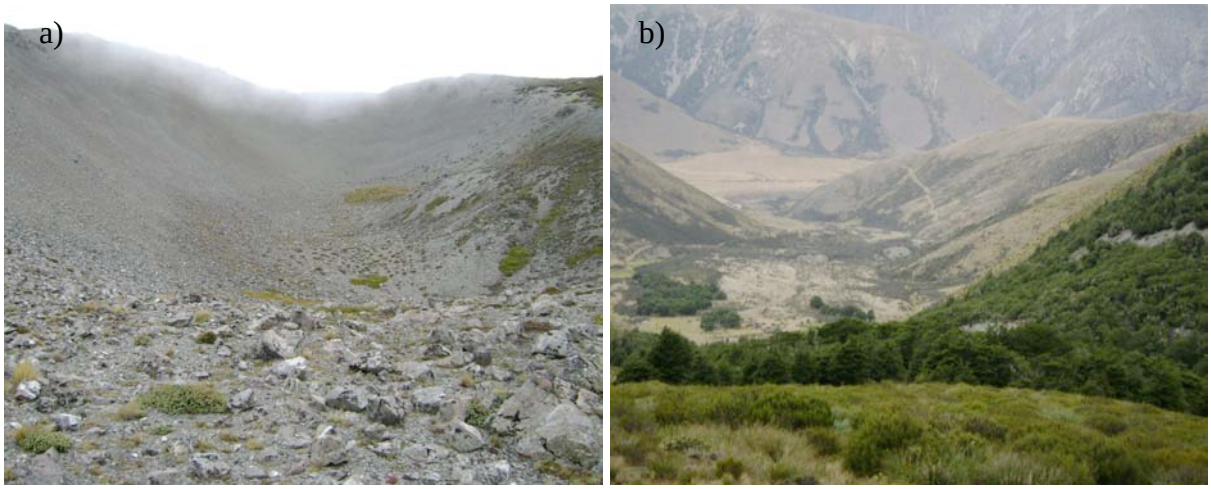

Figure 50: Acheron rock avalanche, a) source and b) deposit.

Dams

The Wanganui-Wilberg rock avalanche runout probably blocked the Wanganui River. The result of this dam was the creation a lake upstream of the river as many other landslides have done in New Zealand (Korup, 2004 and 2005). However the lake was probably small in volume and short-lived. The presence of historic lakes can be deduced by chemical studies and granulometric determination of the deposit occurring while the lake is in place. For

instance, finding silt upstream of a river with landslide deposits on both banks would prove the presence of a lake (if they are from the same source). The presence of a lake, even for a very short time, is likely in the case of the Wanganui-Wilberg rock avalanche. Yet no traces of such a lake, or even such a dam, have been found. However the rather low (because of the small deposit depth; ~ 10 m) dam that once blocked the Wanganui River is not thought to have suffered a dramatic collapse. Then a continuous overtopping may have started near the true right bank, where the runout likely met the moraine. It is considered to be the lowest point of the dam, and so water evacuation likeliest point. This dynamic eventually gave its current shape to the deposit.

Conclusion

Being one of the most active tectonic regions on Earth, New Zealand displays remarkable morphological features. Its west coast is the place of incredible erosion, either chemical (eg. rainfalls) or physical (e.g. earthquake, rainstorm). The recent Alpine fault earthquakes, which have a recurrence time of *c.* 200-300 years in this region (Rhoades and Van Dissen, 2002), have caused numerous rock avalanches, including the one treated herein: the Wanganui-Wilberg rock avalanche. They are "*among the most dangerous landslides triggered by seismic events*" (Keefer, 1984).

The Wanganui-Wilberg rock avalanche is the result of a high ground shaking that rendered possible the detachment of *c.* 33 million cubic metres of rock on the north slope of Mount Wilberg, leaving a clear scar visible from miles away (fig. 35).

The landslide fell initially as an intact block (Davies *et al*. 2006) at a velocity of tens to a hundred metres per second (Keefer, 1984; Jibson *et al.*, 2005) spreading over pre-existing geomorphological surfaces (moraine, fluvial terraces and riverbed), covering the trace of the Alpine fault and creating a new component to the landscape.

The dynamics, although likely to be more accurate with the use of numerical models due to the extreme erosion of the deposit, are proposed to have been as follows:

- An earthquake shook Mount Wilberg and created the failure (sliding) surface.
- The initial blockslide accelerated rapidly, and collapsed to form a fragmenting debris mass moving at high speed, overtopping the moraine terraces on the true left of the Wanganui River, probably reaching the moraine on the other bank and then damming the Wanganui River.
- Once the deposit stabilised (few seconds to minutes (Heim, 1932)), a lake was created, as water could not get through the deposit.

- The lake level rose and water overtopped the dam, probably near the Wanganui River true right bank moraine. No catastrophic breakage of the dam is thought to have happened.
- Slowly but surely, water, rainfall and seismic activity eroded the deposit and gave birth to a series of complex fluvial terraces visible today. This process is still active nowadays.

The age of the deposit has been calculated using trees (Miro and Rimu) growing on its surface. Even if no absolute ages have been found, we deduce that the triggering event is not the AD 1717, nor the AD 1620. AD 1425, 1220, or even maybe the AD 980, is likely to be the triggering event of the Wanganui-Wilberg rock avalanche.

Landslides of all kinds (soil slides, landslides, rock avalanches) in such a region as the West Coast of New Zealand can be of a great significance for communities and other environmental stakeholders. Historic landslide deposits are numerous all along the Southern Alps.

The next large earthquake (Yetton, 1998) is probabilistically expected soon. The Franz Josef site is looked at carefully, as representing a high potential hazard. Future landslides are likely to be triggered, there and elsewhere. The stakes are now to join the economical expansion of the South Island with hazards and disaster management plans. An understood environment is a safe environment.

References

Agnesi, V.; Camarda, M.; Conoscenti, C.; Di Maggio, C.; Diliberto, I. S.; Madonia, P.; Rotigliano, E. (2004): A multidisciplinary approach to the evaluation of the mechanism that triggered the Cerda landslide (Sicily, Italy). *Geomorphology*, 65: 101-116.

Al-Homoud, A. S.; Tahtamoni, W. W. (1999): Reliability analysis of three-dimensional dynamic slope stability and earthquake-induced permanent displacement. *Soil Dynamics and Earthquake Engineering*, 19: 91-114.

Anderson, H.; Beanland, S.; Blick, G.; Darby, D.; Downes, G.; Haines, J.; Jackson, J.; Robinson, R.; Webb, T. (1994): The 1968 May 23 Inangahua, New Zealand, earthquake: an integrated geological, geodetic, and seismological source model. *New Zealand Journal of Geology and Geophysics*, 37: 59-86.

Balance, P. F. (1970): Evolution of the upper Cenozoic magmatic arc and plate boundary in Northern New Zealand. *Earth Planet Sciences Letters*, 28: 356-370.

Benson, A. K. (1995): Applications of ground penetrating radar in assessing some geological hazards: examples of groundwater contamination, faults, cavities. *Journal of applied Geophysics*, 33: 177-193.

Berryman, K. R.; Beanland, S.; Cooper, A. F.; Cutten, H. N.; Norris, R. J.; Wood, P. R. (1992): The Alpine Fault, New Zealand: variations in Quaternary structural style and geomorphic expression. *Annales Tectonicae*, Supplement to Vol. 6: 126-193.

Bird, J. F.; Bommer, J. J. (2004): Earthquake losses due to ground failure. *Engineering Geology*, 75: 147-179.

Bommer, J. J.; Rodriguez, C. E. (2002): Earthquake-induced landslides in Central America. *Engineering Geology*, 63: 189-220.

Bradshaw, J. D.; Weaver, S. D.; Muir, R. J. (1996): Mid-Cretaceous oroclinal bending of New Zealand terranes. *New Zealand Journal of Geology and Geophysics*, 39: 461-468.

Bradshaw, J. D. (1993): A review of the Median Tectonic Zone: terrane boundaries and terrane amalgamation near the Median Tectonic Line. *New Zealand Journal of Geology and Geophysics*, 36: 117-125.

Brunsden, D. (1999): Some geomorphological considerations for the future development of landslide models. *Geomorphology*, 30: 13-24.

Buech, F.; Davies, T. R.; Pettinga, J. R.; Finnemore, M.; Berrill, J. B. (2007): The Little Hill field experiment: Seismic response of an edifice. *In: NZSEE (Editor), New Zealand Society for Earthquake Engineering – 2007 Technical conference and AGM. NZSEE, Palmerston North, New Zealand:* 8p.

Chigira, M.; Wang, W.-N.; Furuya, T.; Kamai, T. (2003): Geological causes and geomorphological precursors of the Tsaoling landslide triggered by the 1999 Chi-Chi earthquake, Taiwan. *Engineering Geology*, 68: 259-273.

Cox, S. C. and Barrell, D. J. A. (2007): Geology of the Aoraki area. *Institute of Geological and Nuclear Sciences 1:250 000 geological map 15*. 1 sheet + 71p. *Lower Hutt, New Zealand. GNS Science.*

Crozier, M. J.; Deimel, M. S.; Simon, J. S. (1995): Investigation of earthquake triggering for deep-seated landslides, Taranaki, New Zealand. *Quaternary International*, 25: 65-73.

Cullen, L. E.; Duncan, R. P.; Wells, A.; Stewart, G. H. (2003): Floodplain and regional scale variation in earthquake effects on forests, Westland, New Zealand. *Journal of the Royal Society of New Zealand*, 33: 693-701.

Dai, F. C.; Lee, C. F.; Deng, J. H.; Tham, L. G. (2005): The 1786 earthquake-triggered landslide dam and subsequent dam-break flood on the Dadu River, southwestern China. *Geomorphology*, 65: 205-221.

Davies, T. R. H.; McSaveney, M. J. (2006): Geomorphic constraints on the management of bedload-dominated rivers. *Journal of Hydrology (NZ)*, 45 (2): 111-130.

Davies, T. R. H.; McSaveney, M. J.; Beetham, R. D. (2006): Rapid block glides: slide-surface fragmentation in New Zealand's Waikaremoana landslide. *Quaterly Journal of Engineering Geology and Hydrogeology*, 39: 115-129.

Davis, P. M.; Rubinstein, J. L.; Liu, K. H.; Gao, S. S.; Knopoff, L. (2000): Northridge Earthquake damage caused by geologic focusing of seismic waves. *Science*, 289: 1746-1750.

Davis, J. L.; Annan, A. P. (1989): Ground-penetrating radar for high-resolution mapping of soil land rock stratigraphy. *Geophysical Prospecting*, 37: 531-551.

De Mets, C.; Gordon, R.G.; Argus, D.F.; Stein, S. (1990): Current plate motions. *Geophysical Journal International*, 101: 425-478.

De Mets, C.; Gordon, R.G.; Argus, D.F.; Stein, S. (1994): Effect of recent revisions to the geomagnetic time scale on estimates of current plate motions. *Geophysics Research letters*, 21: 2191-2194.

Delvaux, D.; Abdrakhmatov, K. E.; Lemzin, I.; Strom, A. L. (2001): Landslides and surface breaks of the 1911, Ms 8.2 Kemin earthquake, Kyrgystan. *Russian Geology and Geophysics*, 42 (20): 1167-1177.

Duncan, R. P. (1989): An evolution of errors in tree age estimates based on increment cores in Kahikatea (*Dacrycarpus dacrydiodes*). *New Zealand Natural Sciences*, 16: 31-37.

Fitzsimons, S. J.; Veit, H. (2001): Geology and geomorphology of the European Alps and the Southern Alps of New Zealand: a comparison. *Mountain Research and Development*, 21: 340-349.

Fuller, M. L. (1912): The New Madrid earthquake. *US Geological Survey Bulletin*, 494: 119p.

Hancox, G. T.; Cox, S. C.; Turnbull, I. M.; Crozier, M. J. (2003): Reconnaissance studies of the landslides and other ground damage caused by the Mw 7.2 Fiordland earthquake of 22 August 2003. *Institute of Geological and Nuclear Sciences science report:* 32p.

Havenith, H.-B.; Strom, A.; Calvetti, F.; Jongmans, D. (2003): seismic triggering of Landslides. Part B: Simulation of dynamic failure process. *Natural Hazards and Earth System Sciences*, 3: 663-682.

Havenith, H.-B.; Strom, A.; Jongmans, D.; Abdrakhmatov, K; Delvaux, D; Tréfois, P. (2003): Seismic triggering of landslides, Part A: Field evidence from the Northern Tien Shan. *Natural Hazards and Earth System Sciences*, 3: 135-149.

Havenith, H.-B.; Vanini, M.; Jongmans, D.; Faccioli, E. (2003): Initiation of earthquake-induced slope failure: influence of topographical and other site specific amplification effects. *Journal of Seismology*, 7: 397-412.

Jiang, D.; White, J. C. (1995): Kinematics of rock flow and the interpretation of geological structures, with particular reference to shear zones. *Journal of Structural Geology*, 17: 1249-1265.

Jibson, R.W.; Harp, E.L.; Schulz, W.; Keefer, D. K. (2004): Landslides triggered by the 2002 Denali Fault, Alaska, Earthquake and the inferred nature of the strong shaking. *Earthquake Spectra*, 20: 669-691.

Jibson, R.W.; Harp, E.L.; Schulz, W.; Keefer, D. K. (2005): Large rock avalanches triggered by the M 7.9 Denali Fault, Alaska, earthquake of 3 November 2002. *Engineering Geology*, 83: 144-160.

Kamp, P. J. J. (1986): The mid-Cenozoic challenger rift system of western New Zealand and its implications for the age of the Alpine Fault inception. *Geological Society America Bulletin*, 97: 255-281.

Keefer, D. K. (1984): Rock avalanches caused by earthquakes: Source characteristics. *Science*, 223: 1288-1289.

Keefer, D. K. (1994): The importance of earthquake-induced landslides to long-term slope erosion and slope-failure hazards in seismically active. *Geomorphology*, 10: 265-284.

Keefer, D. K. (2000): Statistical analysis of an earthquake-induced landslide distribution - the 1989 Loma Prieta, California event. *Engineering Geology*, 58: 231-249.

Keefer, D. K. (2003): Earthquake-induced landslides, shattered landscapes, and hillslope erosion. *Geophysical Research Abstracts*, 5: 02361.

Khazai, B.; Sitar, N. (2003): Evaluation of factors controlling earthquake-induced landslides caused by Chi-Chi earthquake and comparison with the Northridge and Loma Prieta events. *Engineering Geology*, 71: 79-95.

Konagai, K.; Johansson, J.; Mayorca, P.; Yamamoto, T.; Miyajima, M.; Uzuoka, R.; Pulido, N. E.; Duran, F. C.; Sassa, K.; Fukuoka, H. (2002): Las Colinas landslide caused by the January 13 2001 off the coast of El Salvador earthquake. *Journal of Japan Association for Earthquake Engineering*, 2: 1-15.

Koons, P. O.; Norris, R. J.; Craw, D.; Cooper, A. F. (2003): Influence of exhumation of the structural evolution of transpressional plate boundaries: an example from the Southern Alps, New Zealand. *Geology*, 31: 3-6.

Korup, O. (2005): Rockslides and rockslide dams in postglacial fjord environments, New Zealand. In: Senneset, K., Flaate, K., Larsen, J.O. [Eds.] Landslides and Avalanches. Proceedings 11th International Conference and Field Trip on Landslides, 1-10 September 2005. Balkema/Taylor & Francis, London, pp. 221-227.

Korup, O. (2004): Geomorphic implications of fault zone weakening: slope instability along the Alpine Fault, South Westland to Fiordland. *New Zealand Journal of Geology and Geophysics*, 47: 257-267.

Korup, O. (2004): Geomorphometric characteristics of New Zealand landslide dams. *Engineering Geology*, 73: 13-35.

Korup, O.; McSaveney, M. J.; Davies, T. R. H. (2004): Sediment generation and delivery from large historic landslides in the Southern Alps, New Zealand. *Geomorphology*, 61: 189-207.

Lang, A.; Moya, J.;Corominas, J.; Schrott, L.; Dikau, R. (1999): Classic and new dating methods for assessing the temporal occurrence of mass movements. *Geomorphology*, 30: 33-52.

Larsen, S. H.; Davies, T. R. H.; McSaveney, M. J. (2005): A possible coseismic landslide origin of late Holocene moraines of the Southern Alps, New Zealand. *New Zealand Journal of Geology and Geophysics*, 48: 311-314.

Legros, F. (2002): The mobility of long-runout landslides. *Engineering Geology*, 63: 301-331.

Luo, H. Y.; Zhou, W.;Huang, S. L.; Chen, G. (2004): Earthquake-induced landslide stability analysis of the Las Colinas landslide in El Salvador. *Int. J. Rock Mech. Min. Sci.*, 41:Paper 2B 26 (CD-ROM).

Malamud, B. D.; Turcotte, D. L.; Guzzetti, F.; Reichenbach, P. (2004): Landslides, earthquakes, and erosion. *Earth and Planetary Science Letters*, 229: 45-59.

Marzorati, S.; Luzi, L.; De Amicis, M. (2002): Rock falls induced by earthquakes: a statistical approach. *Soil Dynamics and Earthquake Engineering*, 22: 565-577.

McCahon, I.; Dewhirst R.; Elms, D. (2006): Westland District Council Lifelines Study – Alpine Fault Earthquake scenario. *Westland District Council*.

Mellett, J. S. (1994): Ground penetrating radar applications in engineering, environmental management, and geology. *Journal of Applied Geophysics*, 33: 157-166.

Murphy, W.; Petley, D. N.; Bommer, J.; Mankelow, J. M. (2002): Uncertainty in ground motion estimates for the evaluation of slope stability during earthquakes. *Quaterly Journal of Engineering Geology and Hydrogeology*, 35: 71-78.

Nicoletti, P. G.; Parise, M. (2001): Seven landslide dams of old seismic origin in southeastern Sicily (Italy). *Geomorphology*, 46: 203-222.

Nobes, D. C.; Ferguson, R. J.; Brierley, G. J. (2001): Ground-penetrating radar and sedimentological analysis of Holocene floodplains: insight from the Tuross valley, New South Wales. *Australian Journal of Earth Sciences*, 48: 347-355.

Norris, R. J.; Cooper, A. F. (1997): Erosional control on the structure evolution of a transpressional thrust complex on the Alpine Fault, New Zealand. *Journal of Structural Geology*, 19: 1323-1342.

Norris, R. J.; Cooper, A. F. (2003): Very high strains recorded in mylonites along the Alpine Fault, New Zealand: implications for the deep structure of a plate boundary faults. *Journal of Structural Geology*, 25: 2141-2157.

Norton, D. A.; Ogden, J. (1987): Dendrochronology: a review with emphasis on New Zealand applications. *New Zealand Journal of Ecology*, 10: 77-95.

Norton, D. A.; Palmer, J. G.; Ogden, J. (1987): Dendroecological studies in New Zealand, Part 1: An evaluation of tree age estimates based on increment cores. *New Zealand Journal of Botany*, 25: 373-383.

Okybo, C. H. (2004): Rock mass strength and slope stability of the Hilina slump, Kilauea volcano, Hawai‘i. *Journal of Volcanology and Geothermal Research*, 138: 43-76.

Olsen, K. B.; Archuleta, R. J.; Matarese, J. R. (1995): Three-dimensional simulation of a magnitude 7.75 earthquake on the San Andreas Fault. *Science*, 270: 1628.

Paolucci, R. (2002): Amplification of earthquake ground motion by steep topographic irregularities. *Earthquake Engineering and Structural Dynamics*, 31: 1831-1853.

Parise, M.; Jibson, R. W. (2000): A seismic landslide susceptibility rating of geologic units based on analysis of characteristics of landslides triggered by the 17 January 1994, Northridge, California earthquake. *Engineering Geology*, 58: 251-270.

Petley, D. N.; Allison, R. J. (1997): The mechanics of deep-seated landslides. *Earth Surface Processes and Landforms*, 22: 747-758.

Pollet, N. (2004): Contribution à l'analyse des mouvements gravitaires rapides de grande ampleur par la comparaison des matériaux sources et des dépôts: exemples alpins. *Bull Eng Geol Env*, 63: 353-365.

Reyners, M.; Webb, T. (2002): Large earthquakes near Doubtful Sound, New Zealand, 1989–93. *New Zealand Journal of Geology and Geophysics*, 45: 109-120.

Rhoades, D. A. Van Dissen, R. J. (2003): Estimates of the time-varying hazards of rupture of the Alpine Fault, New Zealand, allowing for uncertainties. *New Zealand Journal of Geology and Geophysics*, 46 479-488.

Romeo, R. (2000): Seismically induced landslide displacements: a predictive model. *Engineering Geology*, 58: 337-351.

Sara, W. A. (1979): Glaciers of Westland National Park. *New Zealand Department of Scientific and Industrial Research Information Series*, 79 (2nd ed.).

Sass, O. (2006): Bedrock detection and talus thickness assessment in the European Alps using geophysical methods. *Journal of Applied Geophysics*, 62: 254-269.

Sass, O.; Krautblatter, M. (2006): Debris flow-dominated and rockfall-dominated talus slopes: Genetic models derived from GPR measurements. *Geomorphology*, 86: 176-192.

Sadura, S; Martini, I. P.; Endres, A. L.; Wolf, K. (2005): Morphology and GPR stratigraphy of a frontal part of an end moraine of the Laurentides Ice Sheet: Paris Moraine near Guelph, ON, Canada. *Geomorphology*, 75: 212-225.

Sepulveda, S. A.; Murphy, W.; Petley, D. N. (2005) Topographic controls on coseismic rock slides during the 1999 Chi-Chi earthquake, Taiwan. *Quaterly Journal of Engineering Geology and Hydrogeology*, 38: 189-196.

Shahrivar, H.; Nadim, H. (undated): Literature survey on earthquake-induced landslides. *Unpublished manuscript, Department of Geosciences, University of Oslo.*

Shou, K.-J.; Wang, C.-F. (2003): Analysis of the Chiufengershan landslide triggered by the 1999 Chi-Chi earthquake in Taiwan. *Engineering Geology*, 68: 237-250.

Smith, G. M.; Davies, T. R. H.; Bell, D. H.; McSaveney, M. J. (2005) The Acheron rock avalanche, Canterbury, New Zealand – morphology and dynamics. *Landslides*, 00.

Somerville, P. G.; Graves, R. W. (2003): Characterization of Earthquake Strong Ground Motion. *Pure and Applied Geophysics*, 160: 1811-1828.

Suggate, R. P. (1990): Late Pliocene and Quaternary glaciations of New Zealand. *Quaternary Science Review*, 9: 175-197.

Strom, A. (2006): Morphology and Internal Structure of Rockslides and Rock Avalanches: Grounds and Constraints for their Modelling. *In: Evans, S.G., Scarascia Mugnozza, G., Strom, A. and Hermanns, R.L. (eds), Landslides from Massive Rock Slope Failure:* 305-326

Sturman, A.; Wanner, H. (2001): A comparative review of the weather and climate of the Southern Alps of New Zealand and the European Alps. *Mountain Research and Development*, 21: 359-369.

Sutherland, R.; Norris, R. J. (1995),: Late displacement rate, paleoseismicity, and geomorphic evolution of the Alpine Fault: evidence from Hokuri Creek, south Westland, New Zealand. *New Zealand Journal of Geology and Geophysics*, 38: 419-430.

Tsai, C.-C. P. (1997): Ground Motion Modelling for Seismic Hazard Analysis in the Near-source Regime: An Asperity Model. *Pure and Applied Geophysics*, 149: 265-297.

Wandres, A. M.; Bradshaw, J. D.; Ireland, T. (2005): The Paleozoic–Mesozoic recycling of the Rakaia Terrane, South Island, New Zealand: sandstone clast and sandstone petrology, geochemistry, and geochronology. *New Zealand Journal of Geology and Geophysics*, 48: 229-245.

Wardle, P. (1973): Variations of the glaciers of Westland National Park and the Hooker Range, New Zealand. *New Zealand Journal of Botany*, 11: 349-388.

Warren, G. (1967): *Sheet 17 Hokitika*. Geological map of New Zealand 1:250,000. *Department of Scientific and Industrial Research, Wellington, New Zealand*.

Weidinger, J. T.; Wang, J.; Ma, N. (2002): The earthquake-triggered rock avalanche of Cui Hua, Qin Ling Mountains, P. R. of China—the benefits of a lake-damming prehistoric natural disaster. *Quaternary International*, 93-94: 207-214.

Whitehouse I. E. (1983): Distribution of large rock avalanche deposits in the central Southern Alps, New Zealand. *New Zealand Journal of Geology and Geophysics* **26**: 271–279.

Wise, D. J.; Cassidy, J.; Locke, C. A. (2003): Geophysical imaging of the Quaternary Wairoa North Fault, New Zealand: a case study. *Journal of Applied Geophysics*, 53: 1-16.

Wright, C. A. (1998): The AD 930 long-runout Round Top debris avalanche, Westland, New Zealand. *New Zealand Journal of Geology and Geophysics*, 41: 493-497.

Wright, C. A. (1998): Geology and paleoseismology of the Central Alpine Fault, New Zealand. *Unpublished MSc Thesis, University of Otago, Dunedin, New Zealand*.

Yetton, M. D.; Nobes, D. C. (1998): Recent vertical offset and near-surface structure of the Alpine Fault in Westland, New Zealand, from ground penetrating radar profiling. *New Zealand Journal of Geology and Geophysics*, 41: 485-492.

Yetton, M. D. (1998): The probability and consequences of the next Alpine Fault earthquake, South Island, New Zealand. *Unpublished Ph'D thesis, University of Canterbury, Christchurch, New Zealand*.

Appendix

Geophysic field trip data processing.

The different profiles obtained are following:

Line 1: Fan

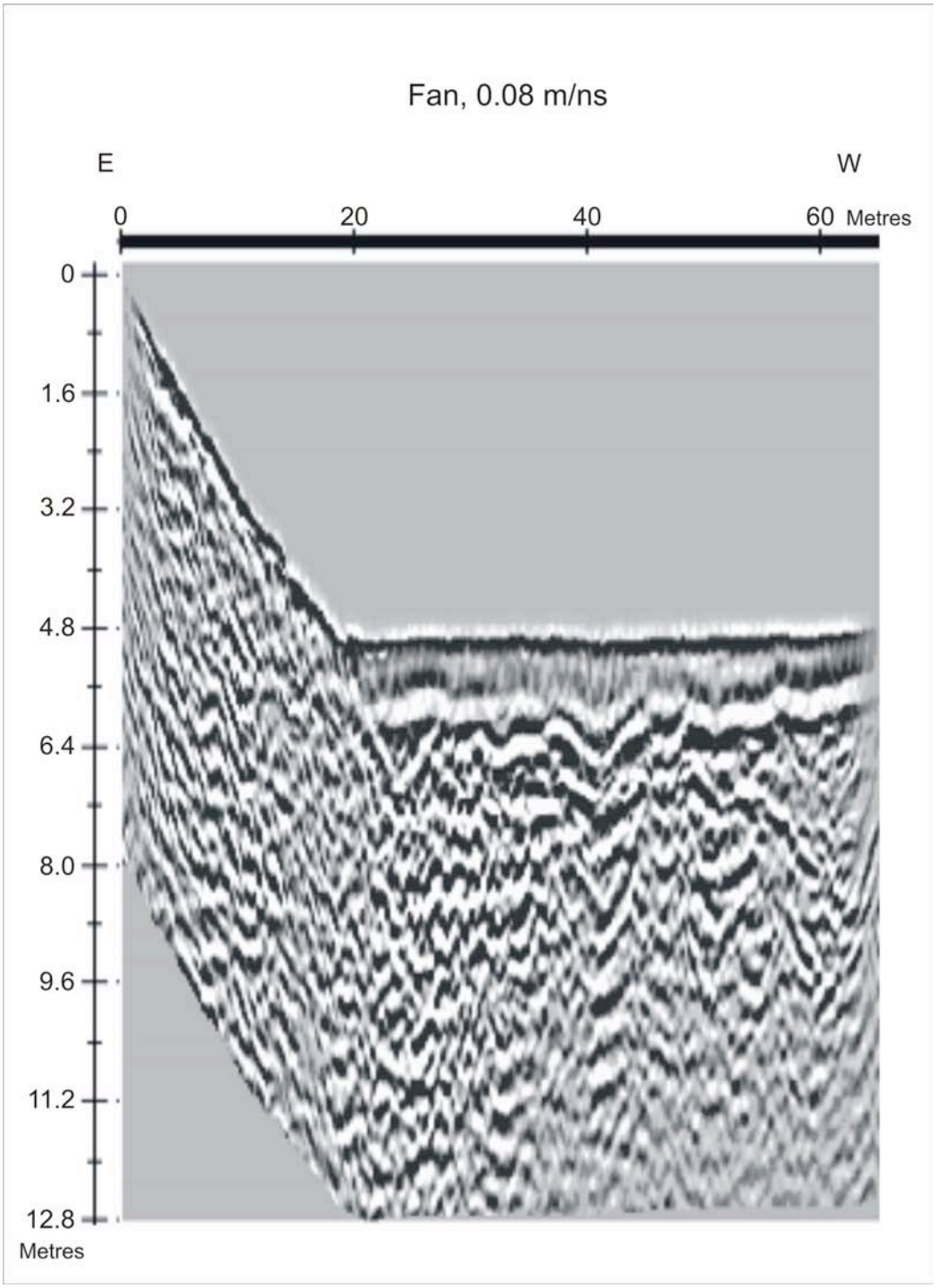

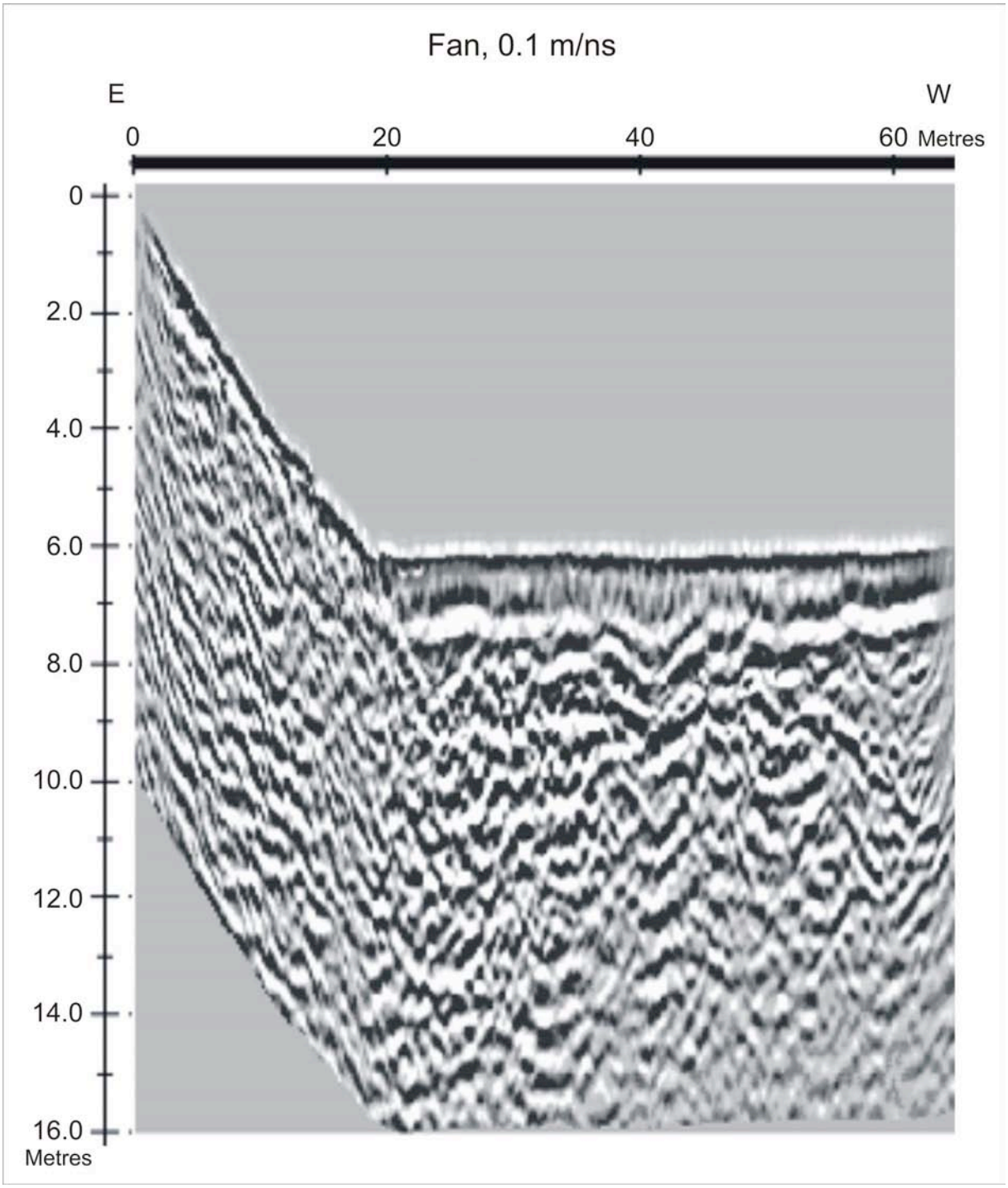
Fan, 0.1 m/ns
E
W
0
20
40
60 Metres
0
2.0
4.0
6.0
8.0
10.0
12.0
14.0
16.0
Metres

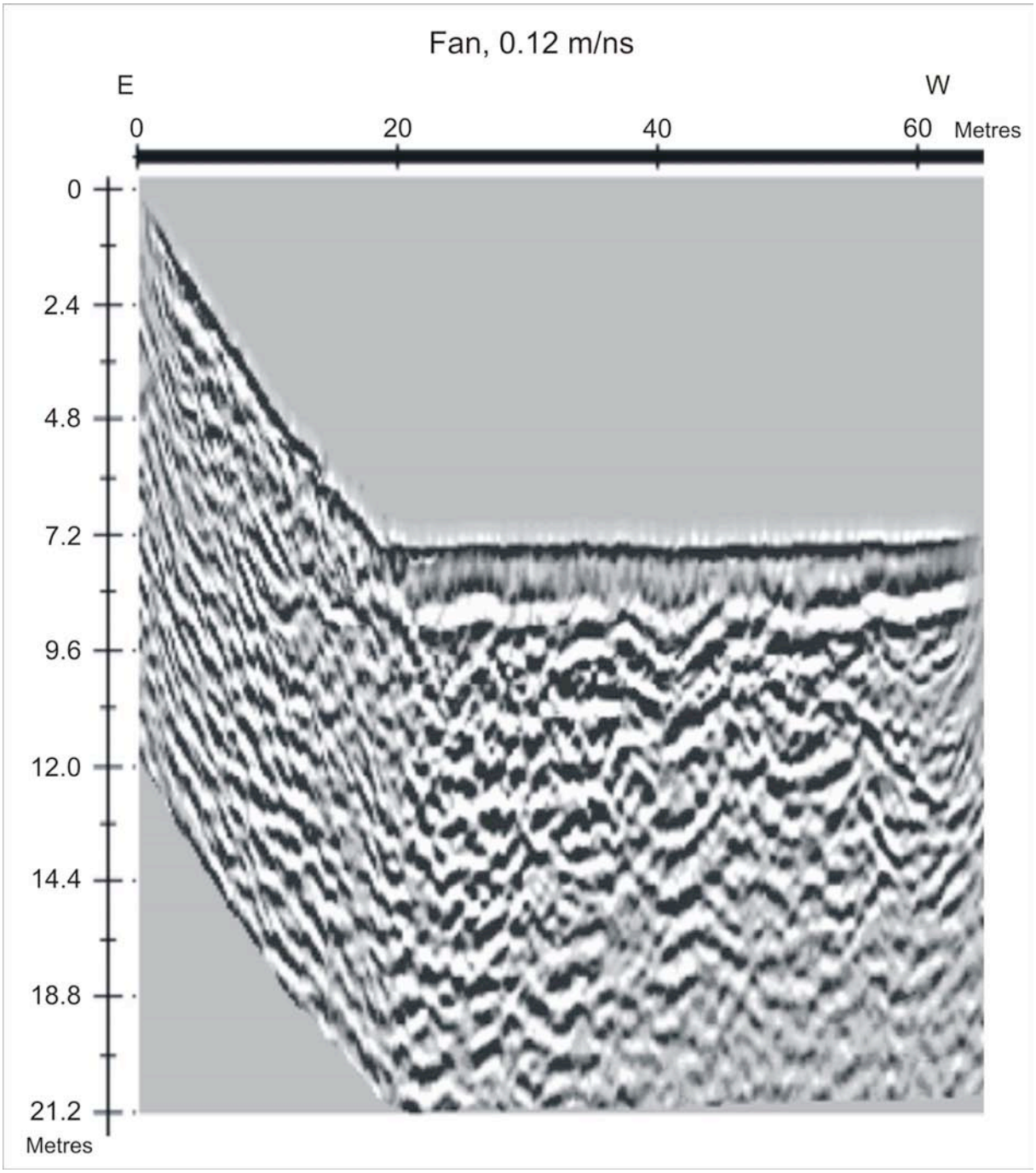
Fan, 0.12 m/ns
E
W
0
20
40
60
Metres
0
2.4
4.8
7.2
9.6
12.0
14.4
18.8
21.2
Metres

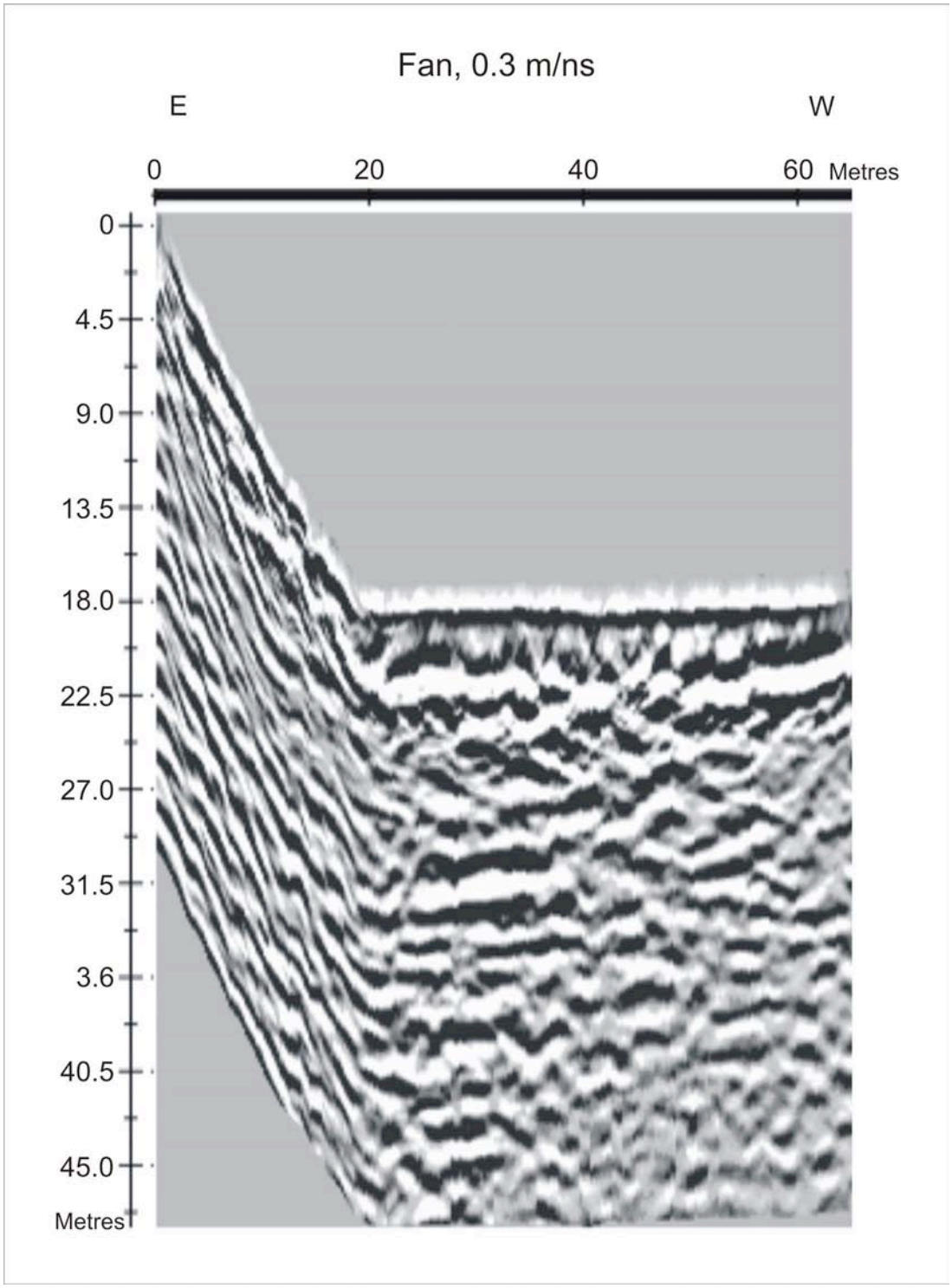
Fan, 0.3 m/ns
E
W
0
20
40
60 Metres
0
4.5
9.0
13.5
18.0
22.5
27.0
31.5
3.6
40.5
45.0
Metres

Line 2: The trench

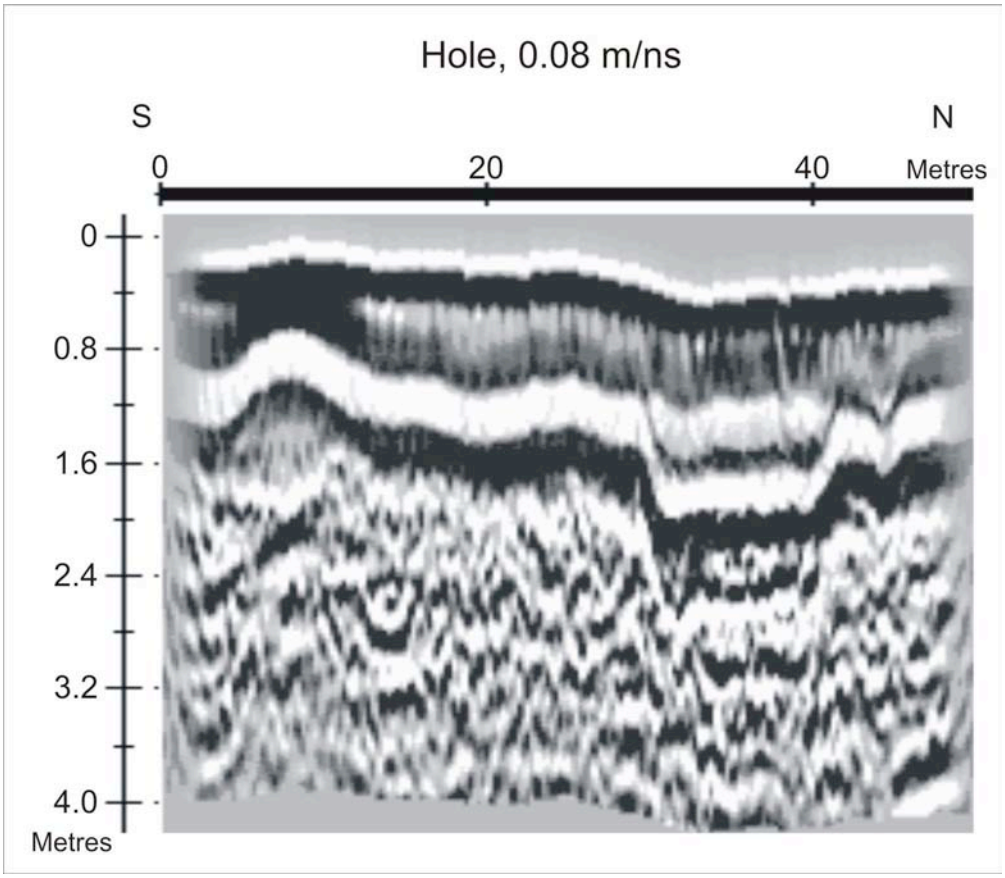

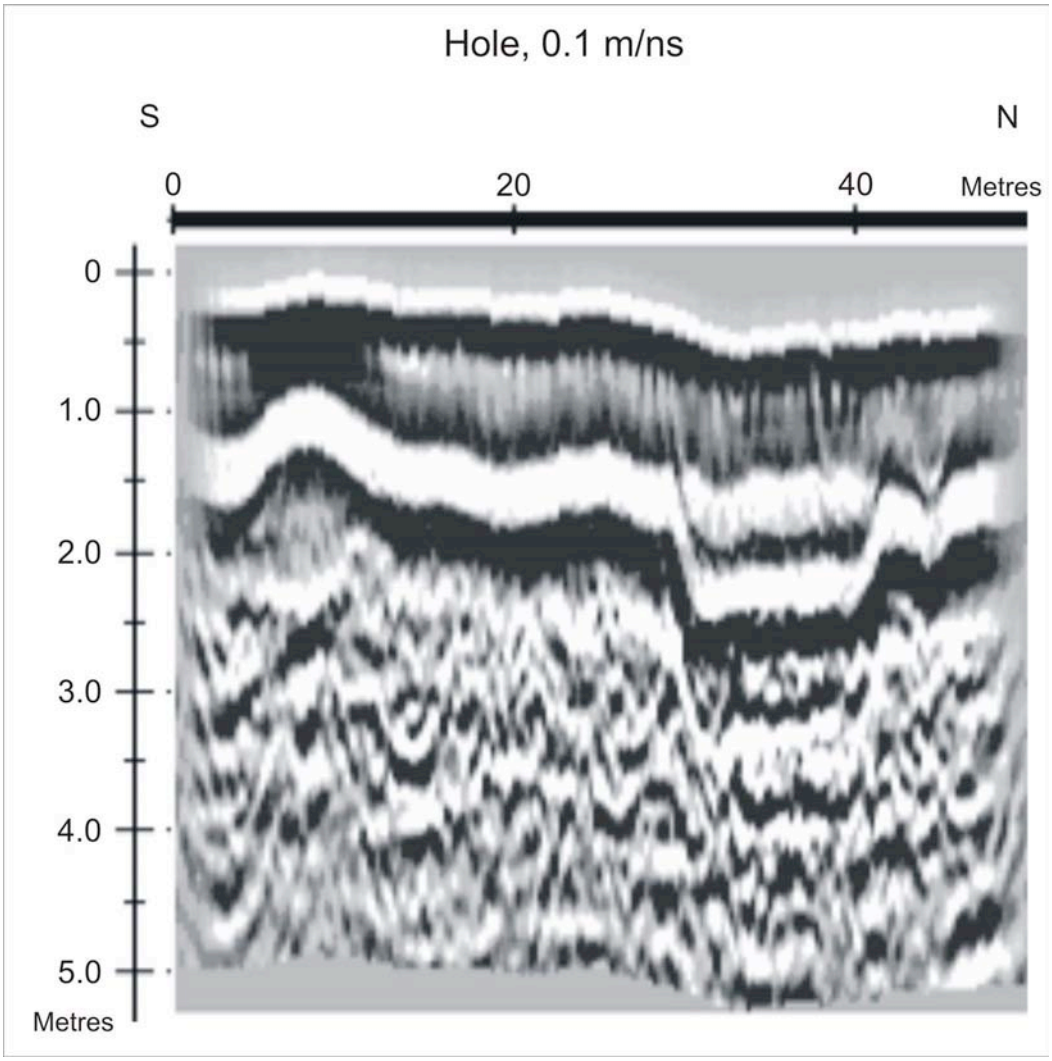
Hole, 0.1 m/ns
S
N
0
20
40
Metres
0
1.0
2.0
3.0
4.0
5.0
Metres

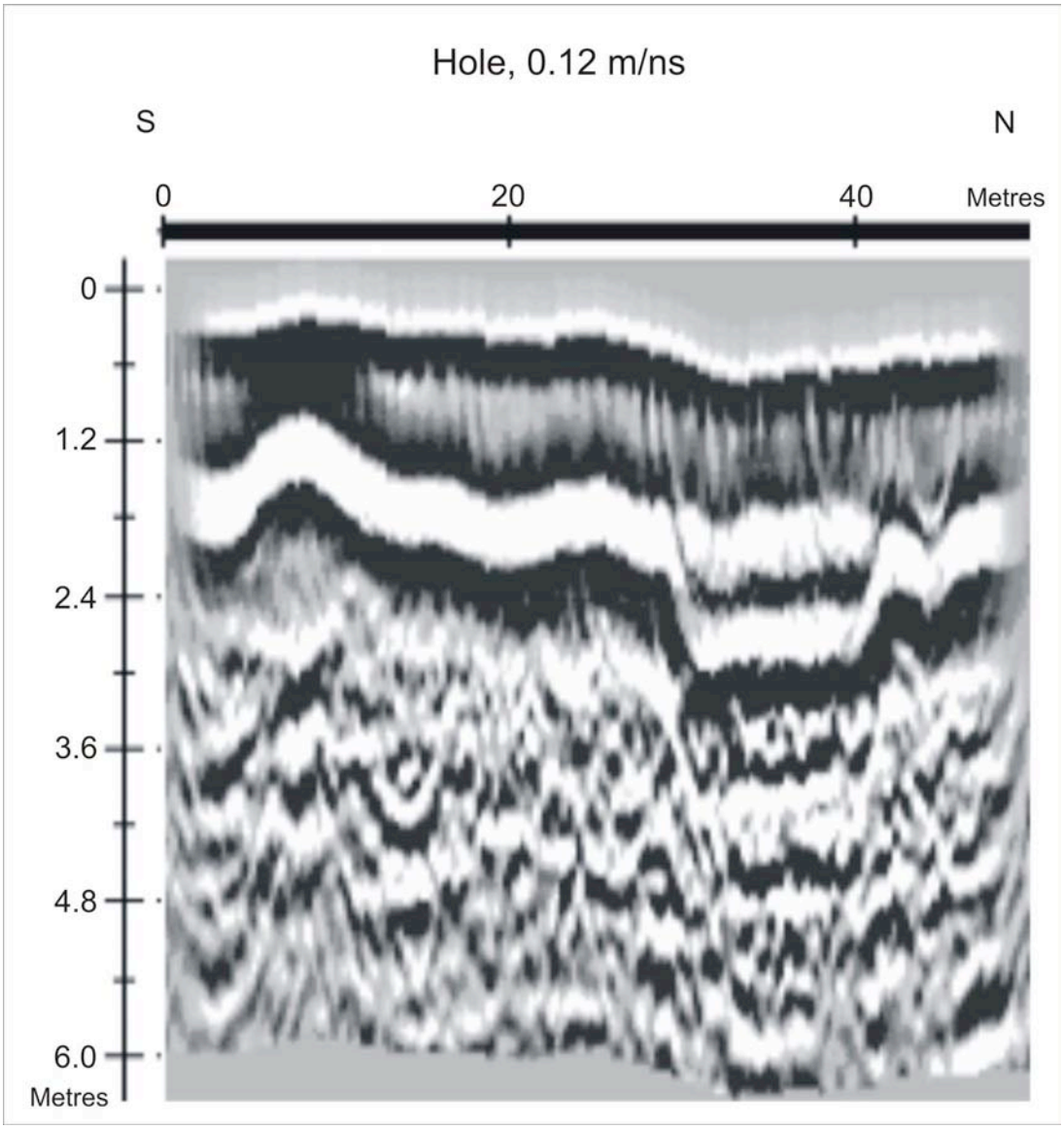
Hole, 0.12 m/ns
S
N
0
20
40
Metres
0
1.2
2.4
3.6
4.8
6.0
Metres

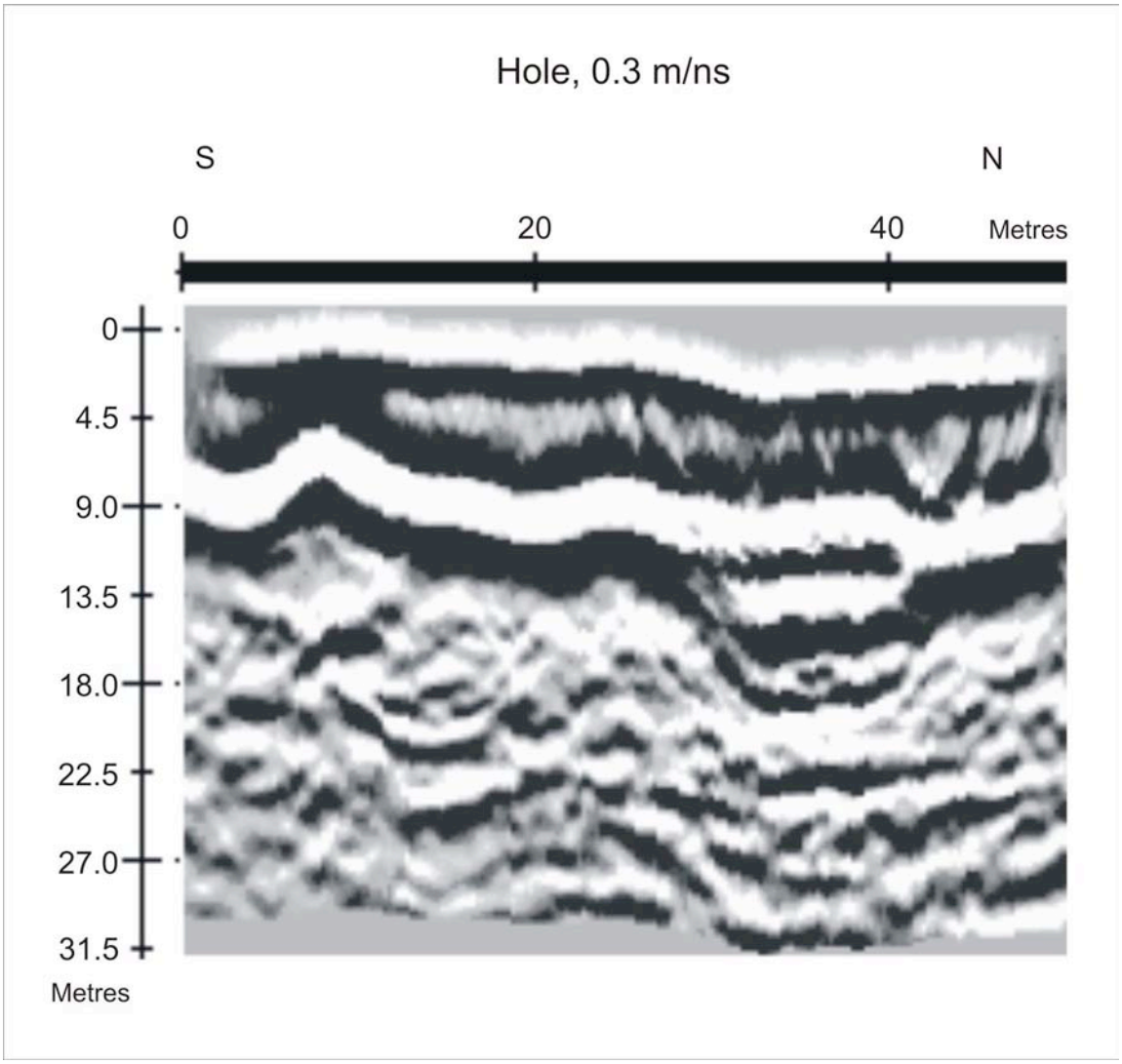
Hole, 0.3 m/ns
S
N
0
20
40
Metres
0
4.5
9.0
13.5
18.0
22.5
27.0
31.5
Metres

Line 3: The flood plain

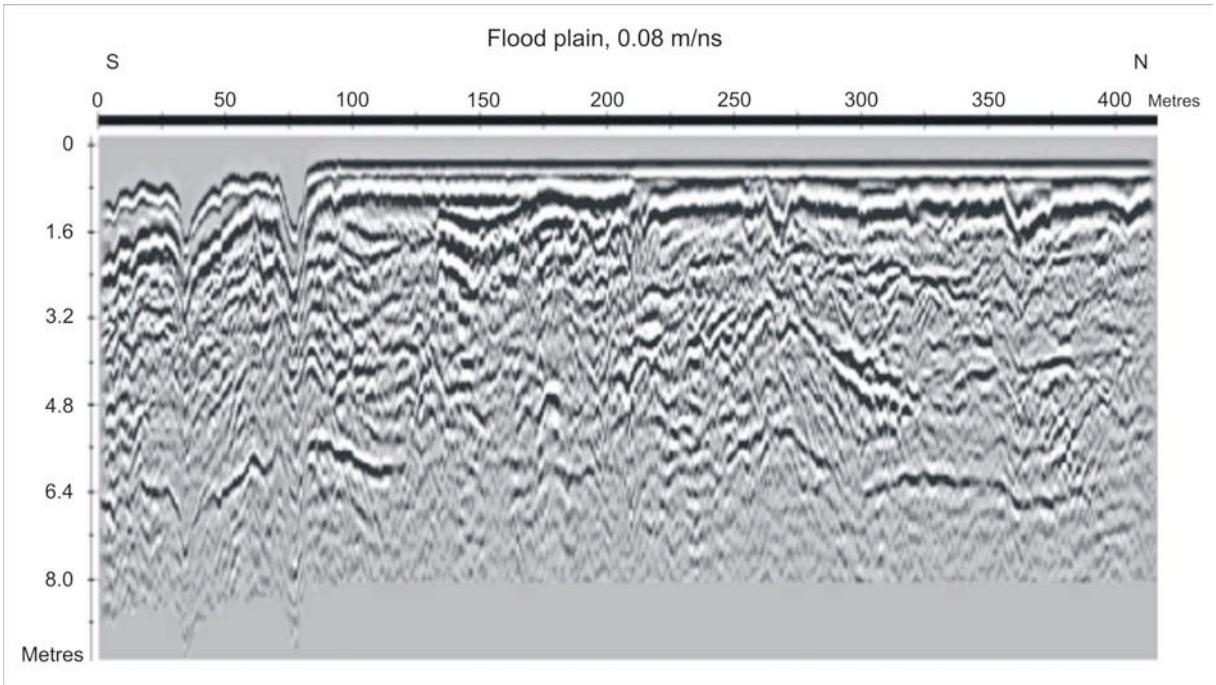

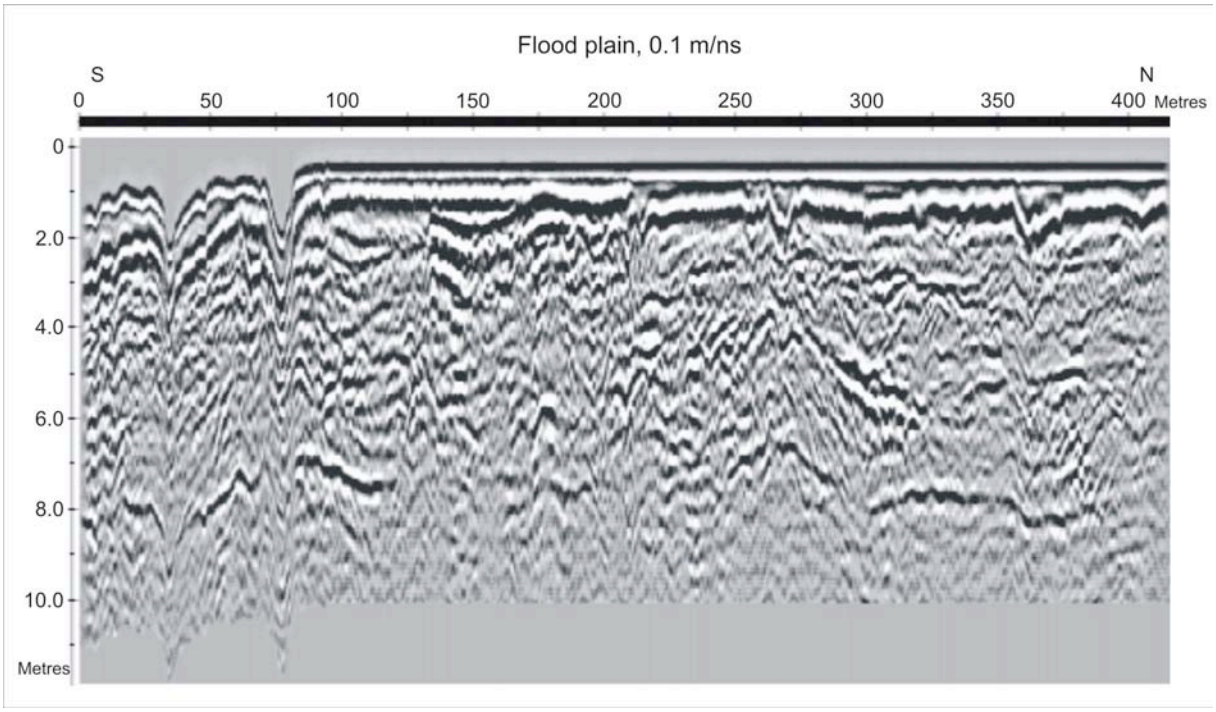

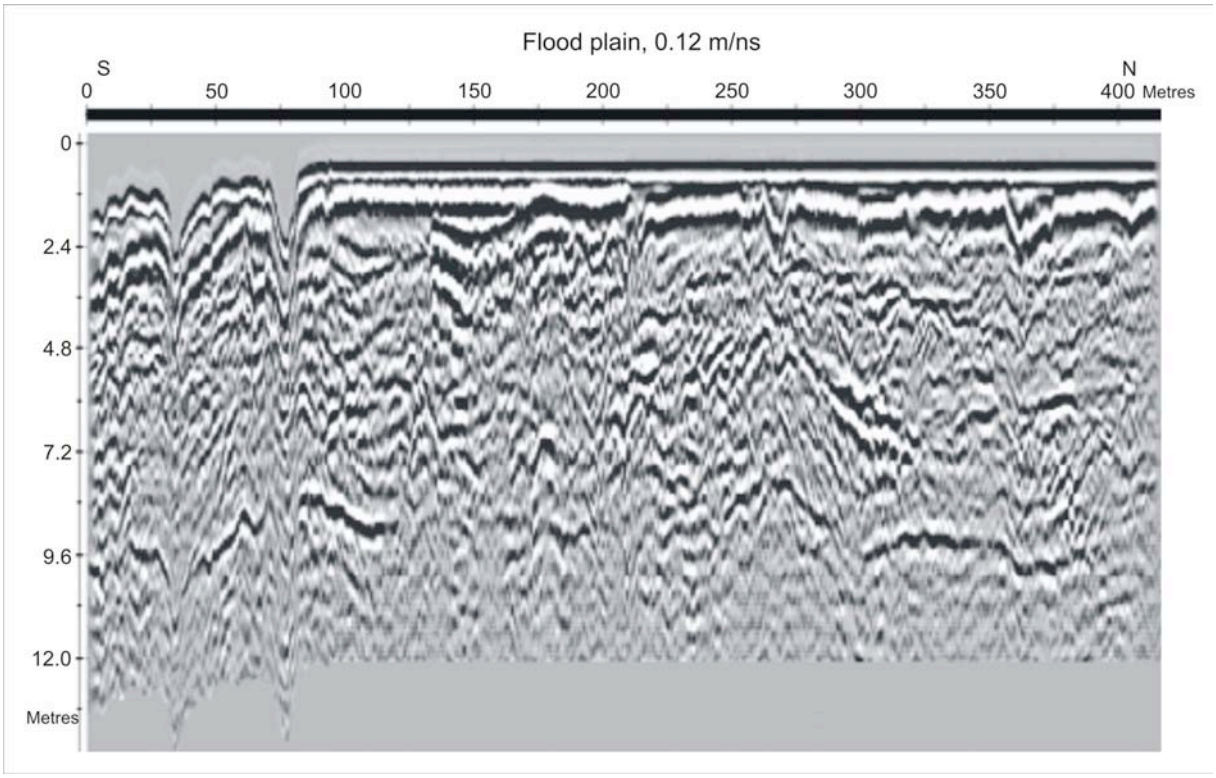
Flood plain, 0.12 m/ns
S
N
0
50
100
150
200
250
300
350
400
Metres
0
2.4
4.8
7.2
9.6
12.0
Metres

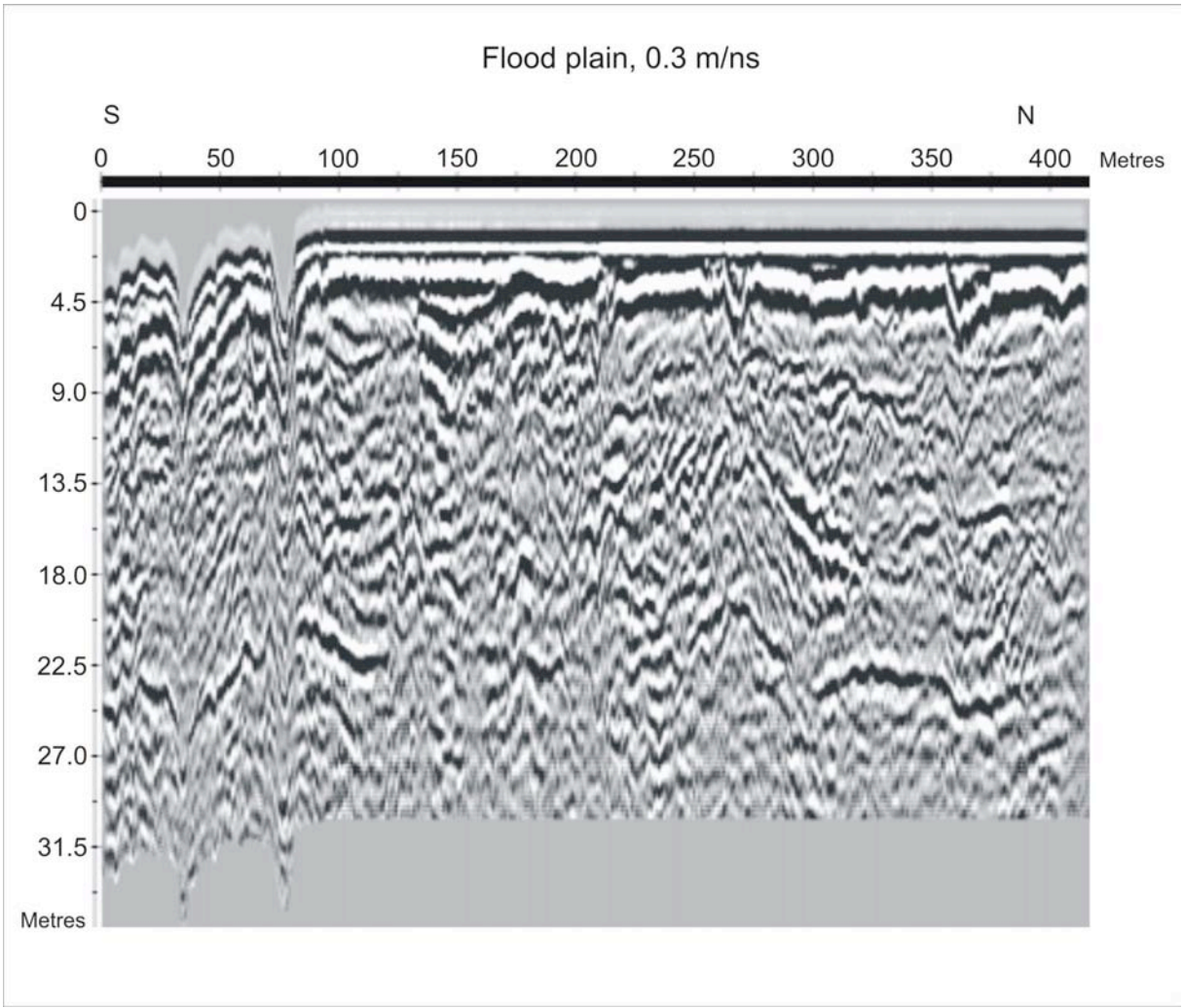
Flood plain, 0.3 m/ns
S
N
0
50
100
150
200
250
300
350
400
Metres
0
4.5
9.0
13.5
18.0
22.5
27.0
31.5
Metres

Line 4: The true right bank

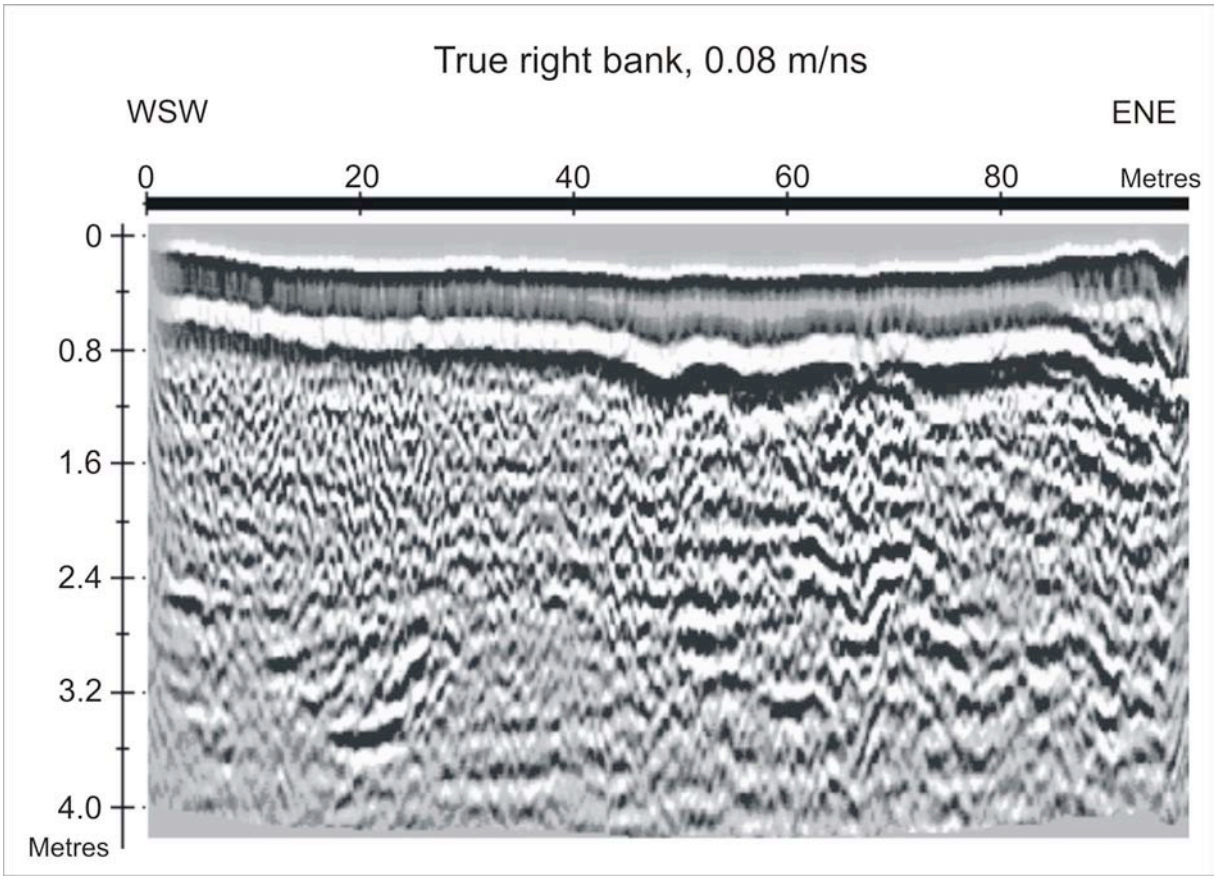

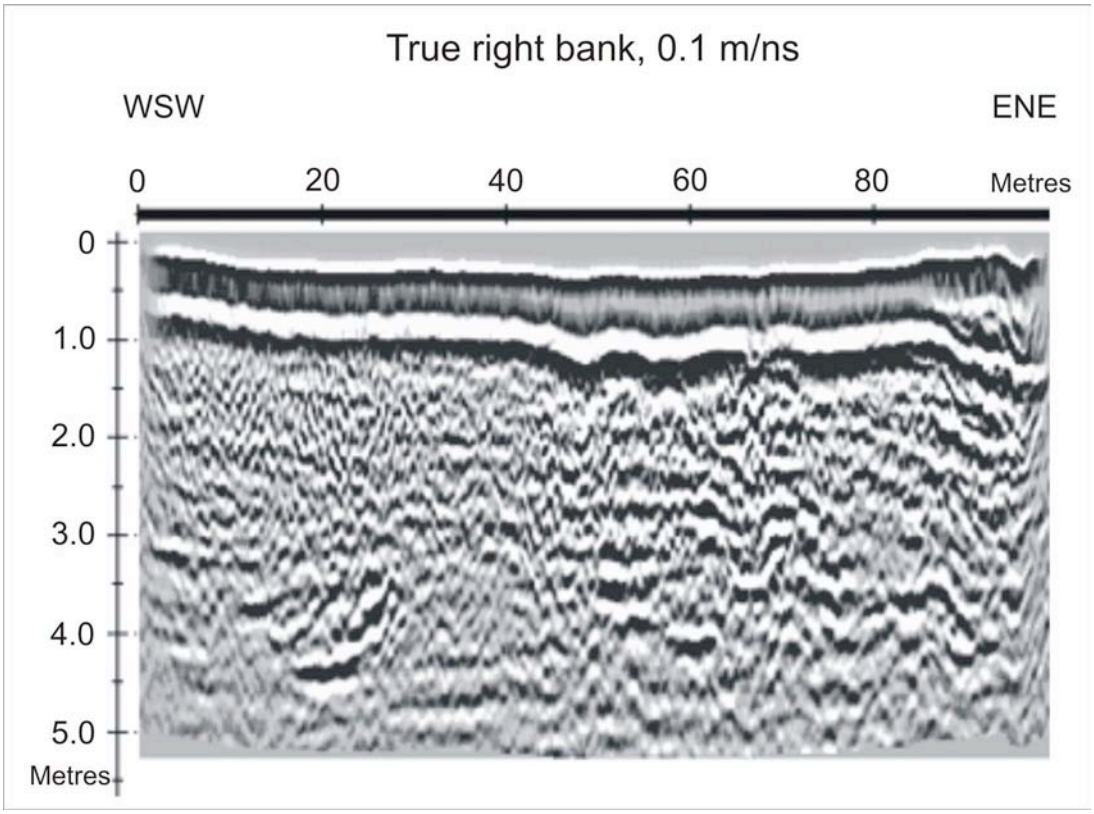

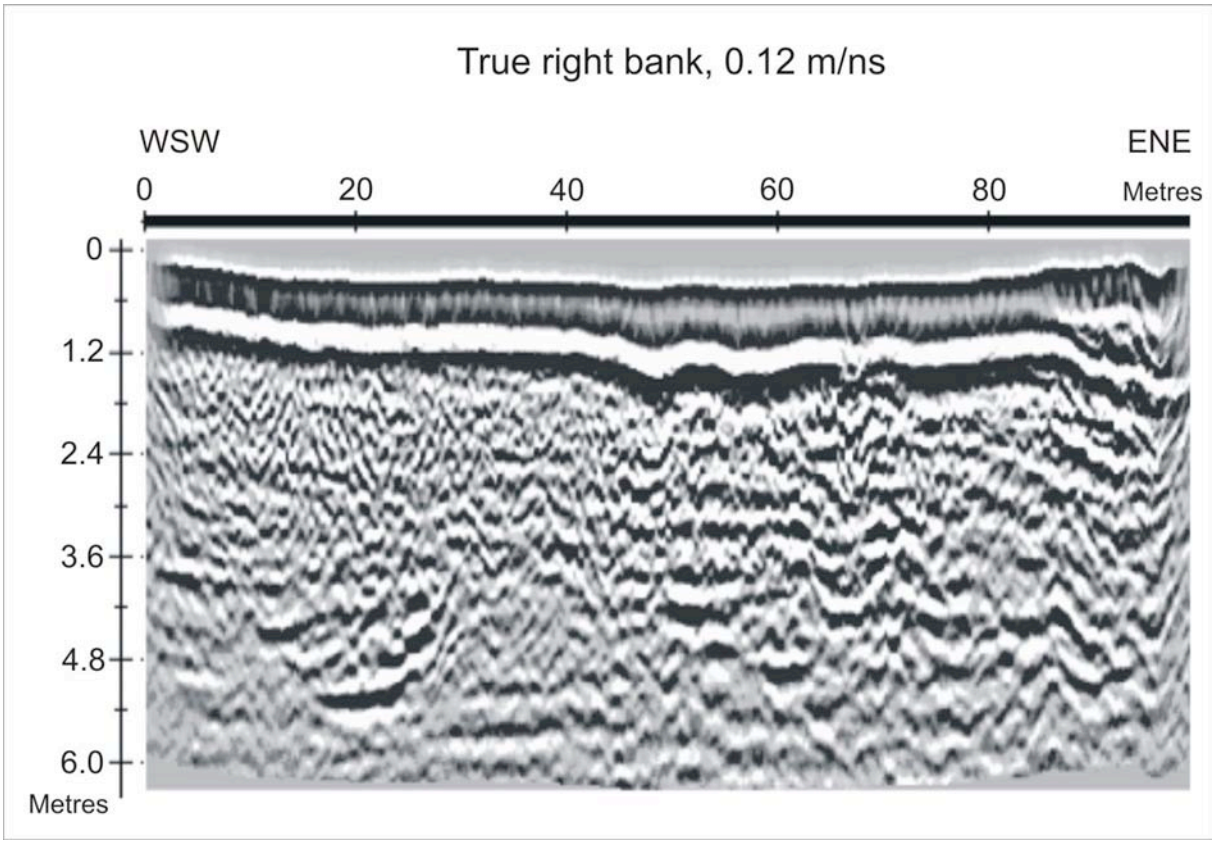
True right bank, 0.12 m/ns
WSW
ENE
0
20
40
60
80
Metres
0
1.2
2.4
3.6
4.8
6.0
Metres

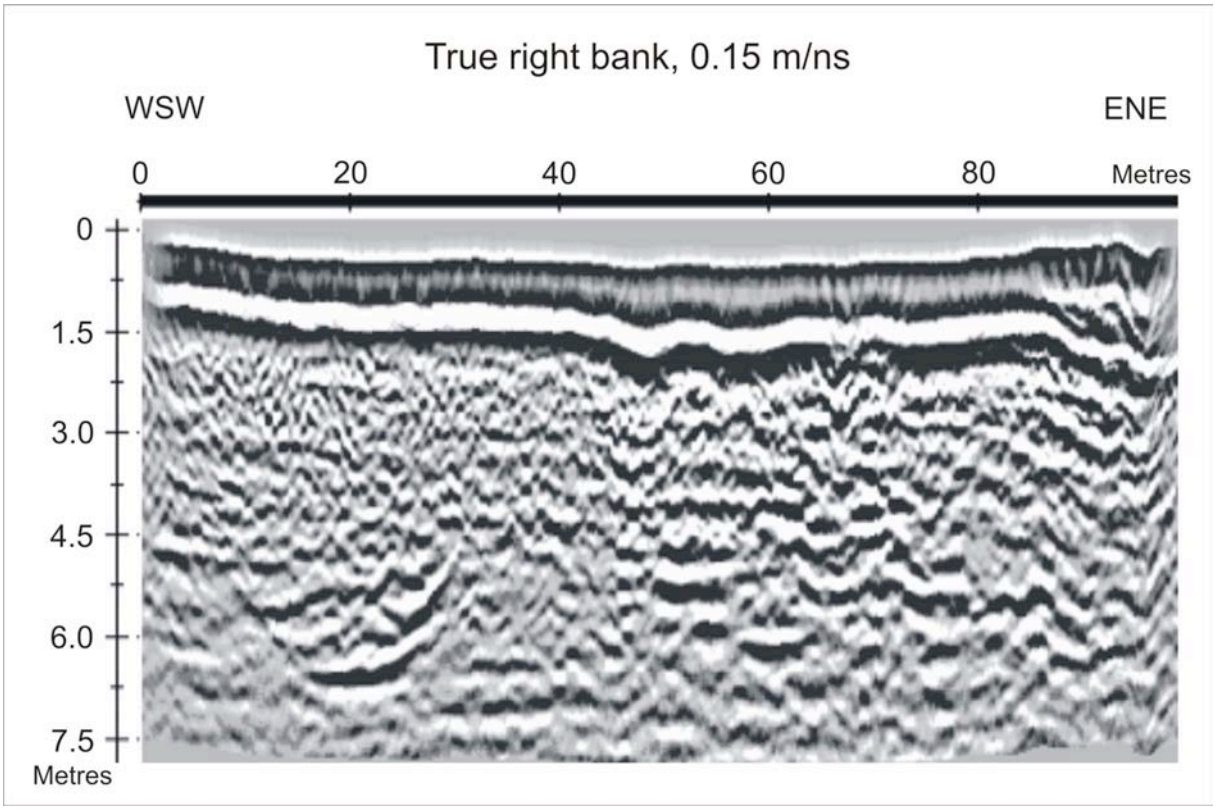
True right bank, 0.15 m/ns
WSW
ENE
0
20
40
60
80
Metres
0
1.5
3.0
4.5
6.0
7.5
Metres

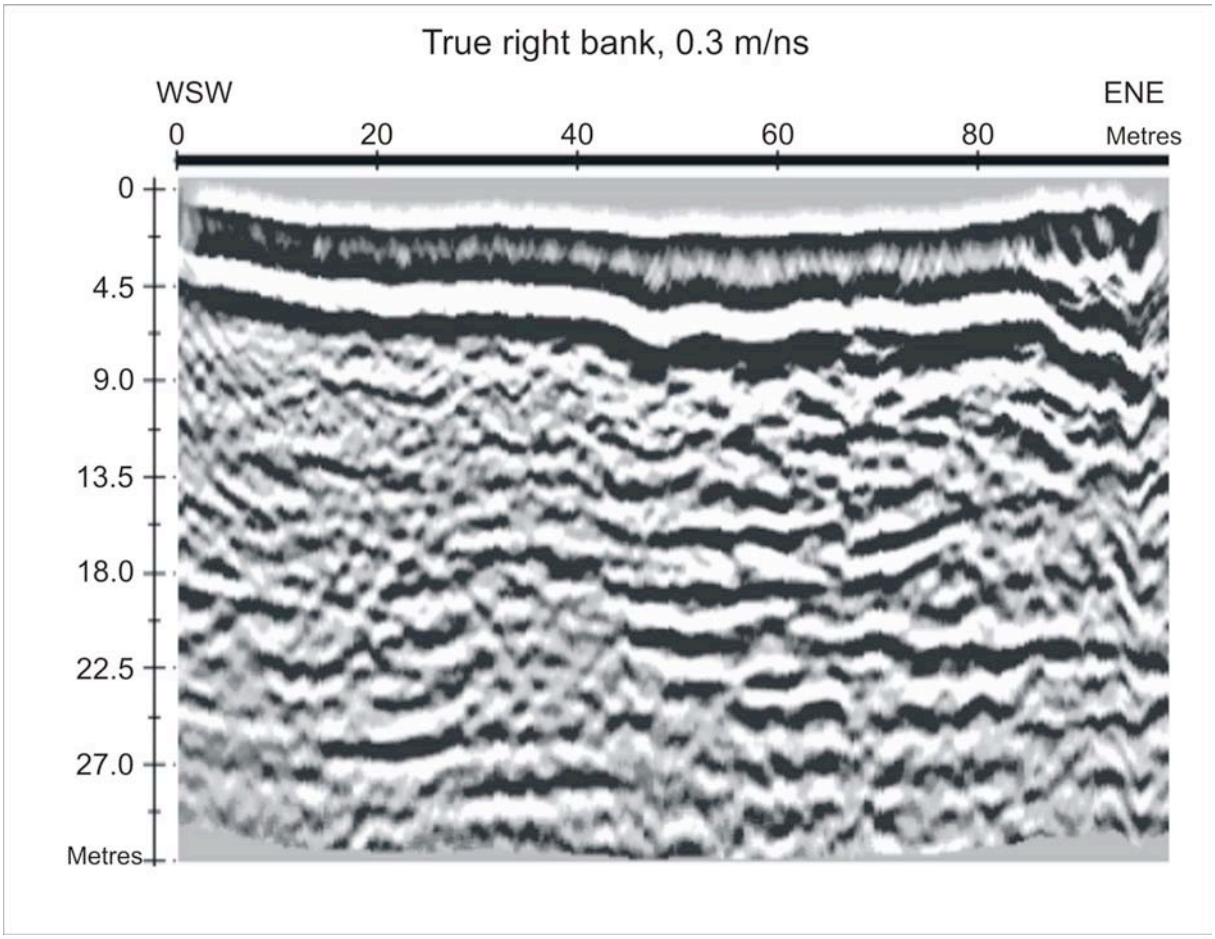

Line 5: The road

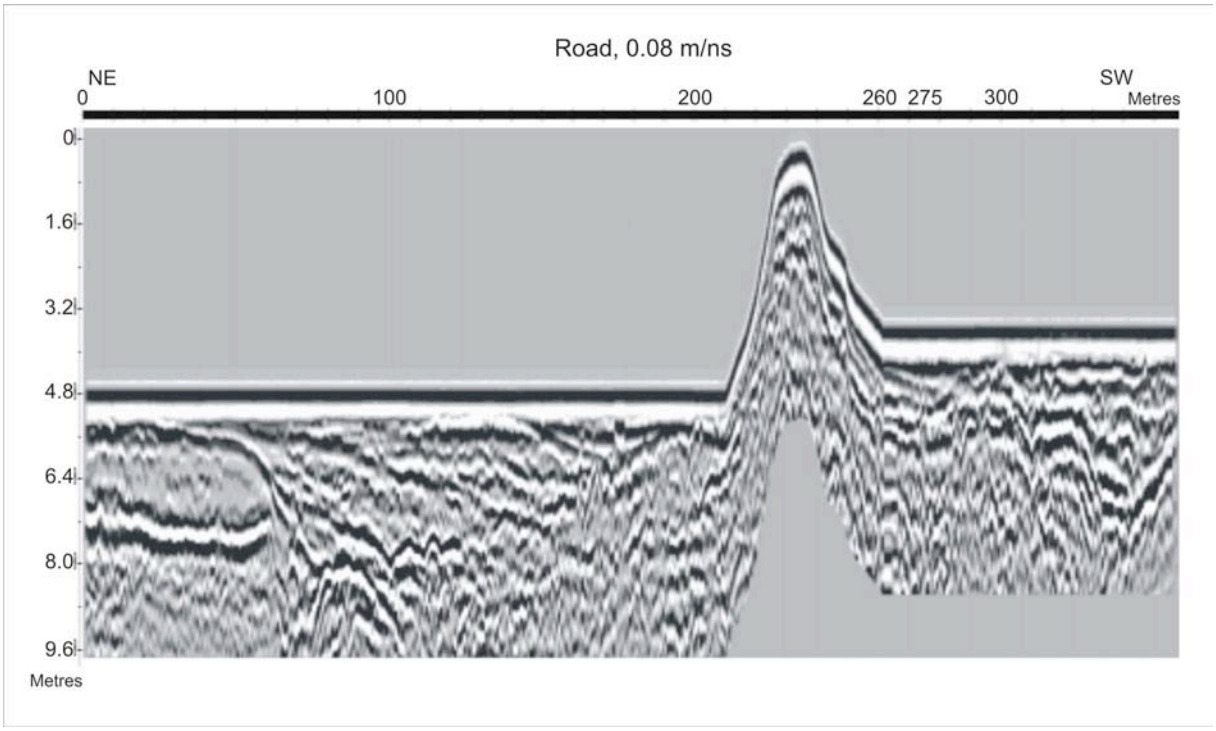

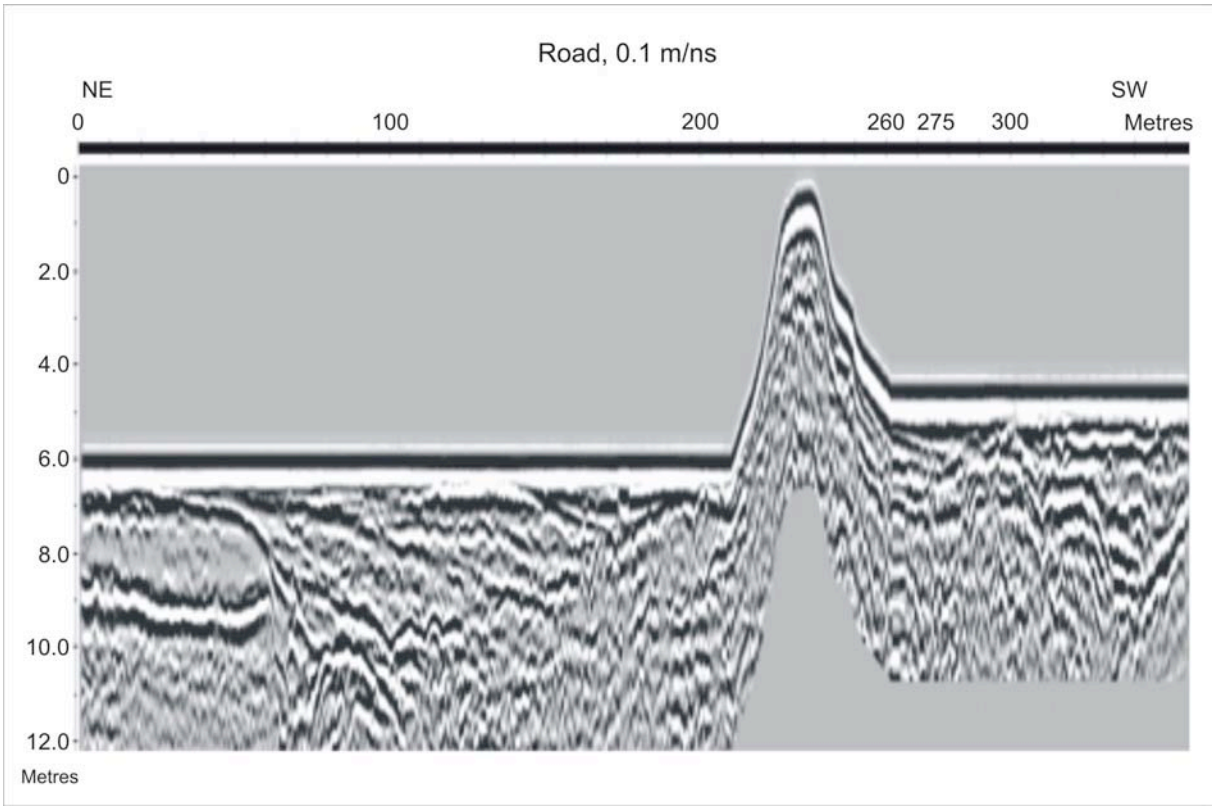
Road, 0.1 m/ns
NE
SW
0
100
200
260 275
300
Metres
0
2.0
4.0
6.0
8.0
10.0
12.0
Metres

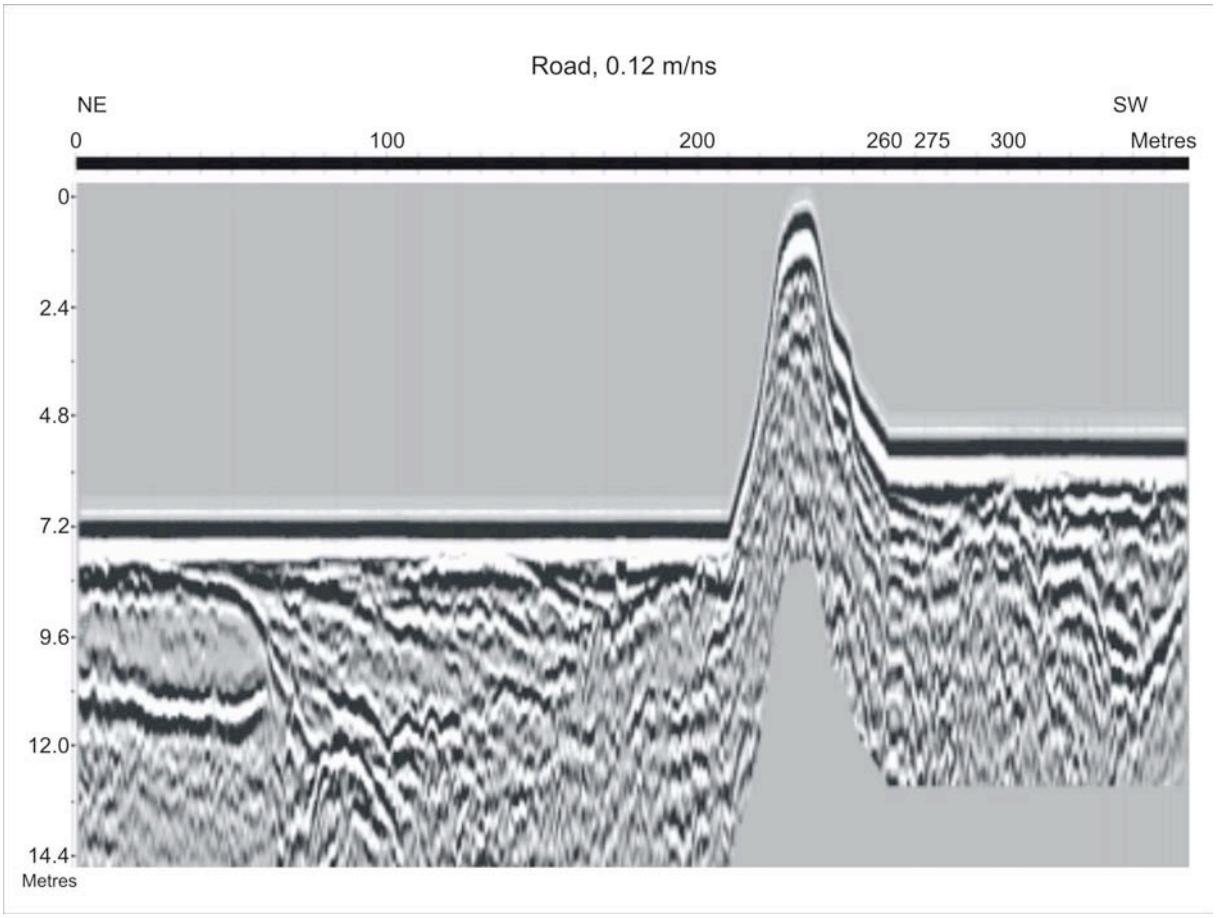
Road, 0.12 m/ns
NE
SW
0
100
200
260 275
300
Metres
0
2.4
4.8
7.2
9.6
12.0
14.4
Metres

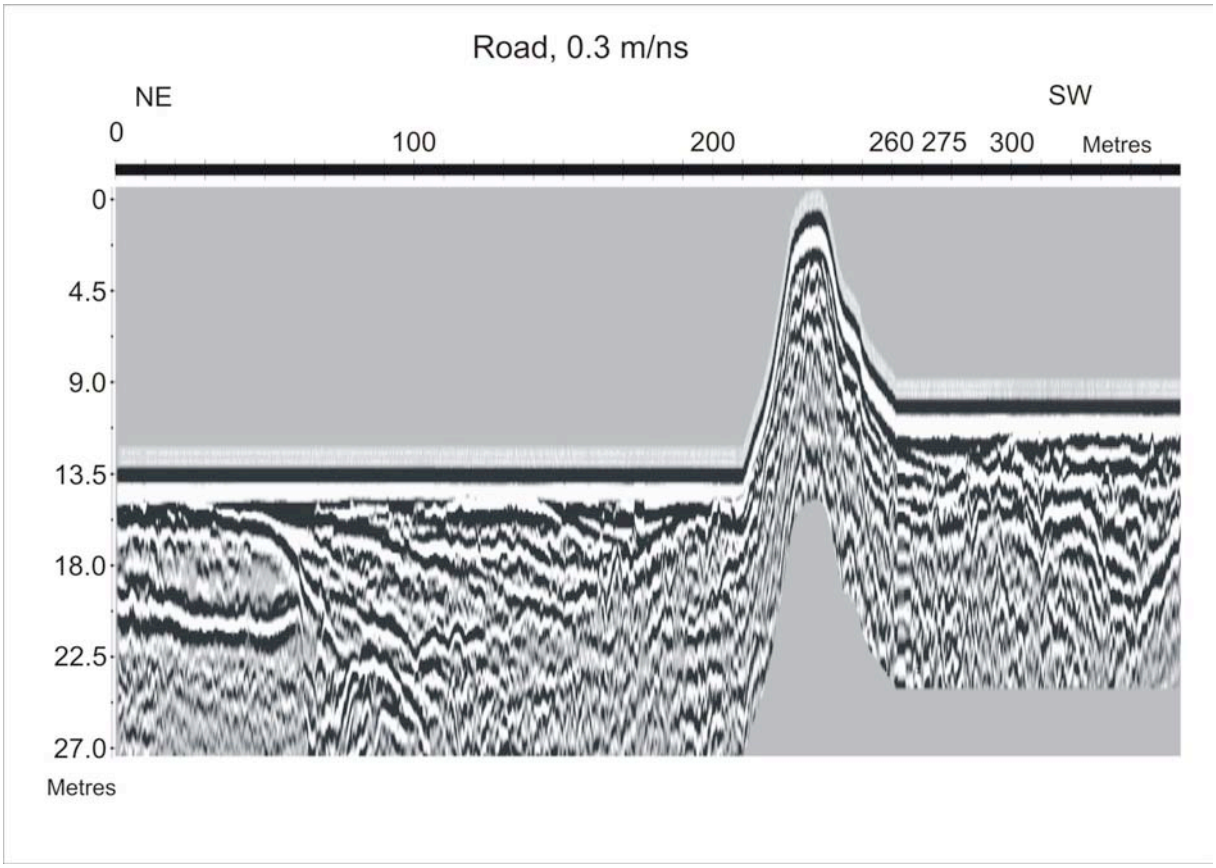
Road, 0.3 m/ns
NE
SW
0
100
200
260 275
300
Metres
0
4.5
9.0
13.5
18.0
22.5
27.0
Metres